DOKUZ EYLÜL UNIVERSITY

GRADUATE SCHOOL OF NATURAL AND APPLIED SCIENCES

DEVELOPMENT OF LABORATORY TESTS ON PERFORMANCES OF ANTIFOULING PAINTS

by

İbrahim KIRKIZ

September, 2023

İZMİR

DEVELOPMENT OF LABORATORY TESTS ON PERFORMANCES OF ANTIFOULING PAINTS

A Thesis Submitted to the

Graduate School of Natural and Applied Sciences of Dokuz Eylül University

In Partial Fulfilment of the Requirements for the Degree of Master of Science

Department of Biochemistry, Biotechnology Program

by

İbrahim KIRKIZ

September, 2023

İZMİR

M.Sc. THESIS EXAMINATION RESULT FORM

We have read the thesis entitled **"DEVELOPMENT OF LABORATORY TESTS ON PERFORMANCES OF ANTIFOULING PAINTS"** completed by **İBRAHİM KIRKIZ** under supervision of **PROF. DR. LEVENT ÇAVAŞ** and we certify that in our opinion it is fully adequate, in scope and in quality, as a thesis for the degree of Master of Science.

Prof. Dr. Levent ÇAVAŞ

Supervisor

Prof. Dr. Merih SARIIŞIK

Jury Member

Assoc. Prof. Sevilay CENGİZ ŞAHİN

Jury Member

Prof. Dr. Okan FISTIKOĞLU

Director

Graduate School of Natural and Applied Sciences

ACKNOWLEDGMENTS

I am grateful to my supervisor, Prof. Dr. Levent ÇAVAŞ, for his valuable knowledge, suggestions, and support throughout the thesis.

I would like to thank my laboratory partners Cengizhan DAĞ, Hacer KANDEMİR, Sema DOĞMAZ and Yeşim YILMAZ ABEŞKA, for their friendships and supports.

I would also like to thank my family for standing behind me in every decision I make. Their endless support and love made me who I am right now.

I am also grateful to the Scientific and Technological Research Council of Türkiye (TÜBİTAK) for the scholarship (Project No: 122Z415, 5200046 and 219M178).

İbrahim KIRKIZ

DEVELOPMENT OF LABORATORY TESTS ON PERFORMANCES OF ANTIFOULING PAINTS

ABSTRACT

Marine biofouling is the attachment of organisms on the surfaces found in the marine ecosystem. Biofouling has serious adverse effects on marine industries. Therefore, antifouling paints are used to deal with the biofouling. But before using, their performance and mechanical properties need to be tested. Field and barnacle adhesion strength tests are some of the performance tests used. In the barnacle adhesion strength test, organisms that adhere to the surface are detached by applying mechanical force. In this thesis, the adhesion strength of the *Amphibalanus amphitrite*, which adhere strongly to the surfaces as a result of the field test were investigated. In addition, the interaction of barnacle cement protein and abietic acid with molecular docking was investigated. At the end of the field test, barnacle and pseudobarnacle adhesion tests were performed on the plates removed from the sea. As a result of the tests, high correlation coefficients were found between the removing strength and the diameter. In addition, very similar barnacle and pseudobarnacle adhesion strength data were obtained in the tests performed on the coating 12. Moreover, in the results of molecular docking analysis, abietic acid was found to bind to cavities in barnacle cement protein with high affinity. This thesis includes the first data on the adhesion strength of *A. amphitrite* on rosin-based self-polishing antifouling paints in the Aegean Sea and shows that molecular docking technology can be used in the production of antifouling paints.

Keywords: Antifouling, biofouling, barnacle, adhesion strength, pseudobarnacle

ANTİFOULİNG BOYALARIN PERFORMANSLARINA YÖNELİK LABORATUVAR TESTLERİNİN GELİŞTİRİLMESİ

ÖZET

Denizsel biyofouling, deniz ekosisteminde yüzeylerin üzerinde organizmaların birikmesidir. Biyofouling olayının denizsel endüstriler üzerine ciddi olumsuz etkileri vardır. Bu nedenle de biyofouling sorunuyla başa çıkmak için antifouling boyalar kullanılmaktadır. Ancak bu boyalar kullanılmadan önce performanslarının ve mekanik özelliklerinin test edilmesi gerekmektedir. Barnacle adhezyon kuvveti ve alan testleri kullanılan performans testlerinden bazılarıdır. Barnacle adhezyon kuvveti testinde, yüzeye tutunan canlılar mekanik kuvvet uygulanarak yüzeyden koparılır. Bu tez çalışmasında alan denemesi sonucunda yüzeylere kuvvetli bir şekilde tutunduğu gözlenen *Amphibalanus amphitrite* türünün adhezyon kuvvetleri incelenmiştir. Bunlara ek olarak, moleküler yanaştırma yöntemi ile barnacle çimento proteini ile abiyetik asidin etkileşimi incelenmiştir. Alan denemesi sonunda denizden çıkarılan plakalar üzerinde barnacle ve sahte barnacle adhezyon testleri gerçekleştirilmiştir. Yapılan testler sonucunda yüzeyden kopma kuvveti ile barnacle çapı arasında yüksek korelasyon katsayıları bulunmuştur. Ayrıca 12 numaralı kaplama üzerinde gerçekleştirilen testlerde çok yakın barnacle ve sahte barnacle adhezyon kuvveti sonuçları elde edilmiştir. Moleküler yanaştırma analizi sonuçlarında ise abiyetik asidin, barnacle çimento proteinindeki oyuklara yüksek afinite ile bağlandığı bulunmuştur. Bu tez, *A. amphitrite* türünün Ege Denizi'ndeki rosin tabanlı self-polishing antifouling boyalar üzerindeki adhezyon kuvveti ile ilgili ilk verileri içermektedir ve moleküler yanaştırma teknolojisinin antifouling boya üretiminde kullanılabileceğini göstermektedir.

Anahtar kelimeler: Antifouling, biyofouling, barnacle, adhezyon kuvveti, sahte barnacle

CONTENTS

Page

M.Sc. THESIS EXAMINATION RESULT FORM ii
ACKNOWLEDGMENTS iii
ABSTRACT iv
ÖZET v
LIST OF FIGURES ix
LIST OF TABLES xiv
ABBREVIATIONS xv

CHAPTER ONE - INTRODUCTION 1

1.1 Marine Biofouling 1
1.2 Effects of Biofouling 2
1.3 Biofouling Species in Aegean Sea 3
1.3.1 *Amphibalanus amphitrite* 3
1.3.2 *Hydroides elegans* 8
1.3.3 *Bugula neritina* 9
1.3.4 *Ulva lactuca* 9
1.4 Antifouling Strategies and Antifouling Paints 10
1.4.1 Insoluble Matrix Paints 11
1.4.2 Soluble Matrix Paints 12
1.4.3 Self-Polishing Co-Polymer Paints 13
1.4.4. Fouling Release Paints 14
1.5 Performance Testing of Antifouling Paints 16
1.5.1 Laboratory Bioassays 16
1.5.2 Fields Tests 18
1.5.3 Mechanical Performance Tests 19
1.6 Bioinformatics 19
1.6.1 The Molecular Docking 20
1.6.2 CB-Docking 20
1.6.3 Scoring Functions 21

1.6.4 Homology Modelling (SWISS-MODEL) 21
1.6.5 ProtParam 22
1.6.6 Multiple Sequence Alignment (Clustal Omega) 22
1.7 The Aims of The Thesis 24

CHAPTER TWO - MATERIALS AND METHODS 25

2.1 Materials 25
2.2 Preparation of the Glass Slides, Plastic Plates and Metal Surfaces 25
2.3 Preparation and Application of Biocide-Free Self-Polishing Coatings 26
2.4 BSA Adsorption Experiments on Coated Glass Slides 28
2.4.1 Preparation of Bradford Reagent 29
2.4.2 Protein Determination 29
2.4.3 BSA Adsorption on Petri Dishes 29
2.5 BSA Adsorption on Plastic Plates 30
2.5.1 Linear Working Range 30
2.5.2 Temperature and Agitating Speed 30
2.5.3 Different ZnR Concentrations 31
2.5.4 Different pH Values 31
2.6 Field Tests 31
2.7 Biofouling Scoring 32
2.8 Protein Determination on Plates (Field Experiment) 32
2.9 Barnacle Adhesion Tests 33
2.10 Pseudobarnacle Adhesion Tests 34
2.11 Statistical Test 35
2.12 Molecular Docking 35

CHAPTER THREE - RESULTS 36

3.1 BSA Adsorption Experiments on Coated Glass Slides 36
3.2 BSA Adsorption on Plastic Plates 37
3.2.1 Linear Working Range 37
3.2.2 Temperature and Agitating Speed 37

3.2.3 Different ZnR Concentrations 38
3.2.4 Different pH Values 39
3.3 Results of Field Test and Biofouling Scores 39
3.4 Protein Determination on Plates (Field Experiment) 55
3.5 Barnacle and Pseudobarnacle Adhesion Strength Tests 56
3.6 Molecular Docking 65

CHAPTER FOUR - DISCUSSION 73

CHAPTER FIVE - CONCLUSION 80

REFERENCES 82

LIST OF FIGURES

Page

Figure 1.1 Stages of biofouling 2
Figure 1.2 *Amphibalanus amphitrite* barnacles attached on metal plates (Personal archive, 2022) 4
Figure 1.3 Schematic of the life cycle stages of a barnacle: nauplius (I-VI), cyprid, juvenile, adult (Inspired from Liang et al., 2019). 5
Figure 1.4 Cements left behind after removing barnacles from the surface (Personal archive, 2022) 6
Figure 1.5 A surface heavy covered with *Hydroides elegans* tubes (Personal archive, 2022) 8
Figure 1.6 Settlement of *Bugula neritina* on a polyvinyl chloride (PVC) pipe (Personal archive, 2022) 9
Figure 1.7 Metal plate fouled by *Ulva lactuca* and *Hydroides elegans* (Personal archive, 2022) 10
Figure 1.8 Diagram of insoluble matrix paints (Inspired from Dafforn et al., 2011) 11
Figure 1.9 Diagram of soluble matrix paints (Inspired from Dafforn et al., 2011) ... 12
Figure 1.10 Chemical structures of resin acids (a) abietic acid, (b) levopimaric acid, (c) palustric acid, (d) neoabietic acid, (e) dehydroabietic acid, (f) sandaracopimaric acid, (g) isopimaric acid, (h) pimaric acid 13
Figure 1.11 Diagram of self-polishing paints (Inspired from Dafforn et al., 2011) .. 14
Figure 1.12 Cation form of tributyltin 14
Figure 1.13 Diagram of fouling release paints (Inspired from Dafforn et al., 2011). 15
Figure 1.14 Structure of a poly(dimethyl)siloxane chain 16
Figure 2.1 Preparation of rosin-based coatings (Personal archive, 2022) 26
Figure 2.2 The sample coatings on a) metal, b) glass, c) plastic surfaces (Personal archive, 2022) 28
Figure 2.3 Petri dishes containing (a, b, c) uncoated slides; (d, e, f) ZnR-coated slides immersed in 0.1 mg/mL, 30 mL BSA solution (Personal archive, 2022)30
Figure 2.4 Some of the plates in the area where the field trial was carried out (Personal archive, 2022) 31

Figure 2.5 The coatings used for protein determination (Personal archive, 2022) 32
Figure 2.6 Analog dynamometer used in the adhesion tests (Personal archive, 2022) 33
Figure 2.7 Wooden pseudobarnacles that used in the adhesion tests (Personal archive, 2022)..... 35
Figure 3.1 Standard calibration graph of BSA..... 36
Figure 3.2 Amount of BSA on (a) petri dish; (b) petri dish with uncoated slide; (c) petri dish with ZnR-coated slide; (d) post-wash solution of uncoated slide; (e) post-wash solution of ZnR-coated slide; (f) petri dish after uncoated slide removal; (g) petri dish after ZnR-coated slide removal after 4 hours The asterisk indicates statistical difference ($p<0.05$) when compared to "amount of BSA on (a) petri dish"..... 37
Figure 3.3 Change of BSA adsorption with different temperature and agitating speeds 38
Figure 3.4 Change of BSA adsorption with different ZnR ratios 38
Figure 3.5 Change of BSA adsorption with different pH values 39
Figure 3.6 The field test results of uncoated plate (a) before immersion, (b) after 2 weeks, (c) after 4 weeks, (d) after 7 weeks, (e) after 10 weeks (Personal archive, 2022)..... 41
Figure 3.7 The field test results of anti-corrosive primer coated plat (a) before immersion, (b) after 2 weeks, (c) after 4 weeks, (d) after 7 weeks, (e) after 10 weeks (Personal archive, 2022)..... 41
Figure 3.8 The field test results of Coating-1 (a) before immersion, (b) after 2 weeks, (c) after 4 weeks, (d) after 7 weeks, (e) after 10 weeks (Personal archive, 2022)..... 42
Figure 3.9 The field test results of Coating-2 (a) before immersion, (b) after 2 weeks, (c) after 4 weeks, (d) after 7 weeks, (e) after 10 weeks (Personal archive, 2022)..... 42
Figure 3.10 The field test results of Coating-3 (a) before immersion, (b) after 3 weeks, (c) after 6 weeks (Personal archive, 2022)..... 43
Figure 3.11 The field test results of Coating-4 (a) before immersion, (b) after 3 weeks, (c) after 6 weeks (Personal archive, 2022)..... 43

Figure 3.12 The field test results of Coating-5 (a) before immersion, (b) after 3 weeks, (c) after 6 weeks (Personal archive, 2022) 43
Figure 3.13 The field test results of Coating-6 (a) before immersion, (b) after 3 weeks, (c) after 6 weeks (Personal archive, 2022) 44
Figure 3.14 The field test results of commercial paint (a, d) before immersion, (b, e) after 3 weeks, (c, f) after 6 weeks (Personal archive, 2022) 44
Figure 3.15 The field test results of Coating-7 (a) before immersion, (b) after 2 weeks, (c) after 4 weeks, (d) after 7 weeks, (e) after 10 weeks (Personal archive, 2022) 45
Figure 3.16 The field test results of Coating-8 (a) before immersion, (b) after 2 weeks, (c) after 4 weeks, (d) after 7 weeks, (e) after 10 weeks (Personal archive, 2022) 45
Figure 3.17 The field test results of Coating-9 (a) before immersion, (b) after 2 weeks, (c) after 4 weeks, (d) after 7 weeks, (e) after 10 weeks (Personal archive, 2022) 46
Figure 3.18 The field test results of Coating-10 (a) before immersion, (b) after 2 weeks, (c) after 4 weeks, (d) after 7 weeks, (e) after 10 weeks (Personal archive, 2022) 46
Figure 3.19 The field test results of Coating-11 (a) before immersion, (b) after 2 weeks, (c) after 4 weeks, (d) after 7 weeks, (e) after 10 weeks (Personal archive, 2022) 47
Figure 3.20 The field test results of Coating-12 (a) before immersion, (b) after 2 weeks, (c) after 4 weeks, (d) after 7 weeks, (e) after 10 weeks (Personal archive, 2022) 47
Figure 3.21 The field test results of Coating-13 (a) before immersion, (b) after 2 weeks, (c) after 4 weeks, (d) after 7 weeks, (e) after 10 weeks (Personal archive, 2022) 48
Figure 3.22 The field test results of Coating-14 (a) before immersion, (b) after 2 weeks, (c) after 4 weeks, (d) after 7 weeks, (e) after 10 weeks (Personal archive, 2022) 48

Figure 3.23 The field test results of Coating-15 (a) before immersion, (b) after 2 weeks, (c) after 4 weeks, (d) after 7 weeks, (e) after 10 weeks (Personal archive, 2022)..... 49
Figure 3.24 The field test results of Coating-16 (a) before immersion, (b) after 2 weeks, (c) after 4 weeks, (d) after 7 weeks, (e) after 10 weeks (Personal archive, 2022)..... 49
Figure 3.25 The field test results of Coating-17 (a) before immersion, (b) after 2 weeks, (c) after 4 weeks, (d) after 7 weeks, (e) after 10 weeks (Personal archive, 2022)..... 50
Figure 3.26 The field test results of Coating-18 (a) before immersion, (b) after 2 weeks, (c) after 4 weeks, (d) after 7 weeks, (e) after 10 weeks (Personal archive, 2022)..... 50
Figure 3.27 The field test results of Coating-19 (a) before immersion, (b) after 2 weeks, (c) after 4 weeks, (d) after 7 weeks, (e) after 10 weeks (Personal archive, 2022)..... 51
Figure 3.28 The field test results of Coating-20 (a) before immersion, (b) after 2 weeks, (c) after 4 weeks, (d) after 7 weeks, (e) after 10 weeks (Personal archive, 2022)..... 51
Figure 3.29 The field test results of Coating-21 (a) before immersion, (b) after 2 weeks, (c) after 4 weeks, (d) after 7 weeks, (e) after 10 weeks (Personal archive, 2022)..... 52
Figure 3.30 The field test results of Coating-22 (a) before immersion, (b) after 2 weeks, (c) after 4 weeks, (d) after 7 weeks, (e) after 10 weeks (Personal archive, 2022)..... 52
Figure 3.31 The field test results of Coating-23 (a) before immersion, (b) after 3 weeks, (c) after 6 weeks (Personal archive, 2022)..... 53
Figure 3.32 Relationship between removal strength and stud diameter on coating 10 after drying 6 hours 60
Figure 3.33 Relationship between removal strength and stud diameter on coating 12 after drying 6 hours 60
Figure 3.34 Relationship between removal strength and stud diameter on coating 14 after drying 6 hours 61

Figure 3.35 Adhesion strengths of different-sized pseudobarnacles on different coatings after 6 hours of drying. Different letters indicate statistical difference at 0.05. The comparisons were carried within groups (5, 10, 15 and 20 stud diameter) 62
Figure 3.36 Relationship between removal strength and stud diameter on coating 10 after drying an hour 63
Figure 3.37 Relationship between removal strength and stud diameter on coating 12 after drying an hour 64
Figure 3.38 Relationship between removal strength and stud diameter on coating 14 after drying an hour 64
Figure 3.39 Adhesion strengths of different-sized pseudobarnacles on different coatings after an hour of drying. Different letters indicate statistical difference at 0.05. The comparisons were carried within groups (5, 10, 15 and 20 stud diameter) 65
Figure 3.40 Modelled 3D structure of CP-20k-1, CP-20k-2 and CP-20k-3 by using SWISS-MODEL 66
Figure 3.41 Clustal Omega result of *Megabalanus rosa* CP-20k and 72

LIST OF TABLES

Page

Table 2.1 Prepared coating and their contents 27
Table 3.1 Antifouling performance scores of prepared coatings 54
Table 3.2 Protein concentrations on plates that used in field experiment..... 55
Table 3.3 The adhesion strengths of *Amphibalanus amphitrite* on the coating 4 56
Table 3.4 The adhesion strengths of *Amphibalanus amphitrite* on the coating 10 57
Table 3.5 The adhesion strengths of *Amphibalanus amphitrite* on the coating 12 57
Table 3.6 The adhesion strengths of *Amphibalanus amphitrite* on the coating 14 58
Table 3.7 Pseudobarnacle test results on anticorrosive primer coated panels (± standard deviation) 59
Table 3.8 Pseudobarnacle tests results on all coatings after 6 hours of drying. Different letters indicate statistical difference at 0.05. Comparisons were carried within groups (Coating 10, 12, 14) and each group compared to adhesion strength of 5 mm diameter (± standard deviation) 59
Table 3.9 Pseudobarnacle tests results on all coatings after an hour of drying. Different letters indicate statistical difference at 0.05. Comparisons were carried within groups (Coating 10, 12, 14) and each group compared to adhesion strength of 5 mm diameter (± standard deviation) (± standard deviation) 63
Table 3.10 The molecular docking results of abietic acid with *Amphibalanus amphitrite* CP-20k-1 67
Table 3.11 The molecular docking results of abietic acid with *Amphibalanus amphitrite* CP-20k-2 68
Table 3.12 The molecular docking results of abietic acid with *Amphibalanus amphitrite* CP-20k-3 69
Table 3.13 The molecular docking results of abietic acid with *Megabalanus rosa* cement protein MrCP-20 70
Table 3.14 ProtParam results of *Megabalanus rosa* and *Amphibalanus amphitrite* CP-20k 71
Table 5.1 Correlations of diameters and removal strengths between barnacles and pseudobarnacles 80

ABBREVIATIONS

CP	: Cement protein
DOPA	: 3, 4-dihydroxy phenylalanine
PVC	: Polyvinyl Chloride
TBT	: Tributyltin
IMO	: International Maritime Organization
PDMS	: Polydimethylsiloxane
EC	: Effective Concentration
LD	: Lethal Dose
ZnR	: Zinc rosinate
PVB	: Polyvinyl Butyral
BSA	: Bovine Serum Albumin
PBS	: Phosphate-Buffered Saline
TEOS	: Tetraethyl Orthosilicate
TCBF	: Tertiary Carboxybetaine Dodecafluoroheptyl Ester Ethyl Acrylate
PEG	: Polyethylene Glycol
PTU	: Propylthiouracil
GPCR	: G-protein Coupled Receptor

CHAPTER ONE
INTRODUCTION

1.1 Marine Biofouling

The settlement and colonization of organisms on any surface that they are in contact with is called biofouling. This biofouling process can happen in medical, industrial, and maritime sectors. Unwanted attachment of organisms such as bacteria, diatoms, algae, and macro-organisms on any surface that found in seawater is classified as marine biofouling (Gule et al., 2016).

If the conditions are suitable, formation of biofouling begins on the substrate surface. Marine biofouling occurs in 4 stages (Figure 1.1). First stage is the adhesion of organic and inorganic molecules to form a conditioning film layer. Formation of this layer takes 1-2 minutes in seawater. This film layer consists of polysaccharides, proteins, proteoglycans, and inorganic compounds. van der Waals interactions are one of the forces effective in the formation of the conditioning film layer. This layer provides a sticky surface to facilitate the adhesion of microorganisms (Cao et al., 2011). After formation of conditioning film layer bacteria and diatoms start colonizing on the modified surfaces and form a microbial biofilm. This microbial biofilm helps embedded microorganisms to survive on the substrate surface. It makes capturing nutrients and other microorganisms easier (Yebra et al., 2004). It takes around 1-24 hours for the primary colonization. The third stage begins with the inclusion of cyprids, algal spores, and invertebrate larvae in this bacterial biofilm. Last stage involves developments and growth of macrofouling community. Macrofouling organisms can be divided into soft fouler and hard foulers. Some soft foulers are algae and hydroids while hard foulers are barnacles and tubeworms. Marine biofouling is a dynamic process because many parameters effect the organisms such as substratum material, geographical location, and physicochemical conditions of the seawater (Vinagre et al., 2020).

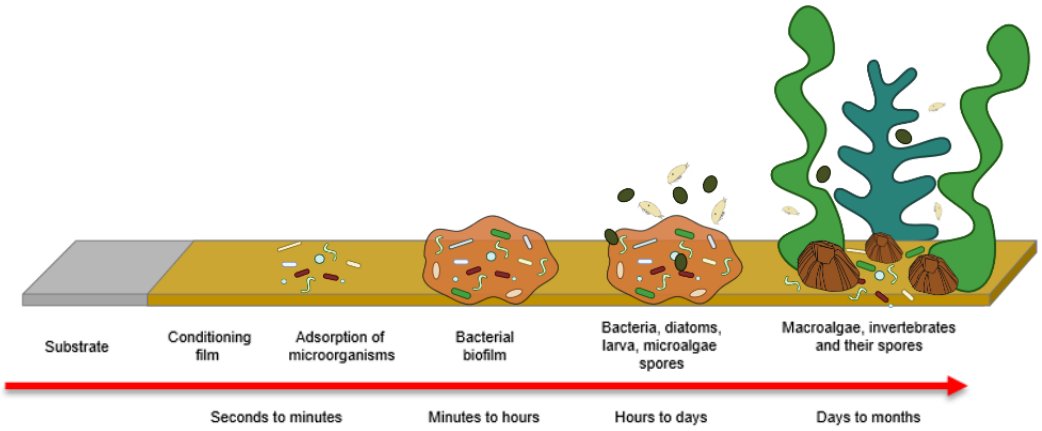


Figure 1.1 Stages of biofouling

1.2 Effects of Biofouling

Biofouling negatively affects especially the marine vessels. Biofouling takes place on the surfaces of all marine vessels. Since these vessels are constantly in the seawater, their surfaces are suitable for biofouling. The problems created by biofouling in the marine industry are as follows (Schultz et al., 2011; Carve et al., 2019).

- Accumulation of biofouling organisms on the ship's parts increase the weight of the ships.
- Ship hulls are smooth surfaces to decrease the surface friction. But biofouling causes roughness on the surfaces. Due to this roughness, the surface friction between surface and seawater increases.
- Increased weight and surface friction cause the speed of the ship to decrease, which causes consumption of more fuel. As fuel consumption increases, carbon emissions also increase.
- In addition, biofouling organisms are transported to different regions by adhering to the ships which causes biodiversity of marine ecosystems to change.

Due to the reasons stated above, ships cannot continue to operate in this way for a long time. For this reason, the ships are taken ashore, and their surfaces are cleaned. This cleaning process is called dry-docking. Even though dry-docking cleans the

surfaces, these operations require time, resource, and labor. Since the dry-docking process causes a serious waste of time and money, nowadays, underwater hull cleaning is carried out using drones and experienced divers. However, this is not a process that can be done in every port now (Yebra et al., 2004; Song and Cui, 2020).

1.3 Biofouling Species in Aegean Sea

Some of the biofouling organisms in marine environment synthetase adhesives to attach underwater surfaces. Those adhesives are quite remarkable since commercial adhesives do not reach the effectiveness of biological adhesives. Because of that, hard foulers such as barnacles, mussels, and tubeworms cause serious issues in maritime industries like transportation, power plants etc. For that reason, understanding the adhesion mechanism of those organisms are crucial for new antifouling paints (Callow and Callow, 2002).

The biofouling species with high populations on the plate surfaces as a result of the field test are explained below. The species found in the field test are similar to those found in the literature (Kocak et al., 1999; Abeşka, 2019; Safarov, 2021).

1.3.1 Amphibalanus amphitrite

Barnacles are a highly studied species because of their widespread and underwater adhesion properties. The most popular areas of work are the development of new adhesives and marine antifouling tests. Barnacles belong to the phylum Arthropoda, and they are one of few sessile crustaceans (Kamino et al., 2012) (Figure 1.2). Their bodies have multi-layered calcareous shell plates (Liang et al., 2019). Barnacles attach their base plates into surfaces using underwater adhesive called cement (Walker, 1972; Kamino, 2013). As mentioned before, they are sessile organisms which mean that they can only be moved by external forces such as water currents. When they become cyprid, they release adhesives that permanently attaches themselves to the surfaces (Kamino, 2016).



Figure 1.2 *Amphibalanus amphitrite* barnacles attached on metal plates (Personal archive, 2022)

The life cycle of barnacles occurs in 4 stages and those are nauplius, cyprid, juvenile and adult (Figure 1.3). Nauplius is the larval stage of the barnacles (Kamino, 2016). When nauplius reaches to sufficient size, it transforms into non-settled cyprid. Cyprid is responsible for exploration and finding an area to settle (Aldred and Clare, 2008). This cyprid seeks marine environments to find a surface to attach and develop. After it finds a surface, it releases a temporary adhesive for reversible adhesion. This temporary adhesive is called footprint (Walker and Yule, 1984). After reversibly settling down, cyprid undergoes metamorphosis and transforms into juvenile (Maruzzo et al., 2012). It also starts calcification process to form several shell plates. Finally, adult barnacles secrete cement proteins (CPs) to attach rigidly onto the surfaces (Kamino, 2016). Adult barnacles continue growing by adding calcium salts to their shell plates.

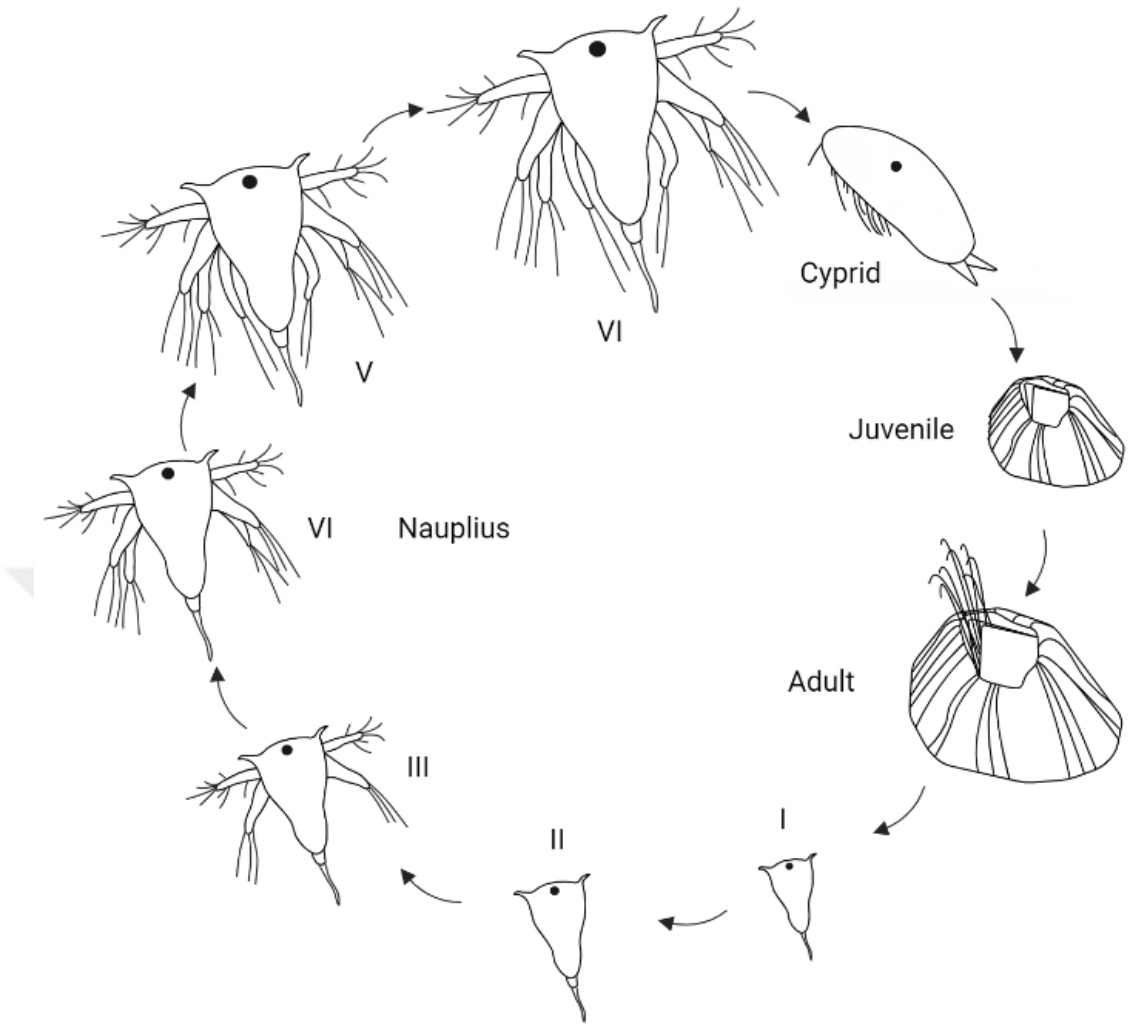


Figure 1.3 Schema of the life cycle stages of a barnacle: nauplius (I-VI), cyprid, juvenile, adult (Inspired from Liang et al., 2019)

Logic behind the temporary attachment is all about finding desirable surface to colonize. If temporary adhesion between cyprid and the surface is strong, then cyprid prefers to colonize there. But if the adhesion is not strong cyprid turns back to seawater for surface exploration. There are some parameters that effects the preference of cyprids. Barnacles prefers to colonize on surfaces that already fouled by other species of adult barnacles (Liang et al., 2019). Also, they can sense physical, chemical, and topological properties of the surfaces. Among that hydrophobicity, surface energy, surface texture etc. can affect the surface exploration for cyprid.

The adhesive is produced at the cement gland and secreted into the gaps between the barnacle base and the surface to fill space (Figure 1.4). Adhesive layer formed between the base and the surface is approximately a few microns (Saroyan et al., 1970). In the lifespan of a barnacle there is 3 stages of adhesion. First one is footprint, which is secreted by cyprid to reversibly attach while exploring for surface. Second, cyprid produces permanent adhesive after finding suitable area. Lastly, adult barnacle secretes cement to rigidly attach to the surface and continues secreting cement to maintain (Liang et al., 2019).



Figure 1.4 Cements left behind after removing barnacles from the surface (Personal archive, 2022)

Composition of barnacle cement differ between species but is a structure with very high protein content. Quantitative analysis shows that cement of *Balanus hameri* and *Balanus crenatus* contain around 85% protein, 5% inorganic residues, 1% carbohydrate and 1% lipid (Walker, 1972; Kamino et al., 1996). When the secondary structure of cement was examined, it was found that it mostly consists of β-sheets, but it also contains α-helix in small amounts (Barlow et al., 2009). The structures of 6 cement proteins have been identified and these proteins have been classified according to their functions. The two proteins with the high molecular weight are CP-100k and CP-52k. Both proteins are hydrophobic, and they contain very low amounts of Cys residues. The main components of cement are CP-100k and CP-52k, which together

constitute the insoluble framework that holds other CPs together and gives adhesive strength. (Urushida et al., 2007; Kamino, 2008; Kamino, 2016). CP-68k is a protein containing high residues of Ser, Thr, Gly, Ala, and Lys (Yuvaraj et al., 2021; Kamino, 2008). Although more research is needed for CP-68k's function, it is thought that it may be effective in interacting with foreign surfaces because it contains charged and hydrophobic amino acids. CP-20k is a simple polypeptide that mostly contains Asp, Glu, His and Cys on its primary structure. CP-20k does not form intermolecular bonds with the other CPs, because of that it might be a specific coupling agent between cements of different barnacles (Kamino, 2001). CP-19k is a simple polypeptide version of CP-68k. It consists of similar amino acids such as Ser, Thr, Gly, Ala, Lys, and Val. As a result of the studies, it has been found that surfaces such as gold, glass and polystyrene adsorb this protein. Considering that barnacles can adhere to a wide variety of surfaces underwater, it is thought that the CP-19k may be involved in the adhesion to foreign surfaces (Urushida et al., 2007). CP-16k is a minor CP and it has structural similarities with lysozyme enzyme. Since crude cement shows lytic activity, CP-16k may be responsible for protecting the cement from microorganisms (Kamino and Shizuri, 1998).

Underwater attachment of barnacles is a complex procedure (Mori et al., 2007). Barnacles have multiple proteins for different functions and each protein is responsible for one of the steps (Waite, 1987; Kamino, 2008). This process can be divided into stages such as removing weak boundary layers (displacement of water), spreading adhesive onto the surface, developing interfacial adhesion and curing. In the light of the studies carried out, Kamino (2016) designed a mechanism for underwater barnacle adhesion. In this mechanism, every protein has different target molecules such as foreign surface, cement molecules and water molecules. The first stage is the movement of water molecules bonded to the surface, followed by cement spreading and coupling. Two CPs are candidate for these functions which are CP-19k and CP-68. CP-20k can also be used in this process since it helps a barnacle to adhere on another barnacle. Following successful coupling, CPs must be produced to attach the barnacle base plate and the foreign surface. CP-100k and CP-52k are the ones that responsible forming that adhesive bulk and ensuring its integrity.

1.3.2 Hydroides elegans

A particularly aggressive aspect of the fouling organisms in tropical and subtropical waters is the serpulid polychaete *Hydroides elegans* (Unabia and Hadfield, 1999). *H. elegans* species live in the calcareous tubes that they secrete (Figure 1.5). These species are very troublesome because they colonize quickly on submerged surfaces, grow and reach maturity very fast, their larval period is very short, and their tubes can reach several centimeters in short time. *H. elegans* also uses cement to attach surfaces. Cement used by tubeworms, as in barnacles, contains a high percentage of protein. Tubeworm cement contains three proteins, and their molecular weights are lower than barnacle CPs. Two of those proteins are rich in Gly and contain high percentage of 3, 4-dihydroxy phenylalanine (DOPA) (Stewart et al., 2004). Unlike other two, third protein has high content of phosphorylated Ser. Tubeworm cement uses these DOPA and Pho-Ser for surface coupling to foreign surfaces (Stevens et al., 2007; Kamino, 2012).



Figure 1.5 A surface heavy covered with *Hydroides elegans* tubes (Personal archive, 2022)

1.3.3 Bugula neritina

Bugula neritina is a common fouling organism that also known as brown bryozoan. It is an invasive species in the tropical, subtropical, and coastal seas (Li et al., 2019). *B. neritina* is less aggressive than *H. elegans*, but it is also a troublesome species. Since it forms large and dense calcified colonies, it heavily covers any surface in seawater (Figure 1.6). Just like barnacles, *B. neritina* also uses larvae to explore seawater to find a surface to settle. After finding a surface larva metamorphose into a first unit of a colony (Sharp et al., 2007).



Figure 1.6 Settlement of *Bugula neritina* on a polyvinyl chloride (PVC) pipe (Personal archive, 2022)

1.3.4 Ulva lactuca

Ulva lactuca, belonging to the phylum Chlorophyta, is a macroalgae and is also known as sea lettuce (Figure 1.7) (Roleda and Heesch, 2021). It is a worldwide common species because it can exist in fresh water and even in very salty waters (Oliveira et al., 2019). Since *U. lactuca* is a species that can reproduce very quickly, it can increase its population outrageously. Because of its reproductive capabilities it can cause green tides and decrease the growth of other species (Tang and Gobler, 2011).



Figure 1.7 Metal plate fouled by *Ulva lactuca* and *Hydroides elegans* (Personal archive, 2022)

1.4 Antifouling Strategies and Antifouling Paints

Many different methods have been used over the years to deal with the biofouling problem. All these methods developed to prevent biofouling are called antifouling. In the times when humanity used wooden marine vessels, vax, tar, oil and hot pitch were used to prevent biofouling on the surfaces. Pitch was frequently utilized, particularly between the 13th and the 15th centuries, to prevent ships from fouling. Later, ship surfaces began to be sheathed with hide and wood with other animal sources. In the 16th century, lead sheathing began to be used. Later, it became the most used antifouling system of its time. Although the protection of wooden ships was very effective, lead sheathing could not be used on iron ships because of the corrosion. Copper sheets were used to cover up the wooden ships to protect them from fouling organisms. Copper was already used in some parts of the ships, but using copper as sheathing was new at the time. In 1780, copper was widely used for covering wooden ships. In order to produce much larger and more strong ships, iron ships were started to be built. But the issue with the copper sheathing, it was causing corrosion on iron ships same as lead. To solve this problem, copper was treated with different materials, but this time it was very costly. In line with the efforts carried out to solve this situation, antifouling paints started to be used. By the mid-1800s, many types of antifouling paints were produced using chemicals such as copper oxide and mercury oxide. At that

time, copper was used as an antifoulant in most of the paints. By the 1900s, hot plastics began to be used in antifouling paints. While hot plastics were used as paint, temperature applications were needed during the process. However, this situation was difficult when working around the ship, so cold plastics were developed. With the use of these paints, the time between dry-dock operations has been increased. After the Second World War, organotin compounds began to be used in antifouling paints. Since these compounds have very high antifouling performances, they have been a solution to the biofouling problem for a long time. Tributyltin (TBT)-based coatings were the most successful and widely used among them (Yebra et al., 2004; Chambers et al., 2006; Jones, 2009; Dafforn et al., 2011). Antifouling paints can be classified into 4 groups.

1.4.1 Insoluble Matrix Paints

In insoluble matrix paints, binder is not soluble because of that it does not polish in the seawater. Different kinds of polymers can be used as binder but mainly vinyl, epoxy, acrylic and rubber polymers are used. After immersion in seawater soluble pigments dissolve with the seawater but since matrix in insoluble they left a porous structure behind which will help seawater to penetrate further into the insoluble matrix (Figure 1.8). However, as time passes, it will be difficult for seawater to diffuse into the insoluble matrix, and with that the release of biocides slow down significantly, reducing the antifouling performance of the paint (Kiil et al., 2003; Yebra et al., 2004).

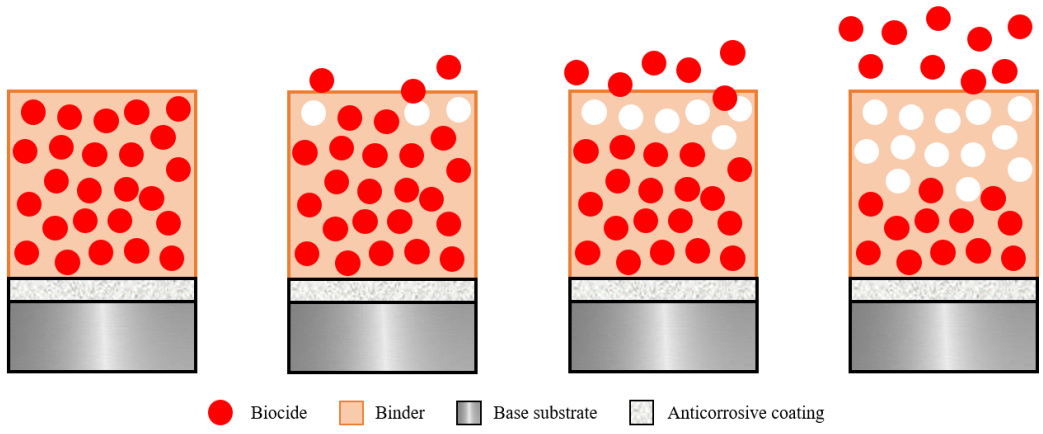


Figure 1.8 Diagram of insoluble matrix paints (Inspired from Dafforn et al., 2011)

1.4.2 Soluble Matrix Paints

When antifouling paints with soluble matrix immersed in the seawater, they start to dissolve. While matrix is dissolving, it also releases its contents like biocides and pigments (Figure 1.9) (Cahill et al., 2013). For this kind of paints high amounts of rosin and its derivatives (such as abietic acid) are used since rosin is a natural and highly soluble in seawater (Rascio et al., 1988). Main issue with soluble matrix paints is that they are affected by the movements of the seawater. Which means biocide release of these paints greatly increases with the vessel speed (Yebra et al., 2004). This leads to a reduction in the half-life of the paint. Likewise, when the marine vessel is not moving, the antifouling effectiveness of the AF paint will decrease, as the release of biocide will slow down.

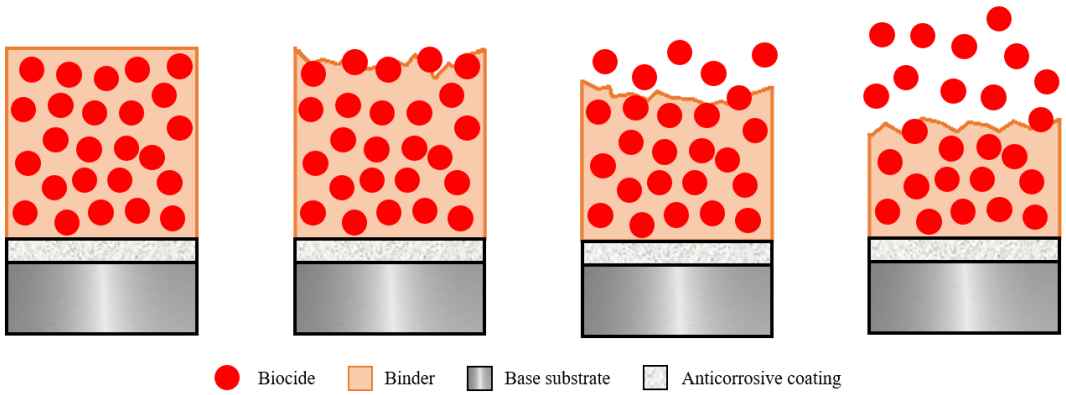


Figure 1.9 Diagram of soluble matrix paints (Inspired from Dafforn et al., 2011)

Rosin also known as colophony, is a brittle solid material that contains resin acids. Rosin can have many colors with shades of yellow and brown. It is used in many areas because it is cheap, abundant in nature and non-toxic. Pine trees are the primary source of rosin. Resin acids have the general molecular formula $C_{19}H_{29}COOH$ and their structures are given in Figure 1.10 (Silvestre and Gandini, 2008; Kugler et al., 2019).

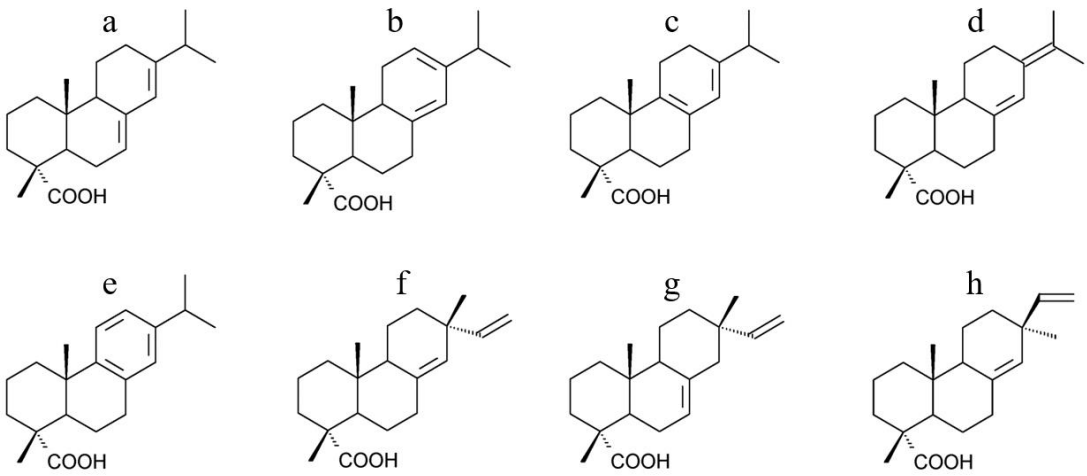


Figure 1.10 Chemical structures of resin acids (a) abietic acid, (b) levopimaric acid, (c) palustric acid, (d) neoabietic acid, (e) dehydroabietic acid, (f) sandaracopimaric acid, (g) isopimaric acid, (h) pimaric acid

1.4.3 Self-Polishing Co-Polymer Paints

The self-polishing co-polymer paints contain hydrolysable binder such as acrylic polymer or rosin (Kwon et al., 2020). After immersion in seawater, binder starts to hydrolyze and release its content layer by layer (Figure 1.11). With each hydrolyzed layer, fouling organisms that already attached to the top layer also cleaned off from the coating surface. Additionally, this is the most controlled biocide releasing way (Chambers et al., 2006). TBT self-polishing co-polymer coatings were one of most used and most effective type of antifouling paints but in 2003 usage of TBT in coating were banned by the International Maritime Organization (IMO) (Cao et al., 2011; Nwuzor et al., 2021). TBT was also affecting the non-target organisms, causing imposex which means development of male characteristics in female organisms (Hunsucker et al., 2019).

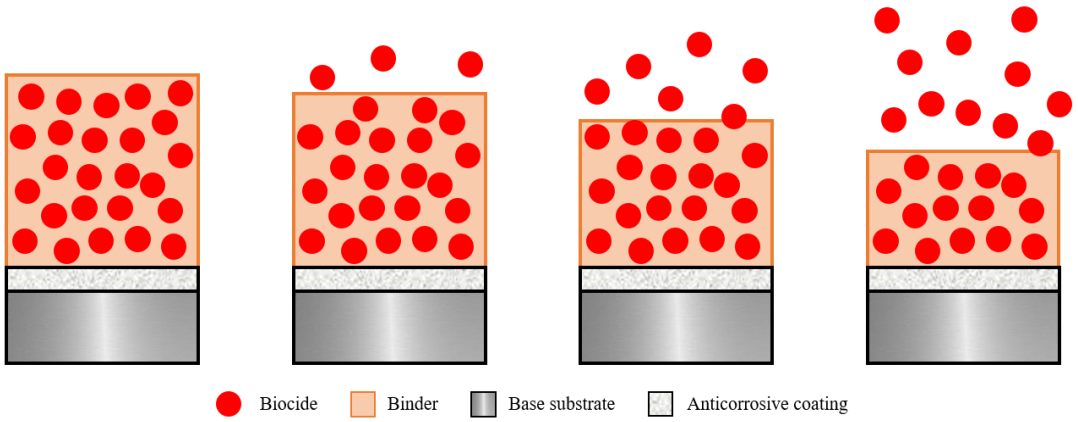


Figure 1.11 Diagram of self-polishing paints (Inspired from Dafforn et al., 2011)

TBT is a synthetically made organotin compound. TBT has three covalently bonded n-butyl groups to a tin (Sn^{4+}) atom and general formula for this compound is $(CH_3CH_2CH_2CH_2)_3Sn{-}X$ (Figure 1.12). The −X is either a halogen or a function group (Du et al., 2014). Properties of the −X slightly affects the toxicity and physicochemical properties of the compounds (Antizar-Ladislao, 2008).

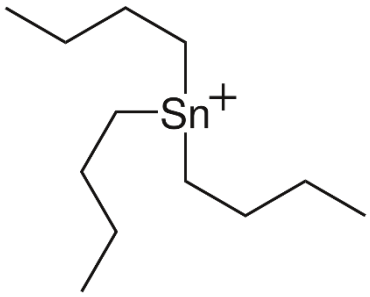


Figure 1.12 Cation form of tributyltin

1.4.4. Fouling Release Paints

Fouling release paints do not contain any toxic chemicals in their formulations. Their antifouling performance is based on their surface characteristic such as having low friction, low surface energy and a smooth surface (Hu et al., 2020). Reduced fouling organism adherence to the surface is the primary mechanism of fouling release

paints (Brady, 2005). This way, fouling organisms either fail to attach to the surface or do so extremely weakly (Nurioglu and Esteves, 2015). Since fouling organisms adhere weakly, they can be removed from the surface by movements of the seawater (Figure 1.13) (Lejars et al., 2012). After the ban of TBT, fouling release paints gained importance because of the advantages it provides. As mentioned, before fouling release coating are biocide free. Because of their smooth surface marine vessels can move at maximum speed, reducing fuel consumption and CO_2 emission. Since they are not soluble in seawater, they last longer than other paints and they are more durable (Yebra et al., 2004).

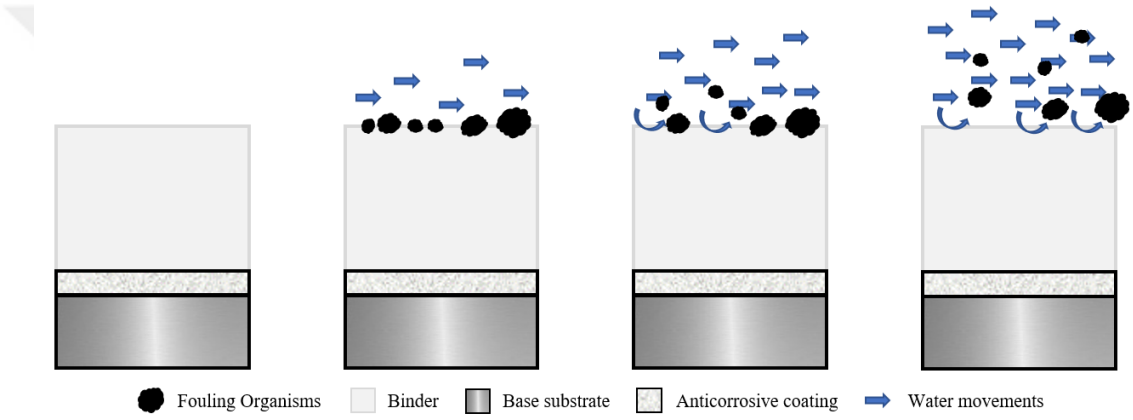


Figure 1.13 Diagram of fouling release paints (Inspired from Dafforn et al., 2011)

Performances of the fouling release coatings are affected by surface hydrophobicity, surface energy, surface roughness, elastic modulus, and thickness of the coating. Silicone elastomers are used as coating matrix since they provide these features. Typical polymer chains used in the antifouling coatings are poly(dimethyl)siloxane (PDMS) (Figure 1.14). PDMS elastomers have flexible backbones and low surface energy (Bressy and Lejars, 2014).

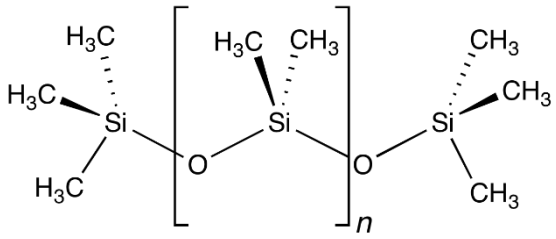


Figure 1.14 Structure of a poly(dimethyl)siloxane chain

1.5 Performance Testing of Antifouling Paints

Antifouling depends on fouling species, physicochemical conditions, and seasonal changes. Due to that, effectiveness of an antifouling paint can differ according to the region. To fix this problem, different performance analysis methods developed. Basically, there are 2 types of performance tests.

1.5.1 Laboratory Bioassays

Laboratory bioassays are used in the early stage of paint development. These tests are used when quick results are needed, or coating is not durable enough for the field test. 2 types of biofouling organisms are used in the laboratory bioassays. First one is microfouling organisms from the maritime environment, such as diatoms and bacteria. The other one is macro fouling organisms such as barnacle cyprids, bryozoans, mussel larvae and spores of algae (Briand, 2009).

Usage of multi-well plates, fluorescence staining of organisms, and automated procedures have helped develop new bioassays. In these studies, Effective Concentration (EC) and Lethal Dose (LD) values are found, and the results are evaluated according to those values (Briand, 2009).

In such studies, inhibition of bacterial growth is usually studied (Idora et al., 2015). However, since biofouling is direct related to adhesion of marine organisms to surfaces, the determination of antifouling performance through growth inhibition may not always be the right method. Utilizing this technique for antifouling performance is

more reliable since the adhesion of diatoms and bacteria to the surface is the initial step of biofouling (Banerjee et al., 2011). Attachment assays either can be inhibition of adhesion or toxicity against the microorganism. Adhesion studies of microorganisms are generally conducted using flow chambers (D'Souza et al., 2010). Since surface energy and chemistry directly affects the adhesion, those parameters are also studied (Briand, 2009).

Barnacles and mussels are mostly used in these studies, as they are dominant biofouling species that adhere to the ship surfaces (van Dam et al., 2016; He et al., 2023). Both species can be cultured easily, and their larval cycles are short (Briand, 2009). Other than that, bryozoan, polychaeta and seaweed are also used in the laboratory bioassays (Gabilondo et al., 2013; Martinelli et al., 2016; Feng et al., 2018).

Different kinds of macro fouling organisms are used in the laboratory settlement bioassays (Scardino et al., 2009). In most of the studies settlement of barnacle cyprids under static condition are investigated. But even different barnacle species adhere surfaces with the effects of different proteins and molecules (Dahlström et al., 2004). So, using only one organism is not a preferred method to evaluate antifouling performance. To prevent this, settlement assays are carried out in which barnacle, mussel, bryozoan, algae and polychaeta species are used (Briand, 2009).

The application of assays based on the measurement of adhesion strength differs between species. For green macroalgae (*Ulva* spp.), water-channel and water-jet apparatuses are used to simulate a ship that moves in the seawater. The measurement of the adhesion strength of green algal spores can be done accurately using any of these two approaches (Briand, 2009). A method created by Swain et al. (1992) is used to measure the barnacles' ability to adhere strongly to surfaces. In addition, this method is described in the ASTM D5618-94. In this method, strength of adhesion is measured by dividing removal strength to base area of the barnacle. External force is applied to the barnacles where their base plate meets the surface. Force is generally applied using a handheld dynamometer but there are also automated systems. Automated methods

are faster and more reliable, but they are expensive, and they cannot be used in the field (Swain et al., 1992).

Toxicity assays are often combined with settlement assays (Rittschof et al., 1992). These assays are usually performed to evaluate the antifouling effects of bioactive molecules. As with other tests, generally barnacle larvae are used in toxicity assays (Briand, 2009). LC and EC can be calculated by counting the swimming and dead barnacle larvae after exposure to the bioactive compound (Maréchal et al., 2004).

During exploration for the desired settlement area, spores and larvae of the biofouling organisms contact with the biofilms formed on the surfaces. Since biofilm formation is a biofouling step, it is crucial for an organism's ability to settle down. (Qian et al., 2007; Zardus et al., 2008). While searching for a surface to attach, most of the organisms choose an area that has fouling organisms or biofilm on the surface. This means that surface characteristics and physicochemical properties of that area is suitable for the settlement (Briand, 2009).

1.5.2 Fields Tests

To learn more about the antifouling paints' performance, field tests are required. These field tests are usually performed according to ASTM D3623-78a (2020). Field tests are used when the biological and physicochemical properties of seawater cannot be achieved in the laboratory assays (Henrikson and Pawlik, 1995). The density of biofouling changes with environmental conditions. For this reason, the control group and a commercial dye with proven activity should also be immersed in seawater to correctly evaluate the results of the field tests. The duration of the field test varies depending on the species and density of fouling organisms in the area where the plates are immersed. Generally, the plates are not left in seawater for more than a year.

1.5.3 Mechanical Performance Tests

Before antifouling paints are placed on the market, their mechanical properties should also be tested. Because the paints must be resistant to the harsh seawater conditions. Salinity, temperature, and dryness are some of the conditions that affect the lifetime of the antifouling paint. If the paint is not strong enough to resist above conditions, cracks and cuts will occur on the surface. Seawater may penetrate to the inner paint layers through those cracks and cuts which will decrease the performance. Therefore, mechanical tests are necessary for the antifouling paints. There are several mechanical tests categories as adhesion, impact, and mandrel bending tests. Adhesion tests are used to evaluate the adhesion strength between paints and substrate surface. To conduct these tests, surface is cut into lines and pressure tape is applied. Then tape is removed to find out weak points of the paints. Adhesion test can be conducted in 4 ways; X-cut, cross-cut (#-cut), knife test and pull-off test. Pull-off test is different than other three. Instead of cutting the surface, dolls are glued into surface and after drying, dolls are removed from the surface using hydraulic testers. In impacts test, metal ball is dropped from different heights to evaluate the damage it causes on the surface. Mandrel bending test is used to evaluate the resistance of paint matrix to cracking and shattering. For this test, coated surface is placed and bended around the mandrel (Yebra and Weinell, 2009).

1.6 Bioinformatics

Bioinformatics is an interdisciplinary field that combines chemistry, biology, mathematics, statistics, and computer science. With the recent developments, huge amounts of biological data are being generated and understanding and storing this complex data has become a major problem (Zhang et al., 2013). Bioinformatics, which emerged for use in biological studies at first, has become a complex field that spreads to much more scientific fields. And it continues its development by dividing into specialized branches such as molecular docking, molecular modelling, and genome sequencing (Fenstermacher, 2005; Diniz and Canduri, 2017).

1.6.1 The Molecular Docking

A sort of computer modeling called molecular docking makes it simpler to predict the preferred binding orientation of one molecule to another (Raval and Ganatra, 2022). It is possible to forecast the energy profiling of complexes, such as the binding free energy, using the preferred molecular positions of coupled molecules. These days, in order to determine the characteristics of a drug candidate's binding to its biomolecular targets, molecular docking is routinely used (Fan et al., 2019). The primary objective of molecular docking is to obtain the best possible docked positions for both the ligand and the receptor to lower the binding free energy (ΔG_{bind}). The search for potential targets and ligands using structural data banks are necessary for the molecular docking studies. There are numerous tools and methodologies to achieve this. These tools rank possible ligands based on their interactions with the target candidates (Agarwal and Mehrotra, 2016).

1.6.2 CB-Docking

Protein and ligand binding affinities are predicted via molecular docking. Today, there are many docking tools that can be used in the academic studies. Finding ligand binding sites in proteins is essential for most docking tools. However, these regions are often unknown, so docking studies are based on the entire protein. This type of docking is called blind docking. Because it is based on the entire protein, blind docking is less accurate than conventional docking. To eliminate this problem, many tools have been developed for binding site detection. These tools show the regions on the protein where the ligand can bind. CB-dock is also a tool that finds the cavities on the protein and performs the docking. Vina scores are used by CB-dock to rank the binding sites it discovers. It also generates a 3D binding site image that can be interacted with (Liu et al., 2020).

1.6.3 Scoring Functions

Scoring functions are computational methods that try to find the best binding position between ligand and protein. Force-field-based, knowledge-based, and empirical scoring functions are the three types of scoring functions (Ragoza et al., 2017). In force-field-based scoring, van der Waals and electrostatic interactions among the molecules are calculated (Huang and Zou, 2010). Knowledge-based scoring function is based on finding binding free energy based on atom pairs between protein and ligand (Gohlke et al., 2000). Empirical scoring utilizes the other two scoring functions to determine the overall binding free energy (Korb et al., 2009).

With the CB-Dock, another scoring function was proposed, which is Cyscore. This scoring function is based on the energy of hydrogen bonds, van der Waals interactions, and hydrophobic free energy. But since this interaction between ligand and protein is the most crucial, it is mainly focused on hydrophobic free energy. In traditional docking techniques, hydrophobic free energy is considered as surface tension and the molecular shape of the protein is ignored. However, such methods cause hydrophobic free energy to be measured incorrectly. Cyscore, on the other hand, enables a more accurate measurement of hydrophobic free energy by including the molecular shape of the protein (Cao and Li, 2014).

1.6.4 Homology Modelling (SWISS-MODEL)

Since proteins are very important for the cellular processes, finding the 3D structure of proteins is at great importance. Finding the 3D structures of proteins is also important in elucidating how they interact with other molecules. In line with the studies, a lot of information about proteins is obtained and databases are used to store this excessive data. However, determining the structures of these proteins is slow due to the time-consuming experimental processes. Nowadays, computational methods are used to eliminate this deficiency (Hillisch et al., 2004; Waterhouse et al., 2018).

The primary structure of the protein is a straight chain made of amino acids joined together with peptide bonds. Homology modelling is a method that used to construct a model protein structure by using known protein structures and sequences that have similarities. A popular server for protein homology modeling is SWISS-MODEL. Working principle of SWISS-MODEL is quite easy. First amino acid sequence of the target protein is provided. Then, this sequence is searched in the template library to find accurate templates. After that, it offers top-ranked templates for the analyst to choose. After choosing the desired template, it generates the 3D structure for the target protein. In this way, fast and highly accurate protein modeling is performed (Waterhouse et al., 2018; Studer et al., 2021).

1.6.5 ProtParam

ProtParam is used to find out the physicochemical properties of a protein by using its sequence. ProtParam uses either accession number or amino acid sequence of the protein (Gasteiger et al., 2005). Parameters calculated by ProtParam are given below.

- Molecular weight,
- Theoretical pI,
- Amino acid composition,
- Atomic composition,
- Extinction coefficient,
- *In-vivo* half-life,
- Instability index,
- Aliphatic index,
- Grand average of hydropathicity.

1.6.6 Multiple Sequence Alignment (Clustal Omega)

Multiple sequence alignment is very important to find out the similarities among different protein groups and those similarities can be used to predict the function of an unknown protein. There are several sequence alignment analysis methods but some of

them have drawbacks. Some of the methods analysis bigger data but with a low quality of results. Others give high quality analysis, but their data size is lower. The existence of such obstacles in the multiple sequence alignment technology, which is widely used today, causes problems. For this reason, a new analysis method called Clustal Omega has been discovered recently. Clustal Omega aligns sequences of almost any size quickly and accurately. Also, Clustal Omega performs better with the increasing numbers of sequences (Lassmann and Sonnhammer, 2005; Sievers et al., 2011).

1.7 The Aims of The Thesis

The aim of this thesis is to prepare biocide-free self-polishing paints and evaluate the antifouling performances of the prepared coatings using both field tests and laboratory assays.

The objectives of the thesis to investigate:

- The antifouling performances of different biocide-free self-polishing coating formulations with field test.
- The adhesion mechanisms of biofouling organisms.
- The adhesion strength tests using *A. amphitrite* as a model organism.
- The pseudobarnacle adhesion strengths tests to mimic living organisms.
- The comparison of field tests, laboratory tests and *in silico* analysis results.

CHAPTER TWO
MATERIALS AND METHODS

2.1 Materials

In order to prepare coatings, technical grade rosin, zinc rosinate, xylene, $CaCO_3$, ZnO and $BaSO_4$ (Tekkim) were used. The polyvinyl butyral (PVB) used in the coatings was provided by Shark Solutions. Metal plates ($10x10cm^2$) were provided by Dokuz Eylül University Technical Workshops. The diameters of the barnacles were measured by using a Vernier caliper (Leo, 0-150x0.05 mm). To measure the removal strength of the barnacles, an analog dynamometer (Loyka NK-200) was used.

2.2 Preparation of the Glass Slides, Plastic Plates and Metal Surfaces

Different amounts of glass slides, plastic and metal plates were used throughout the studies. Each of these materials were subjected to different processes before being coated with self-polishing coatings.

- Glass slides (76 mm x 26 mm x 1 mm) used in the adsorption experiments were pre-cleaned with methanol and deionized water before coating.
- Small plates of $4x2\ cm^2$ were cut from a plastic sheet. The surfaces of these plates were lightly sanded to better hold the paint. Finally, they were cleaned with methanol and deionized water and made suitable for use.
- For the field test, series of $10x10\ cm^2$ metal plates were prepared. Holes with a diameter of 5 mm were drilled in the middle of one side of all plates. Afterwards, the plates were sanded, and their surfaces were cleaned with methanol. After these processes, plates were completely painted with anticorrosive primer to prevent from rusting in seawater.

2.3 Preparation and Application of Biocide-Free Self-Polishing Coatings

To prepare rosin and zinc rosinate-based coatings, rosin, or zinc rosinate (ZnR) was dissolved in xylene at 60 ºC and at 200 rpm using magnetic stirrer (Figure 2.1). After obtaining a homogenous texture, supportive materials like $CaCO_3$, ZnO and $BaSO_4$ were added to the mixture. Final mixture was stirred until homogenous and desired texture obtained. PVB-based coatings with different percentages were also used in the field tests. There were total of 23 different formulations that evaluated with the field tests and their contents are given in the Table 2.1.



Figure 2.1 Preparation of rosin-based coatings (Personal archive, 2022)

Table 2.1 Prepared coating and their contents

Coating	Materials (w/w %)							
	Rosin	**Xylene**	**Zinc rosinate**	**PVB**	**Deionized Water**	**$CaCO_3$**	**ZnO**	**$BaSO_4$**
1	25	75	-	-	-	-	-	-
2	50	50	-	-	-	-	-	-
3	75	25	-	-	-	-	-	-
4	-	75	25	-	-	-	-	-
5	-	50	50	-	-	-	-	-
6	-	25	75	-	-	-	-	-
7	-	-	-	36	64	-	-	-
8	-	-	-	18	72	-	-	-
9	-	-	-	9	81	-	-	-
10	40	40	-	-	-	20	-	-
11	40	40	-	-	-	-	20	-
12	40	40	-	-	-	-	-	20
13	40	40	-	-	-	10	10	-
14	40	40	-	-	-	10	-	10
15	40	40	-	-	-	-	10	10
16	-	40	40	-	-	20	-	-
17	-	40	40	-	-	-	20	-
18	-	40	40	-	-	-	-	20
19	-	40	40	-	-	10	10	-
20	-	40	40	-	-	10	-	10
21	-	40	40	-	-	-	10	10
22	35	35	-	-	-	10	10	10
23	-	35	35	-	-	10	10	10

Prepared paint formulations were poured onto glass and plastic surfaces with a pipette and spread evenly on the surfaces. Paint formulations prepared for metal plates were applied evenly on the surfaces with the help of a paint brush. All rosin-based coatings were left to dry for 1 week (Figure 2.2). For the field tests, after all the coatings on the metal plates were dried, they were fixed to PVC pipes to be hung in the seawater.

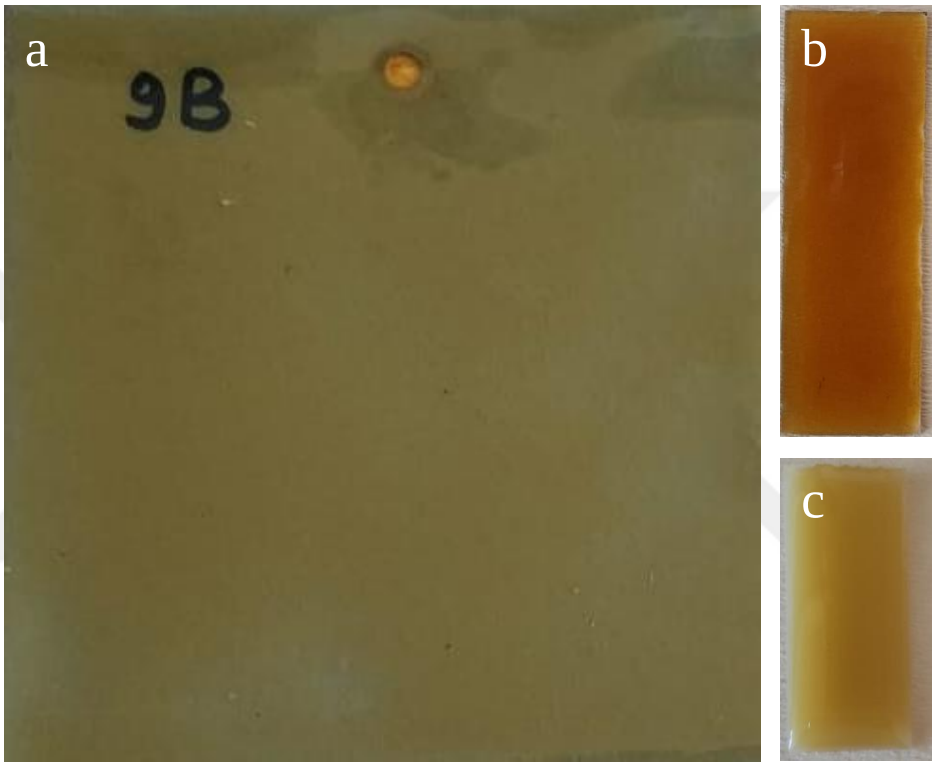


Figure 2.2 The sample coatings on a) metal, b) glass, c) plastic surfaces (Personal archive, 2022)

2.4 BSA Adsorption Experiments on Coated Glass Slides

Bradford Micro-Assay method was used to determine the total protein amount. For this, Bradford Reagent was prepared, and a calibration graph was obtained by using bovine serum albumin (BSA) standard solutions diluted at different ratios. In BSA adsorption experiments, the methodology used by Zhou et al. (2021) was followed.

2.4.1 Preparation of Bradford Reagent

To prepare Bradford Reagent, 50 mg Coomassie Brilliant Blue G250 is dissolved in 25 mL 95% ethanol and 50 mL 85% (w/v) o-phosphoric acid is slowly added to the mixture. Final volume is made up to 100 mL with deionized water. After mixing the solution, it is filtered and stored at 4 °C in the dark (Bradford, 1976).

2.4.2 Protein Determination

In the determination of protein, 50 µL of Bradford reagent and 200 µL of BSA standard solution or sample were added in the microplate well. As blank solution, 200 µL of phosphate-buffered saline (PBS) is used instead of 200 µL of sample. After that equal amounts of pipetting are applied to all of the samples. Then, samples were incubated for 3-5 minutes at room temperature. After incubation, absorbances at 590 nm (A_{590}) were measured using microplate reader. Each sample was measured in triplicate and the average A_{590} values were used in the calculations.

2.4.3 BSA Adsorption on Petri Dishes

After slides were coated with 50% ZnR and completely dried, they were washed with deionized water and PBS before starting the experiment. Washed slides were placed in petri dishes and immersed in 30 mL of 0.1 mg/mL BSA solution for 4 hours at 25 ℃ (Figure 2.3). After 4 hours, slides were rinsed 3 times with PBS solution. Samples were taken from both the petri dishes in which the slides were kept, and the solution obtained as a result of washing. The amount of protein in the samples was determined using above methodology.

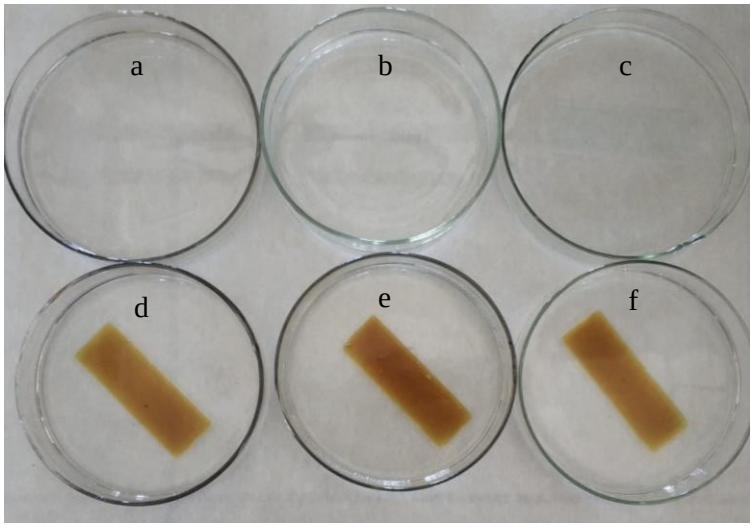


Figure 2.3 Petri dishes containing (a, b, c) uncoated slides; (d, e, f) ZnR-coated slides immersed in 0.1 mg/mL, 30 mL BSA solution (Personal archive, 2022)

2.5 BSA Adsorption on Plastic Plates

Plastic plates coated with 50% ZnR were used to determine the optimum parameters for the BSA adsorption. To determine optimum parameters, linear working range, temperature, agitating speed, zinc rosinate ratio in the coating, time and pH parameters were studied. Coated plastic plates were kept in BSA for 4 hours and samples were taken every hour to measure their absorbance at 590 nm using Bradford assay.

2.5.1 Linear Working Range

Different BSA concentration ranges were used to obtain acceptable standard calibration graph. In addition, the concentration of BSA in which the samples would be kept was determined by using the obtained standard calibration graph.

2.5.2 Temperature and Agitating Speed

To imitate the parameters in the marine environment, the samples were kept at 20-40 °C, in both static and dynamic conditions (100 rpm). All other parameters except temperature and agitating speed were kept constant.

2.5.3 Different ZnR Concentrations

In this study, coatings containing different ratios of ZnR were prepared. All values except the ZnR ratios were kept constant. Coated plastic plates were incubated statically at room temperature.

2.5.4 Different pH Values

Since the BSA stock was prepared with PBS solution under the standard conditions the pH of the medium was around 7.4. However, since it is known that pH has a serious effect on proteins, same experiment was performed under acidic and basic conditions. In this experiment, 40 mL 0.05 mg/mL BSA with pH=3.5, 7.4, 9 were prepared. Samples were measured for 4 hours at room temperature without shaking.

2.6 Field Tests

The metal plates coated with different coatings were immersed in seawater at a depth of 50 cm in İnciraltı coast between July and September (38°24'48.7"N, 27°02'03.9"E, İzmir, Türkiye) (Figure 2.4). After 10 weeks, the plates were removed from seawater and brought to laboratory to conduct the laboratory tests.



Figure 2.4 Some of the plates in the area where the field trial was carried out (Personal archive, 2022)

2.7 Biofouling Scoring

To evaluate field test results, scoring system is used. For this scoring system, a system previously available in the literature was used (Arimura et al., 2004; Mert et al., 2014). The scoring system is as follows:

Level I. There are no fouling organisms on the surface.
Level II. There is thin microfilm layer formation on the surface.
Level III. There is thick microfilm layer and macro foulant spores on the surface.
Level IV. There are soft and hard foulers on the surface (<50% overall coverage).
Level V. The surface is heavily fouled (>50% overall coverage).

2.8 Protein Determination on Plates (Field Experiment)

After immersing in seawater for 10 weeks, coating with the most biofouling and with the commercial paint were chosen for the protein determination experiment (Figure 2.5).



Figure 2.5 The coatings used for protein determination (Personal archive, 2022)

Then the plates were removed from seawater, they were washed with 5 mL of deionized water 3 times. Then, biofouling on the first plate was scraped carefully and the remaining plate was washed with 5 mL of deionized water 3 times. After collecting

all the samples, they were brought to the laboratory. The samples were centrifuged at 800 rpm for 20 minutes and Bradford Micro-Assay was used to determine total protein concentrations in supernatants.

2.9 Barnacle Adhesion Tests

According to ASTM D5618-94 (2017), the test should be carried out on barnacles with a diameter of 5-20 mm, approximately 20 mm from the edges of the plates and not in contact with other barnacles. Because of that, after bringing panels into laboratory, their surfaces must be cleaned from other biofouling organisms such as *U. lactuca* and *H. elegans*. *H. elegans* tubes were carefully scraped from the surface to perform the test properly. After cleaning and isolating barnacles, their diameters were measured using a caliper. Since barnacles are not in a perfect circular shape, 4 diameters were measured in 4 different positions (0°, 45°, 90°, 135°). Then, average base diameters (d_a) of the barnacles were calculated. After obtaining average base diameters, base area for the barnacles can be calculated using below formulation:

$$\text{Base Area (A)} = \frac{1}{4}\,\pi\,{d_a}^2$$

For measuring the removal strengths of barnacles, an analog dynamometer (Loyka NK 200) was used (Figure 2.6). 8 mm rod and a suitable probe were attached to the dynamometer before the tests.



Figure 2.6 Analog dynamometer used in the adhesion tests (Personal archive, 2022)

For the shear force measurements, plates and the dynamometer were placed parallelly, and the force was applied to the barnacles until they were removed from the surface. While performing the tests, care was taken not to disturb the integrity of the barnacles. The barnacles that are crushed during the test were not included in the results. When taking note of the results, the results in which the barnacles were completely detached from the surface were considered.

For the calculation of the strength of adhesion, measured removal strength of barnacle (Newtons, F) is divided by the base area of the barnacle (millimeter square, A):

$$\text{Strength of Adhesion (MPa)} = \frac{\text{Removal Strength (N)}}{\text{Base Area (mm}^2\text{)}}$$

2.10 Pseudobarnacle Adhesion Tests

The same procedure was followed in the pseudobarnacle adhesion test. Instead of using live barnacles, wooden pseudobarnacles with known diameters were adhered to the surfaces with epoxy (Pattex Power Epoxy). These pseudobarnacles can usually be aluminum studs, or they can be made of wood. The same rules and calculations for the barnacle adhesion tests were also applied to this test. One of the important points to be considered is the excess epoxy should be cleaned after the pseudobarnacles are adhered to the surfaces. In the literature, aluminum studs with fixed-known diameters (mostly 7 or 10 mm) are used as pseudobarnacles (Ekin et al., 2007; Sommer et al., 2011; Hu et al., 2021; Pawar et al., 2022). However, barnacles grow by adding calcium carbonate to their shell plates which is called calcification (Burden et al., 2014). Thus, they are found in different sizes in seawater. It was also found that the barnacle adhesion strength was affected by the size and age of the barnacles (Swain et al., 1992). Therefore, pseudobarnacles of different sizes were used to ensure accurate comparison with live barnacles in the present study. Pseudobarnacle tests were repeated 3 times for each coating and stud diameter. The view of the pseudobarnacles is shown in Figure 2.7.

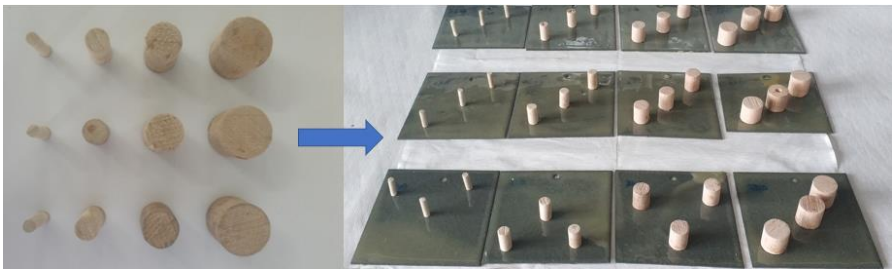


Figure 2.7 Wooden pseudobarnacles that used in the adhesion tests (Personal archive, 2022)

2.11 Statistical Test

Student's T test and correlation test in Excel (Microsoft Office) were used to analyze data. Statistical significance was set at 0.05.

2.12 Molecular Docking

The primer sequences of the *Megabalanus rosa* CP-20k and *A. amphitrite* CP-20k-1, CP-20k-2, CP-20k-3 were obtained from UniProt (Accession numbers are Q9GRC4, K7X3K6, K7XZK5, K7X9M0, respectively) (The UniProt Consortium, 2023). 3D structure of *M. rosa* CP-20k was available on RCSB Protein Data Bank (Berman et al., 2000), but CP-20k structures of *A. amphitrite* were absent on RCSB. For that reason, SWISS-MODEL was used to obtain 3D structures of *A. amphitrite* CP-20k fragments (Waterhouse et al., 2018). 3D structure of abietic acid (PubChem CID: 10569) was retrieved from PubChem (Kim et al., 2023). Molecular docking studies were carried out using CB-Dock2 (Liu et al., 2022). Physical and chemical parameters of the barnacle CPs were retrieved using ProtParam (Gasteiger et al., 2005). The content of CPs differs from species to species. Even in different types of organisms that are members of the same species, differences are observed. For this reason, Clustal Omega was used to align the sequences of the 4 proteins (Sievers et al., 2011).

CHAPTER THREE
RESULTS

3.1 BSA Adsorption Experiments on Coated Glass Slides

Before starting the adsorption experiments, a standard calibration graph was obtained in the range of 5-50 μg/mL BSA concentration to determine the total protein amount (Figure 3.1).

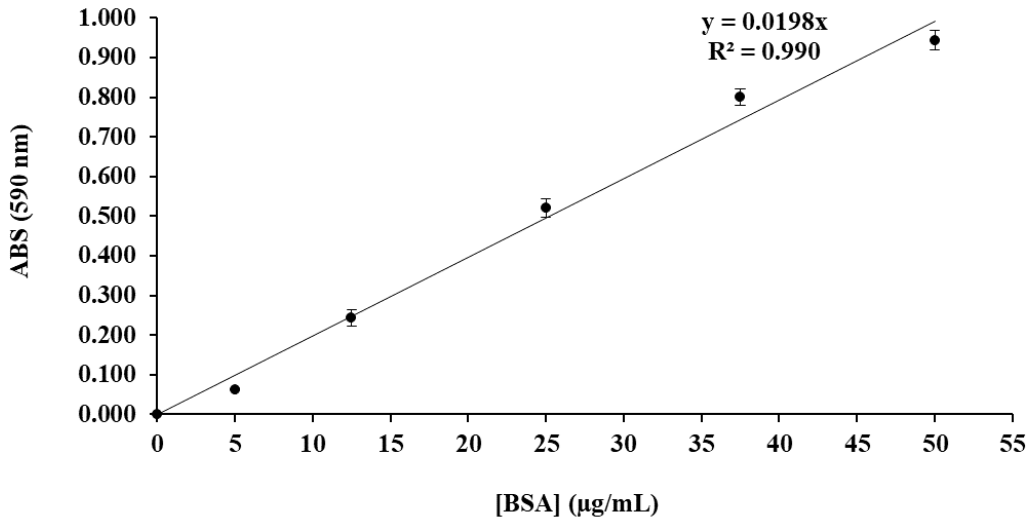


Figure 3.1 Standard calibration graph of BSA

After measuring absorbances at 590 nm, BSA concentrations were found by using the standard calibration graph (Figure 3.1). The results were given in Figure 3.2. According to the result BSA adsorbs to petri dish, uncoated slide, and ZnR-coated slide. As can be seen from Figure 3.2, blank solution (petri dish without coating) has the highest BSA amount. Uncoated and ZnR-coated slides have lower BSA amount because BSA adsorbs on to those surfaces. After the surfaces were washed with deionized water, no BSA was found in the washing solution. Removing glass slides from the petri dishes also lowered the BSA amount.

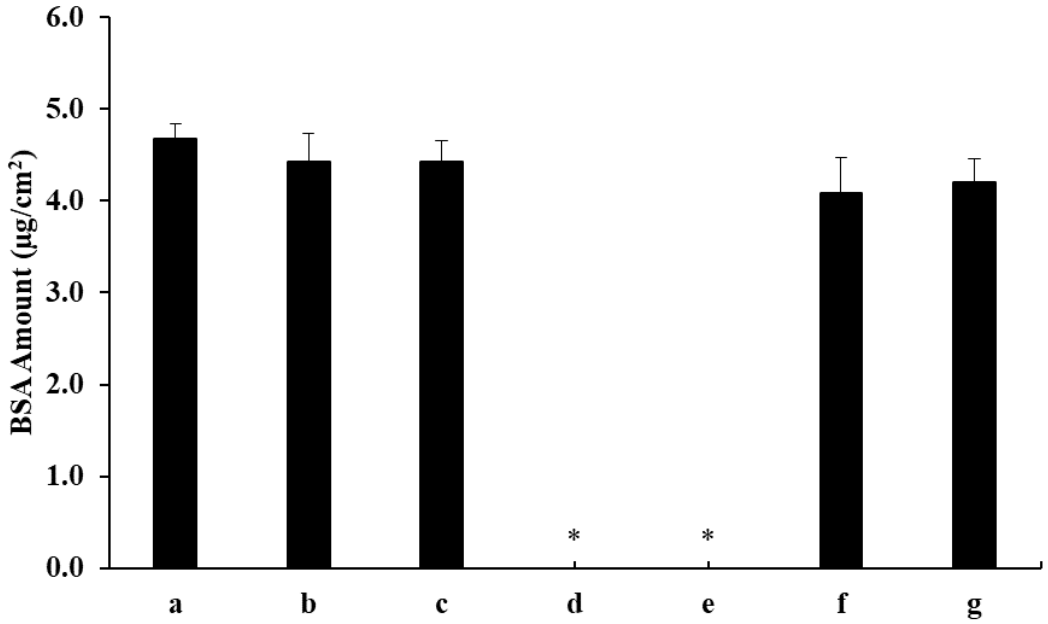


Figure 3.2 Amount of BSA on (a) petri dish; (b) petri dish with uncoated slide; (c) petri dish with ZnR-coated slide; (d) post-wash solution of uncoated slide; (e) post-wash solution of ZnR-coated slide; (f) petri dish after uncoated slide removal; (g) petri dish after ZnR-coated slide removal after 4 hours. The asterisk indicates statistical difference ($p<0.05$) when compared to "amount of BSA on (a) petri dish"

3.2 BSA Adsorption on Plastic Plates

3.2.1 Linear Working Range

Standard calibration graphs of different concentrations were drawn to determine the BSA concentration to be added to the samples. Initially, the range of 0.02-0.15 mg/mL was studied but obtained absorbance values could not be determined in this range. For this reason, the working range was changed to 5-50 µg/mL BSA.

3.2.2 Temperature and Agitating Speed

Figure 3.3 shows the effect of temperature and stirring speed on BSA adsorption. This test was carried out with 2 different stirring speeds (0-100 rpm) and 2 different temperatures (20-40 °C). As can be seen from Figure 3.3, increase in temperature

affects BSA adsorption negatively, but it has been observed that the agitating speed increases BSA adsorption.

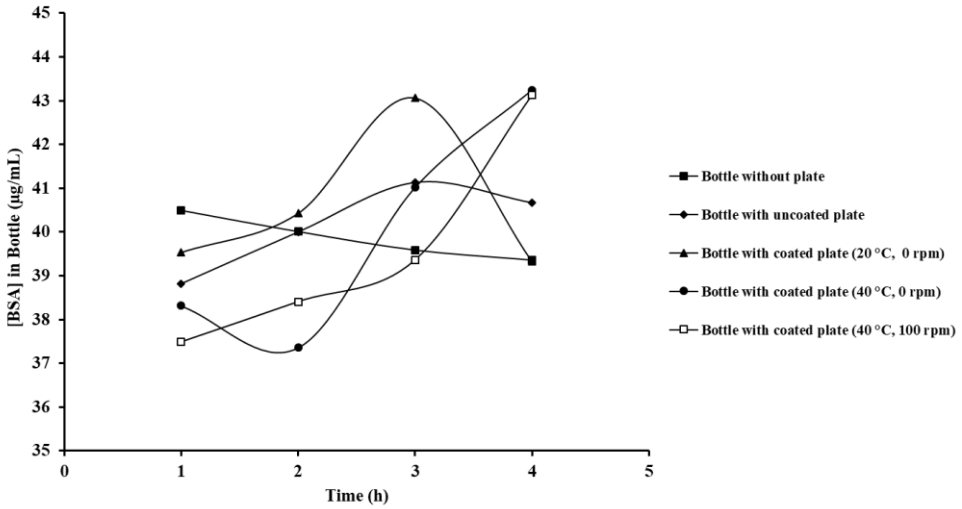


Figure 3.3 Change of BSA adsorption with different temperature and agitating speeds

3.2.3 Different ZnR Concentrations

In this experiment, the variation of BSA adsorption with increasing amount of zinc rosinate was studied. Paint formulations were prepared to contain 25% and 50% ZnR. In accordance with the measurements taken under static conditions, Figure 3.4 was obtained. When the Figure 3.4 was examined, it was found that the amount of ZnR had no effect on BSA adsorption.

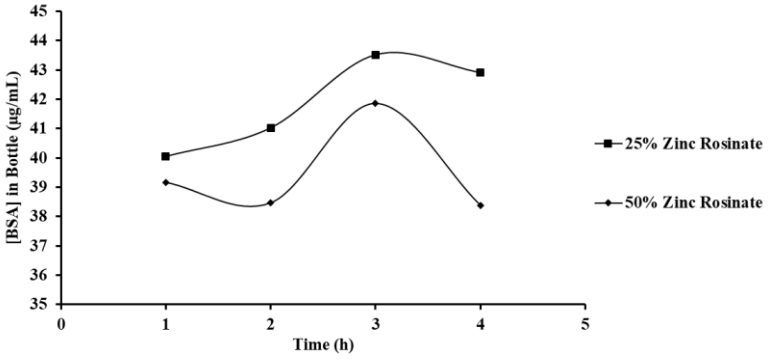


Figure 3.4 Change of BSA adsorption with different ZnR ratios

3.2.4 Different pH Values

With this experiment, the effect of pH on BSA adsorption was investigated. Because of that, BSA solutions with pH 3.5, 7.5 and 9.5 were prepared. Figure 3.5 was obtained with the measurements made for 4 hours. As can be seen from the Figure 3.5, as the pH decreases, the amount of BSA adsorbed to the surfaces increases.

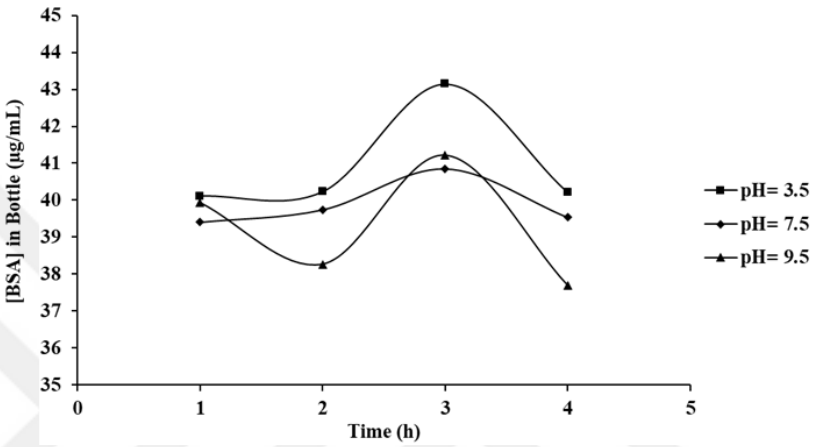


Figure 3.5 Change of BSA adsorption with different pH values

3.3 Results of Field Test and Biofouling Scores

The field test was conducted to examine the performances of rosin-based self-polishing antifouling paints. For this, coated plates were immersed in seawater for 10 weeks in İnciraltı/İzmir. The photographs of these plates were taken periodically to observe the biofouling process on them. The photographs of the plates taken over 10 weeks are shown in Figures 3.6 to 3.31.

As can be seen from Figures 3.6 and 3.7, the surfaces of the uncoated and anticorrosive primer coated plates were completely covered with biofouling organisms. After week 2, biofouling process was started on both surfaces. After 10 weeks, surfaces reached Level V of biofouling. Figures 3.8-3.10 show biofouling processes on the coating 1-3, respectively. The coating 1 and 2 started to cover with microfilm layer and accumulated by biofouling organisms over 10 weeks. But

biofouling process on the coating 3 started between 1-3 weeks. After 6-7 weeks, all 3 plates reached Level V biofouling score. In Figures 3.11-3.13 all 3 coatings had microfilm layer after 3 weeks and after 6 weeks macrofouling organisms adhered to all 3 surfaces. Performance of the coating 4 was evaluated as Level V, while the coating 5 and 6 were evaluated as Level IV. Antifouling effectiveness of the commercial paint was given in Figure 3.14. After 6 weeks both surfaces had minor microfilm layer formation. Antifouling performance of commercial paint was evaluated as Level III. The Figures 3.15-3.17 contain field test results of the PVB coatings. After immersed in seawater for 2 weeks, fouling organisms started to accumulate on the coating surfaces. Then heavily fouled by organisms after 7-10 weeks, because of this, the performances were evaluated as Level V. The Figures 3.18-3.20 show biofouling on the coatings 10-12. After 2 weeks, surfaces had no fouling organisms but started to fade because of self-polishing. 4 weeks later biofouling organisms started accumulating on the surfaces, then reached scoring of Level V. As can be seen from Figures 3.21-3.23 the coatings 13-15 showed similar results. This is because of these coatings have same similar formulations except supporting materials. On week 2, surfaces had no biofouling and reached Level V of biofouling after 10 weeks. In Figures 3.24-3.26, the coatings 16-18 showed microfilm layer after 2 weeks. After 4 weeks microfilm layer got denser and macrofouling organisms started to accumulate on the surfaces. Performances of all 3 coatings were evaluated as Level V after 10 weeks. The coatings in Figures 3.27-3.29 also showed similar results with the previous triplets. Microfilm layer started after 2 weeks and macrofouling started around 4 weeks. Macrofouling processes after 10 weeks were evaluated as Level V. In Figures 3.30 and 3.31 micro and macrofouling started around week 4. Performance of the coating 22 was evaluated as Level V. The coating 23 only had several macrofouling organisms on the coating surface. Because of that it was evaluated as Level IV. All the scorings were given in Table 3.1.

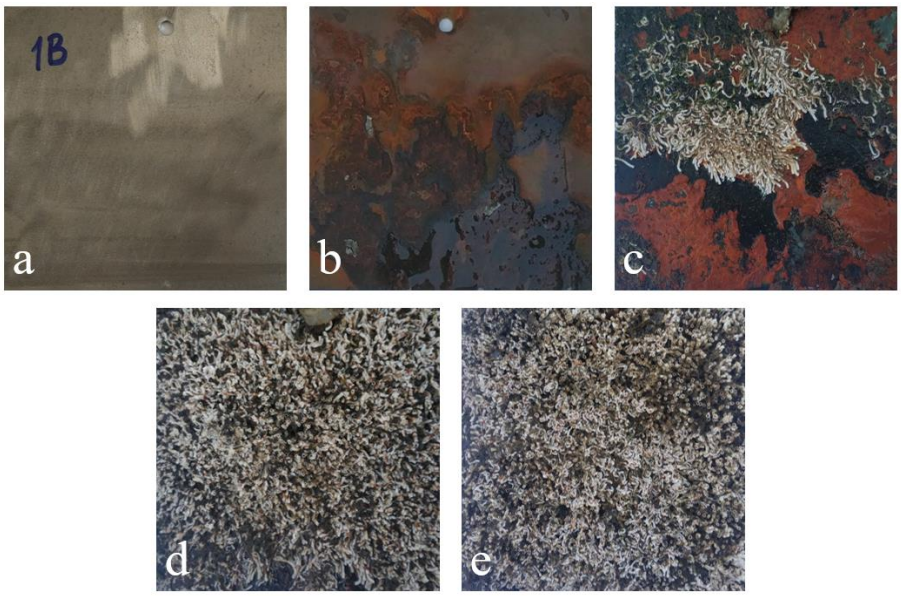


Figure 3.6 The field test results of uncoated plate (a) before immersion, (b) after 2 weeks, (c) after 4 weeks, (d) after 7 weeks, (e) after 10 weeks (Personal archive, 2022)

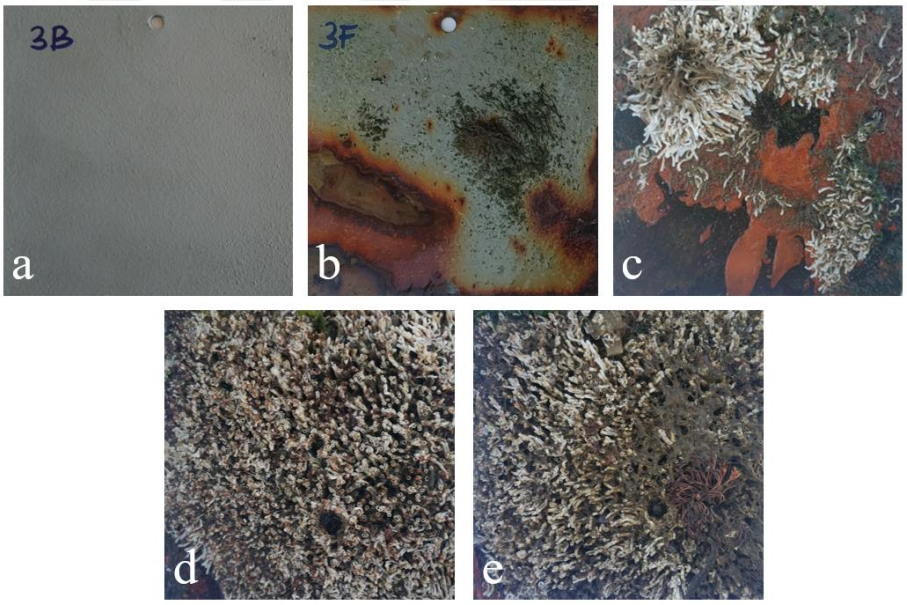


Figure 3.7 The field test results of anti-corrosive primer coated plate (a) before immersion, (b) after 2 weeks, (c) after 4 weeks, (d) after 7 weeks, (e) after 10 weeks (Personal archive, 2022)

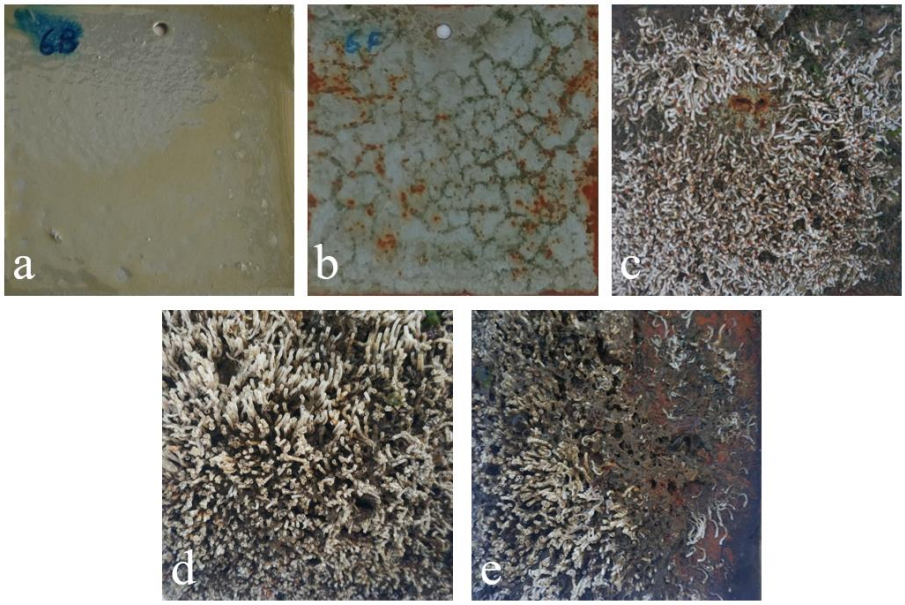


Figure 3.8 The field test results of Coating-1 (a) before immersion, (b) after 2 weeks, (c) after 4 weeks, (d) after 7 weeks, (e) after 10 weeks (Personal archive, 2022)

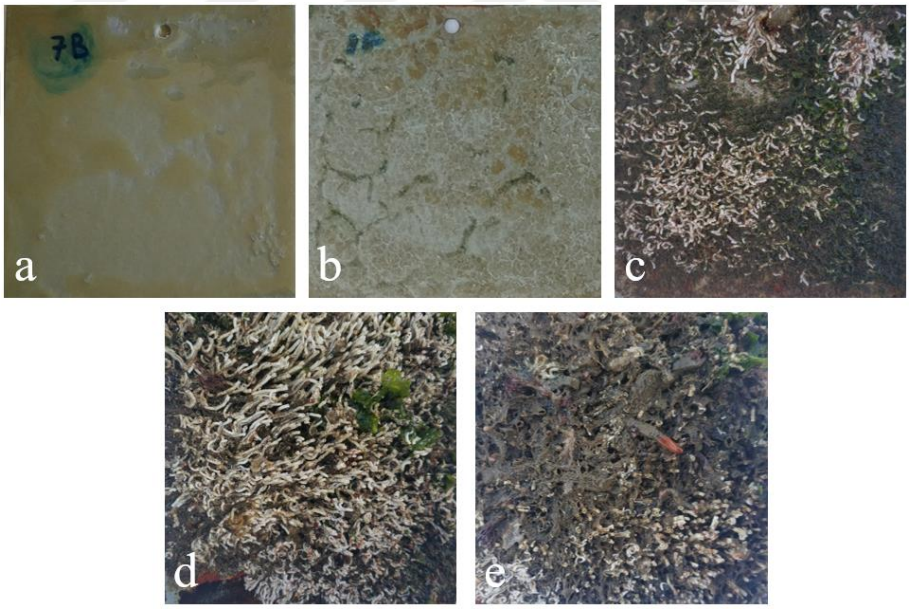


Figure 3.9 The field test results of Coating-2 (a) before immersion, (b) after 2 weeks, (c) after 4 weeks, (d) after 7 weeks, (e) after 10 weeks (Personal archive, 2022)



Figure 3.10 The field test results of Coating-3 (a) before immersion, (b) after 3 weeks, (c) after 6 weeks (Personal archive, 2022)

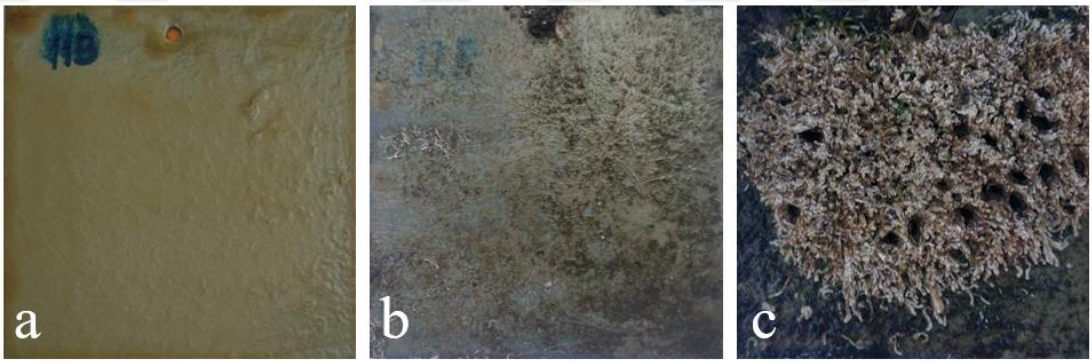


Figure 3.11 The field test results of Coating-4 (a) before immersion, (b) after 3 weeks, (c) after 6 weeks (Personal archive, 2022)

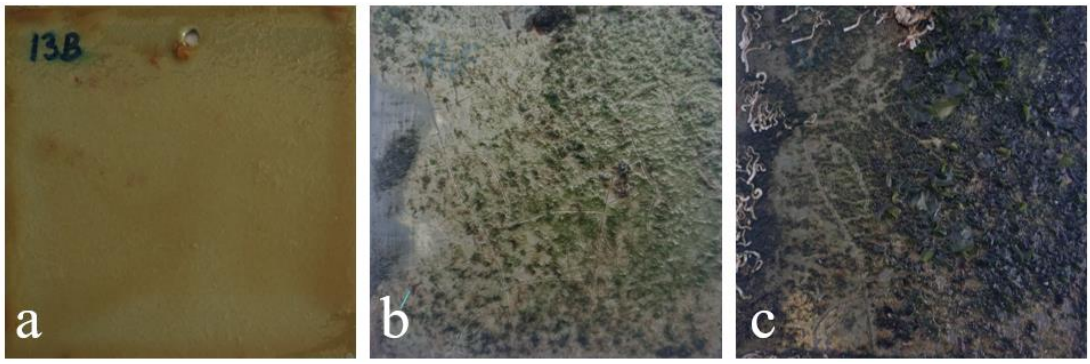


Figure 3.12 The field test results of Coating-5 (a) before immersion, (b) after 3 weeks, (c) after 6 weeks (Personal archive, 2022)

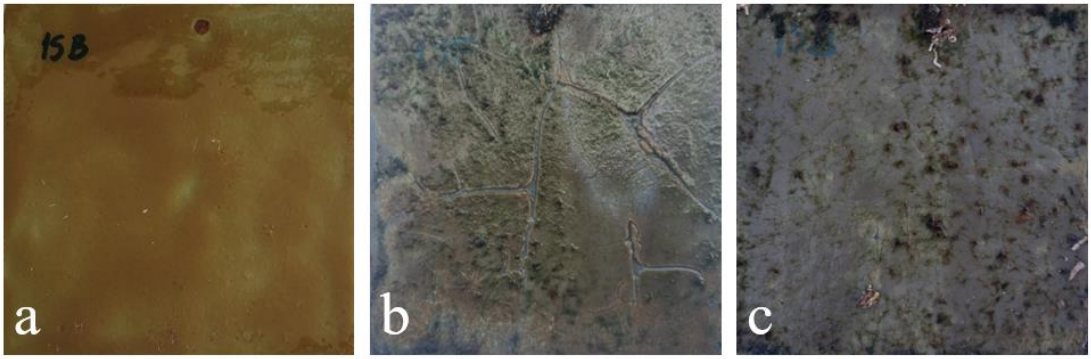


Figure 3.13 The field test results of Coating-6 (a) before immersion, (b) after 3 weeks, (c) after 6 weeks (Personal archive, 2022)

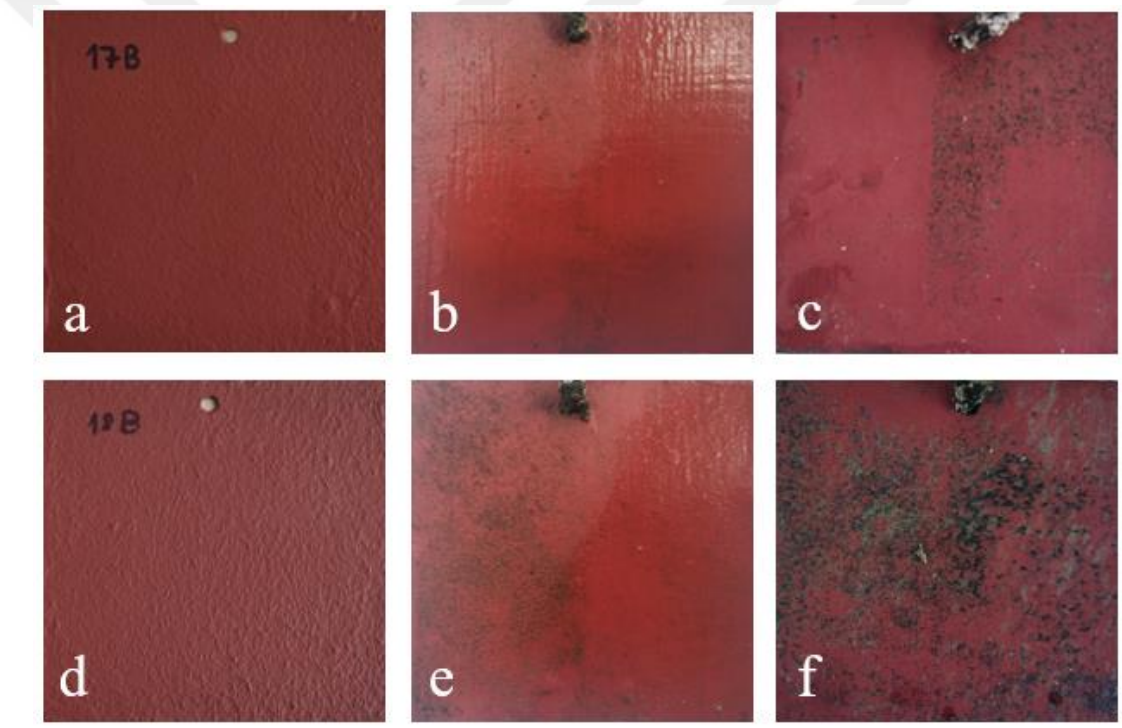


Figure 3.14 The field test results of commercial paint (a, d) before immersion, (b, e) after 3 weeks, (c, f) after 6 weeks (Personal archive, 2022)

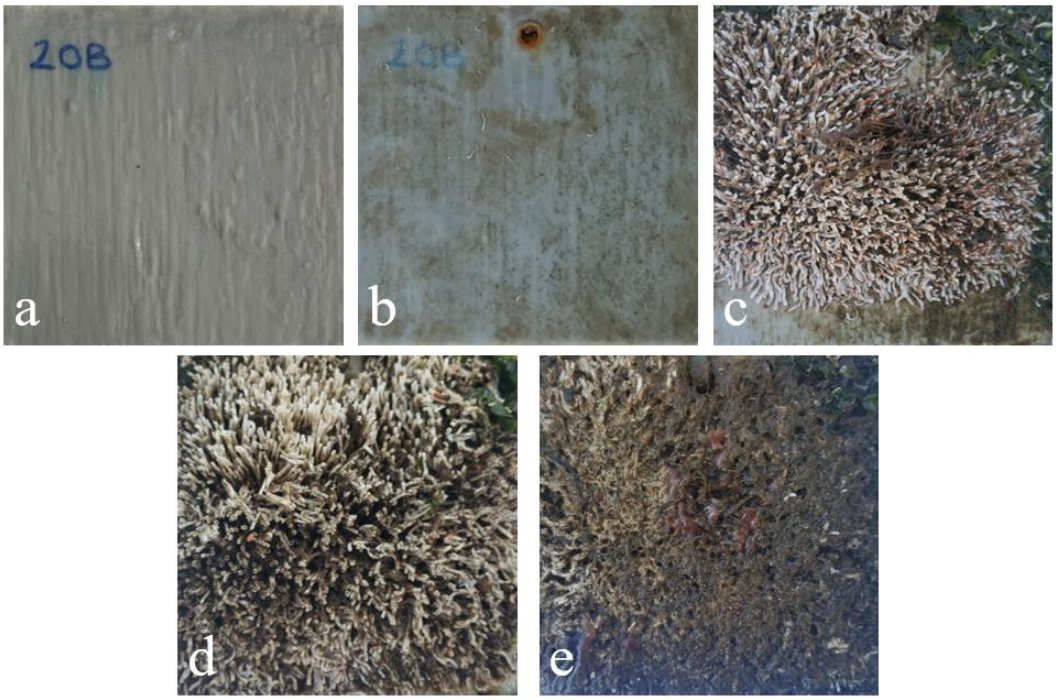


Figure 3.15 The field test results of Coating-7 (a) before immersion, (b) after 2 weeks, (c) after 4 weeks, (d) after 7 weeks, (e) after 10 weeks (Personal archive, 2022)

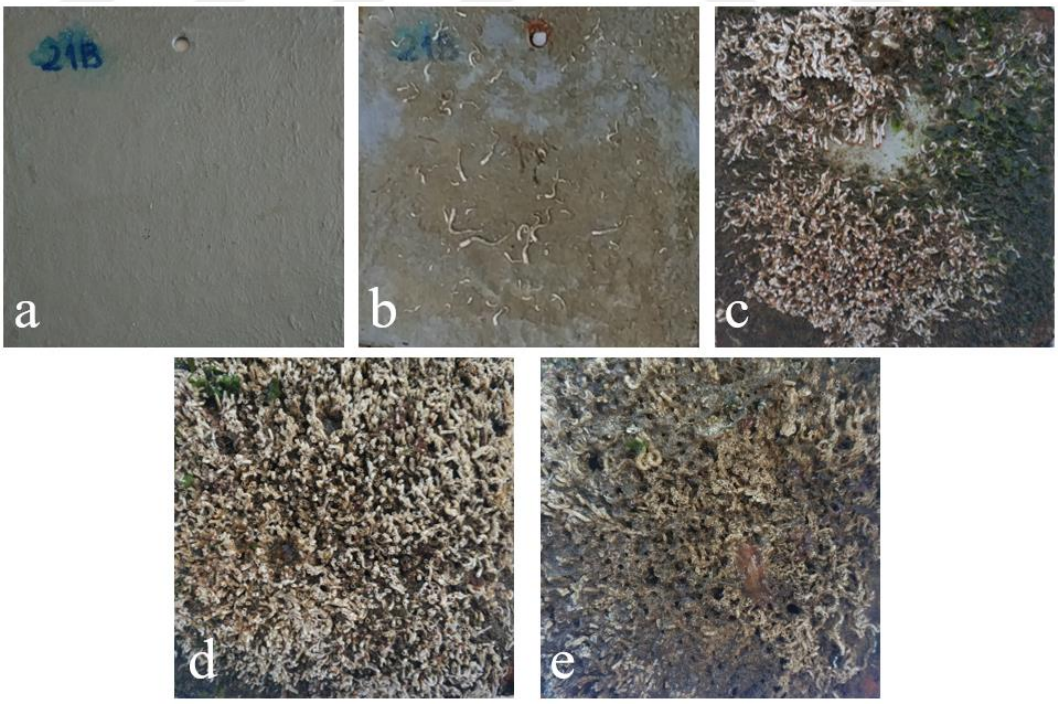


Figure 3.16 The field test results of Coating-8 (a) before immersion, (b) after 2 weeks, (c) after 4 weeks, (d) after 7 weeks, (e) after 10 weeks (Personal archive, 2022)

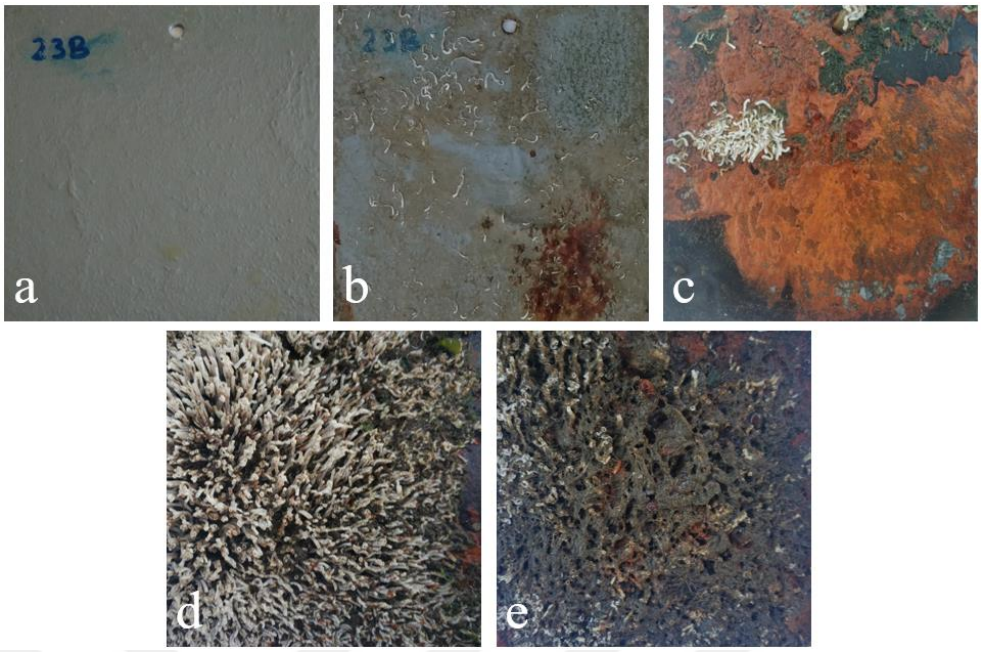


Figure 3.17 The field test results of Coating-9 (a) before immersion, (b) after 2 weeks, (c) after 4 weeks, (d) after 7 weeks, (e) after 10 weeks (Personal archive, 2022)

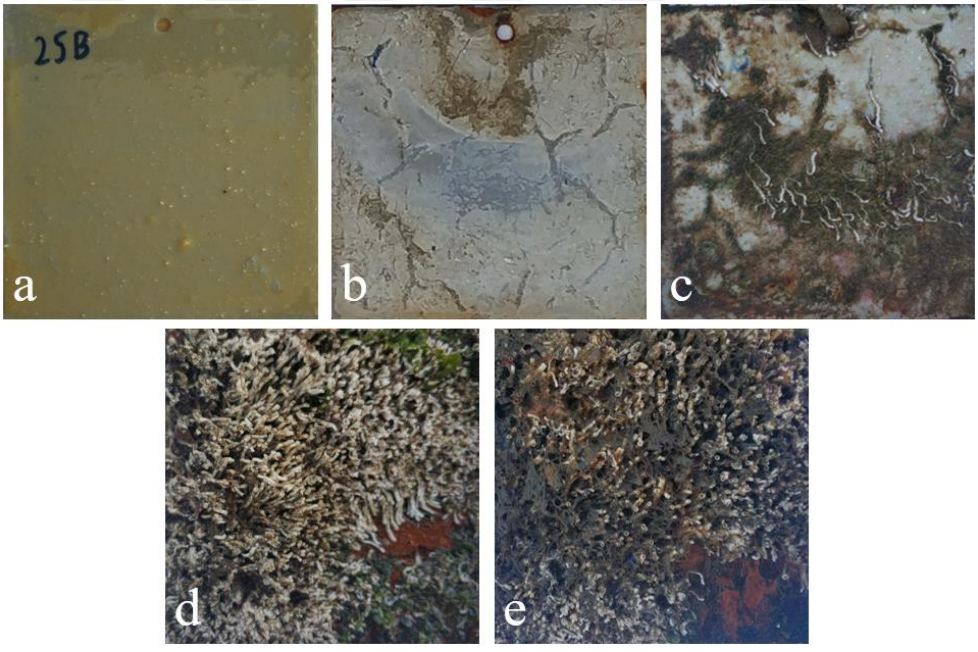


Figure 3.18 The field test results of Coating-10 (a) before immersion, (b) after 2 weeks, (c) after 4 weeks, (d) after 7 weeks, (e) after 10 weeks (Personal archive, 2022)

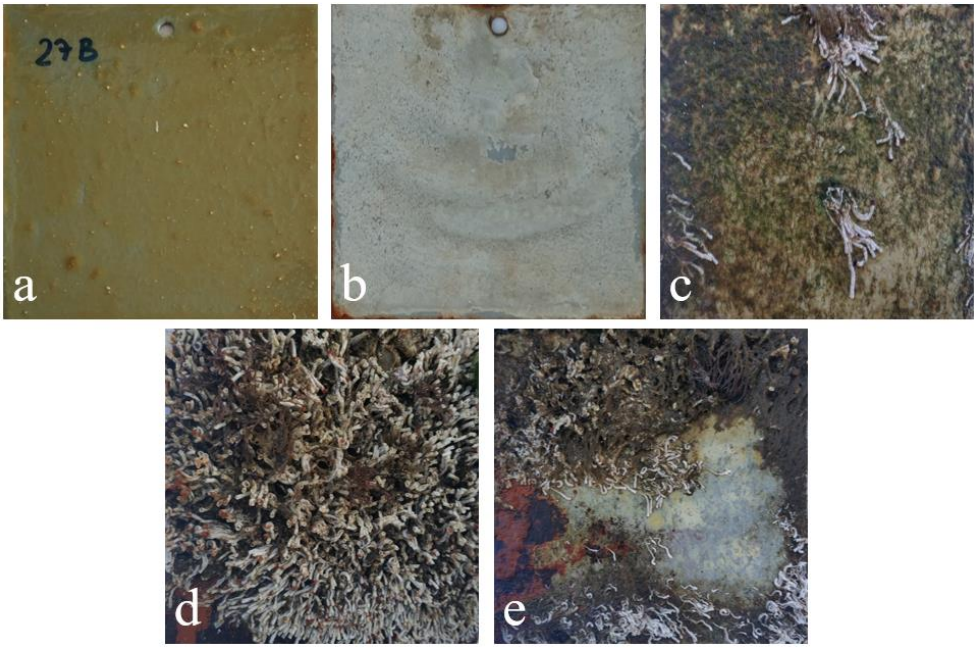


Figure 3.19 The field test results of Coating-11 (a) before immersion, (b) after 2 weeks, (c) after 4 weeks, (d) after 7 weeks, (e) after 10 weeks (Personal archive, 2022)

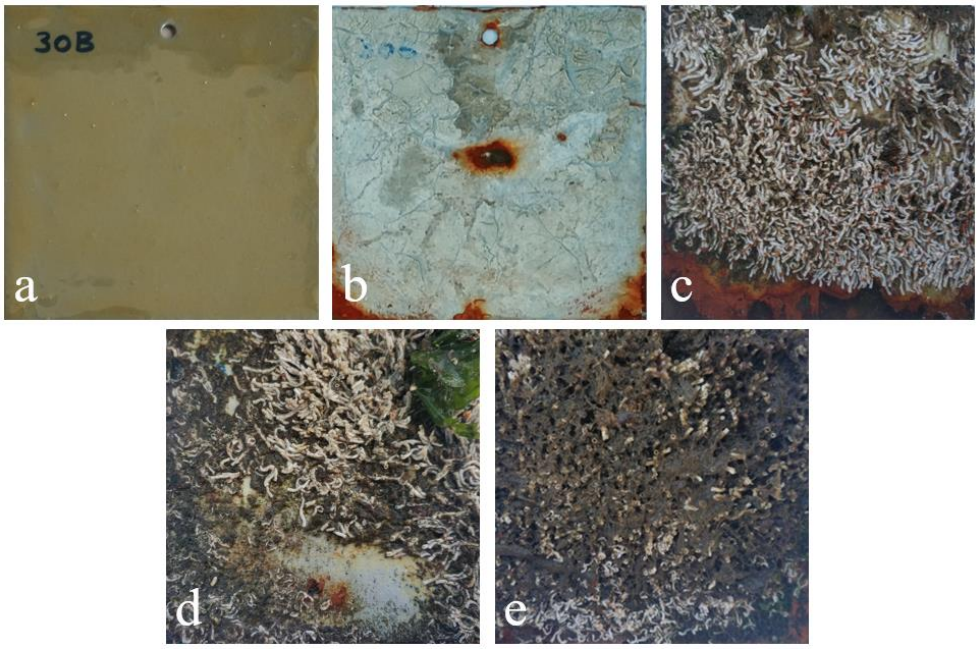


Figure 3.20 The field test results of Coating-12 (a) before immersion, (b) after 2 weeks, (c) after 4 weeks, (d) after 7 weeks, (e) after 10 weeks (Personal archive, 2022)

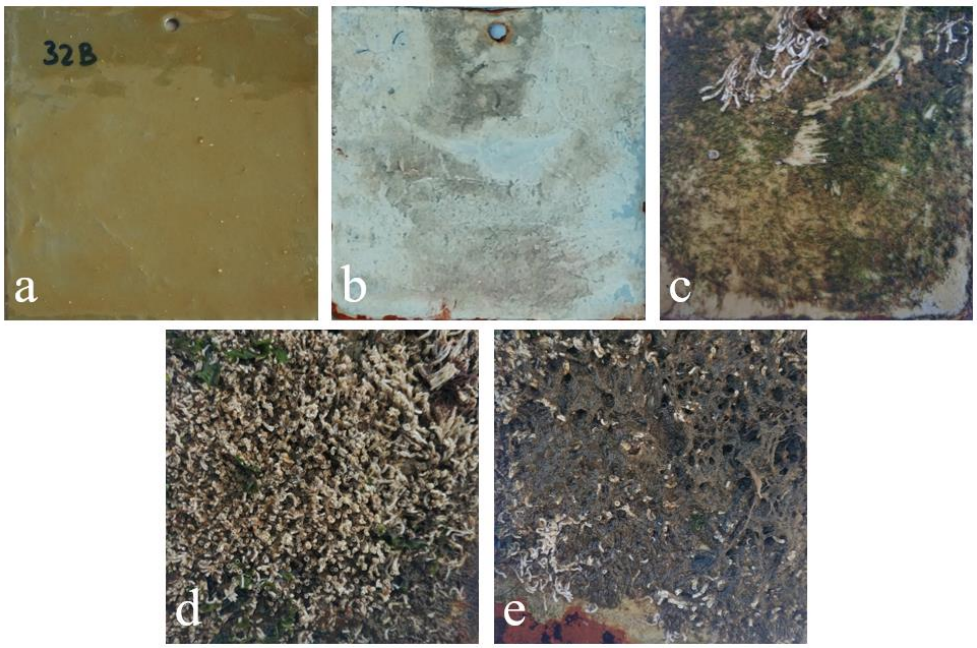


Figure 3.21 The field test results of Coating-13 (a) before immersion, (b) after 2 weeks, (c) after 4 weeks, (d) after 7 weeks, (e) after 10 weeks (Personal archive, 2022)

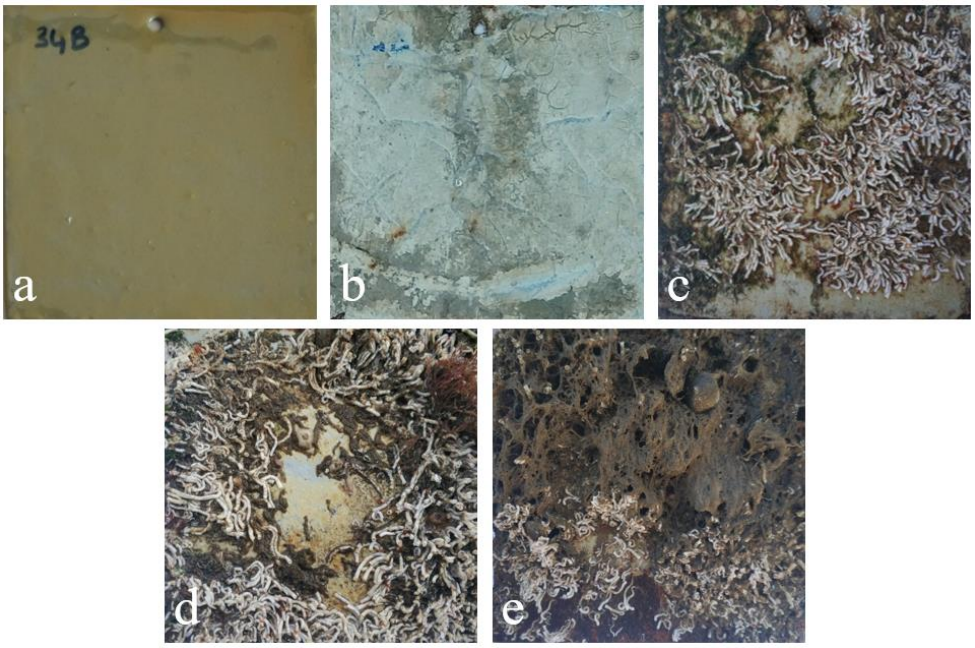


Figure 3.22 The field test results of Coating-14 (a) before immersion, (b) after 2 weeks, (c) after 4 weeks, (d) after 7 weeks, (e) after 10 weeks (Personal archive, 2022)

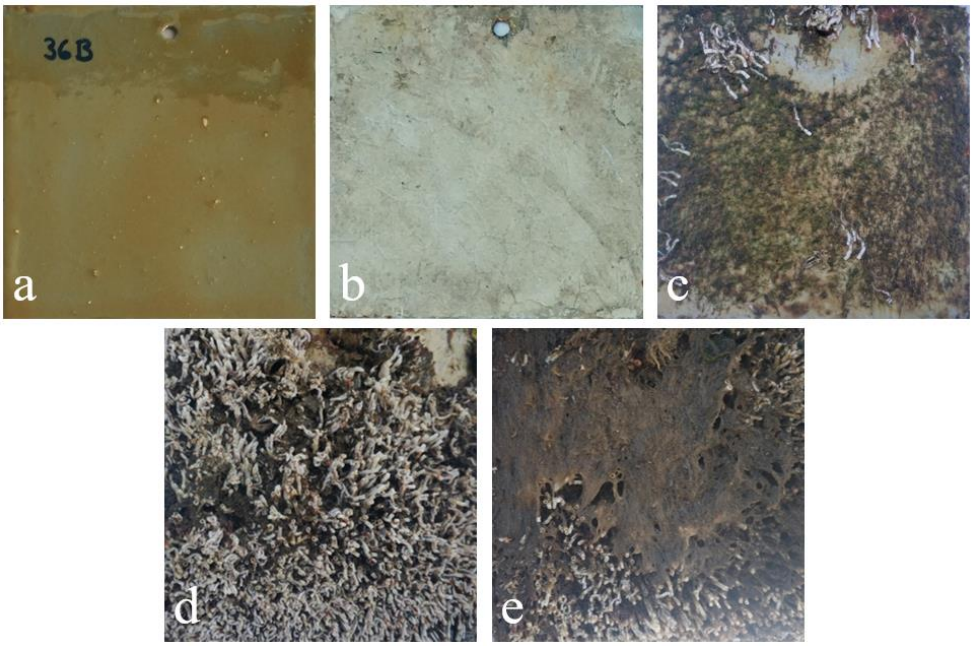


Figure 3.23 The field test results of Coating-15 (a) before immersion, (b) after 2 weeks, (c) after 4 weeks, (d) after 7 weeks, (e) after 10 weeks (Personal archive, 2022)

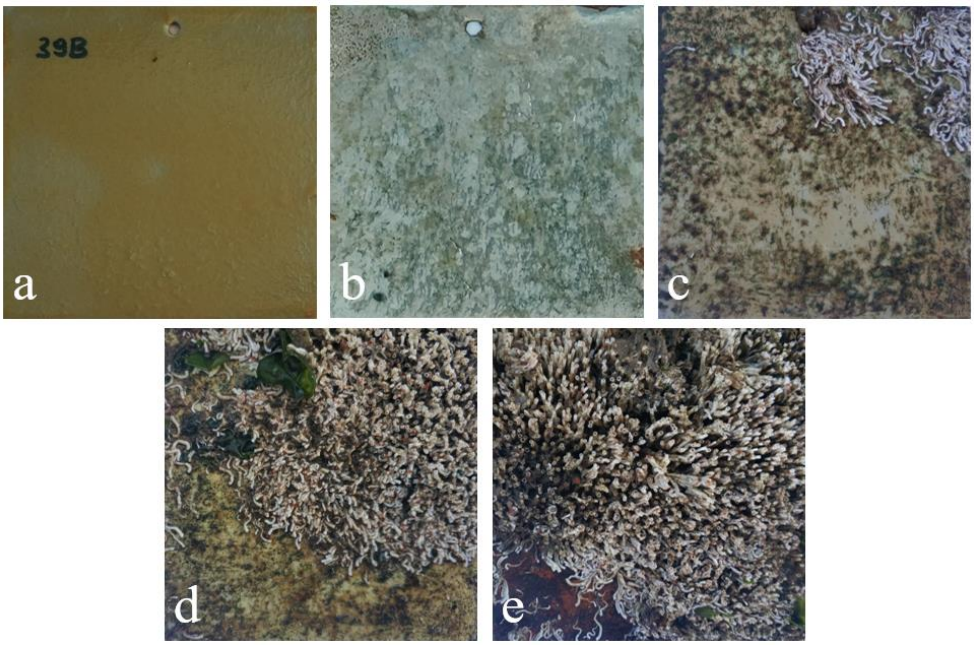


Figure 3.24 The field test results of Coating-16 (a) before immersion, (b) after 2 weeks, (c) after 4 weeks, (d) after 7 weeks, (e) after 10 weeks (Personal archive, 2022)

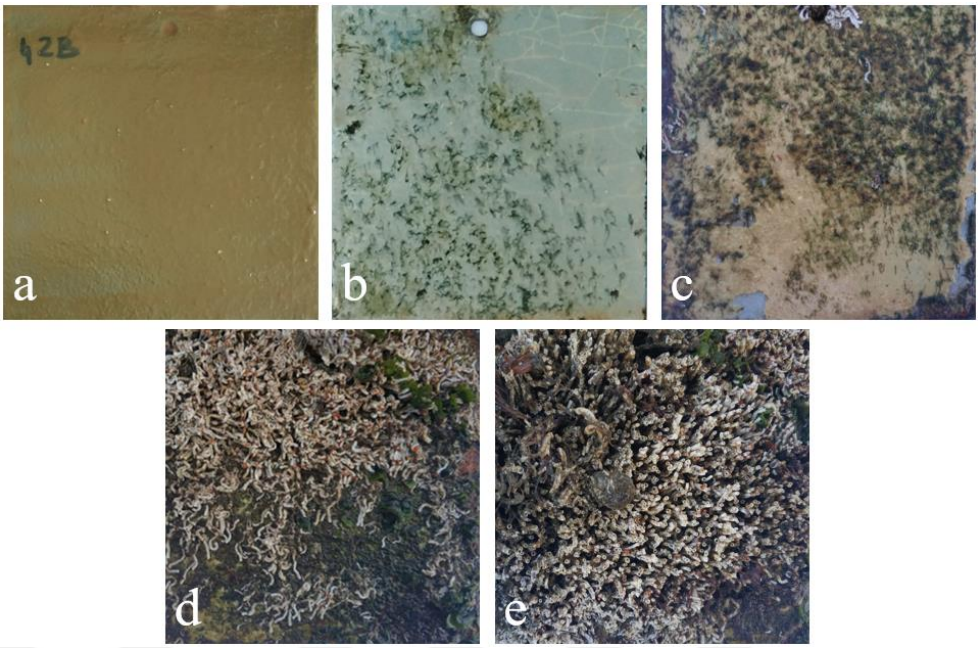


Figure 3.25 The field test results of Coating-17 (a) before immersion, (b) after 2 weeks, (c) after 4 weeks, (d) after 7 weeks, (e) after 10 weeks (Personal archive, 2022)

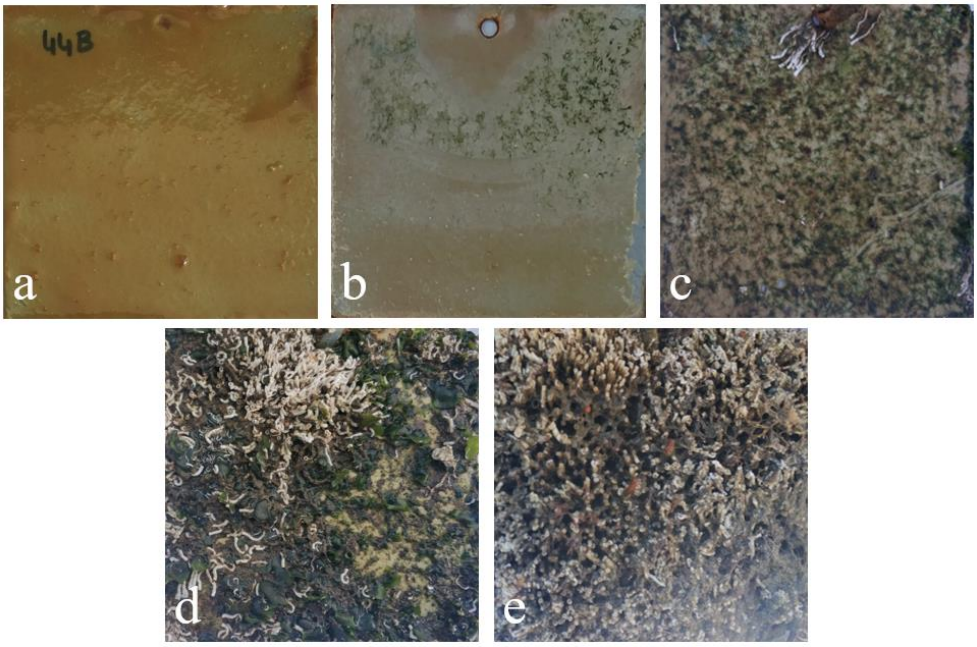


Figure 3.26 The field test results of Coating-18 (a) before immersion, (b) after 2 weeks, (c) after 4 weeks, (d) after 7 weeks, (e) after 10 weeks (Personal archive, 2022)

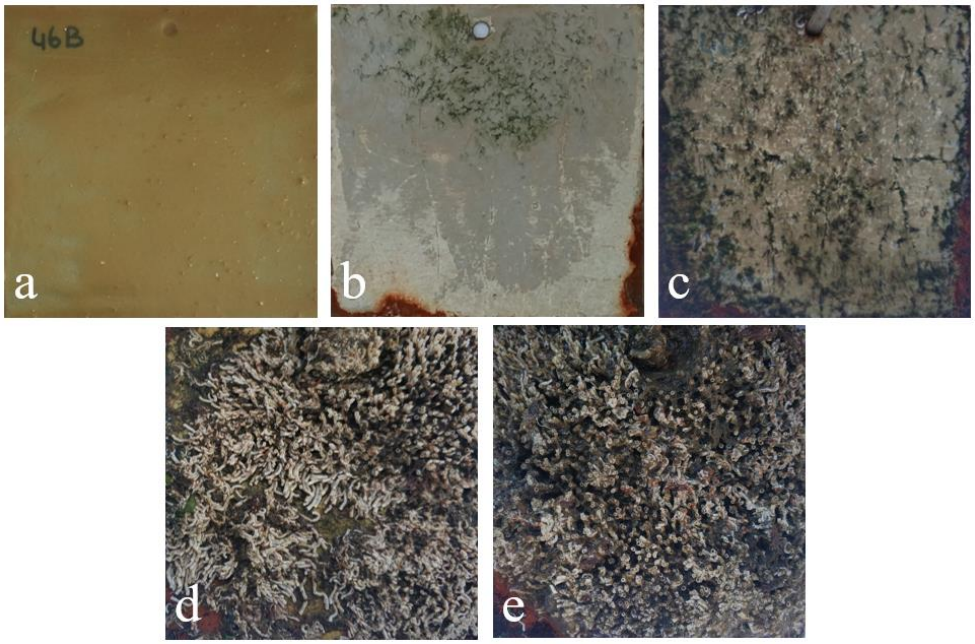


Figure 3.27 The field test results of Coating-19 (a) before immersion, (b) after 2 weeks, (c) after 4 weeks, (d) after 7 weeks, (e) after 10 weeks (Personal archive, 2022)

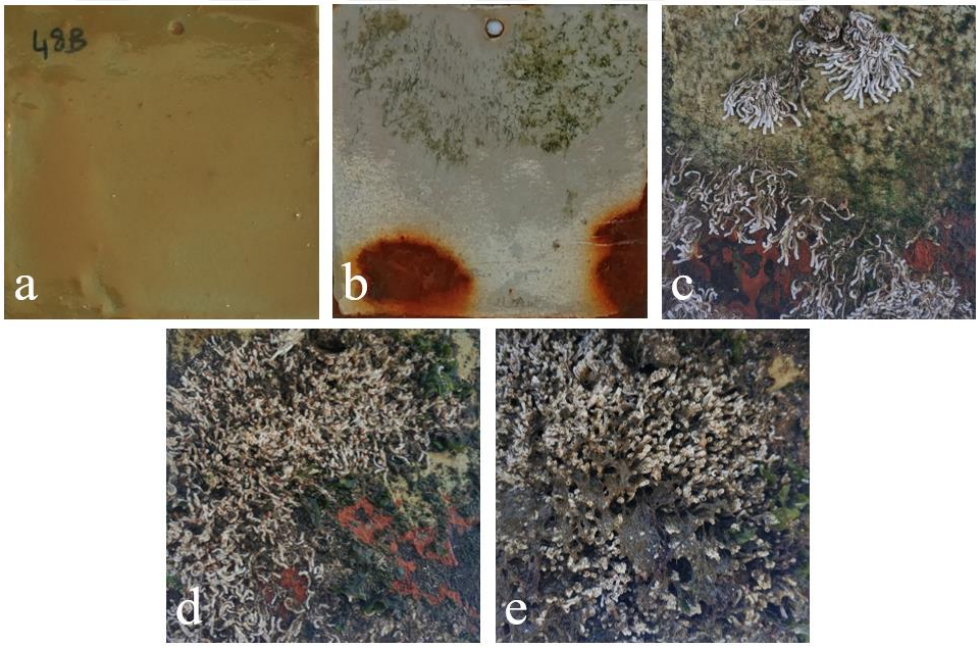


Figure 3.28 The field test results of Coating-20 (a) before immersion, (b) after 2 weeks, (c) after 4 weeks, (d) after 7 weeks, (e) after 10 weeks (Personal archive, 2022)

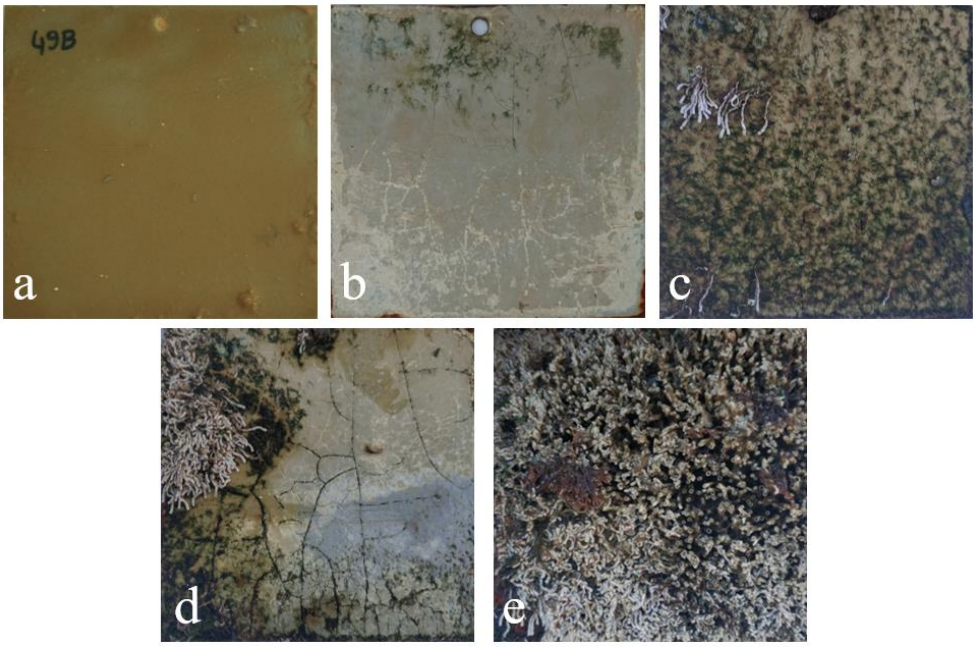


Figure 3.29 The field test results of Coating-21 (a) before immersion, (b) after 2 weeks, (c) after 4 weeks, (d) after 7 weeks, (e) after 10 weeks (Personal archive, 2022)

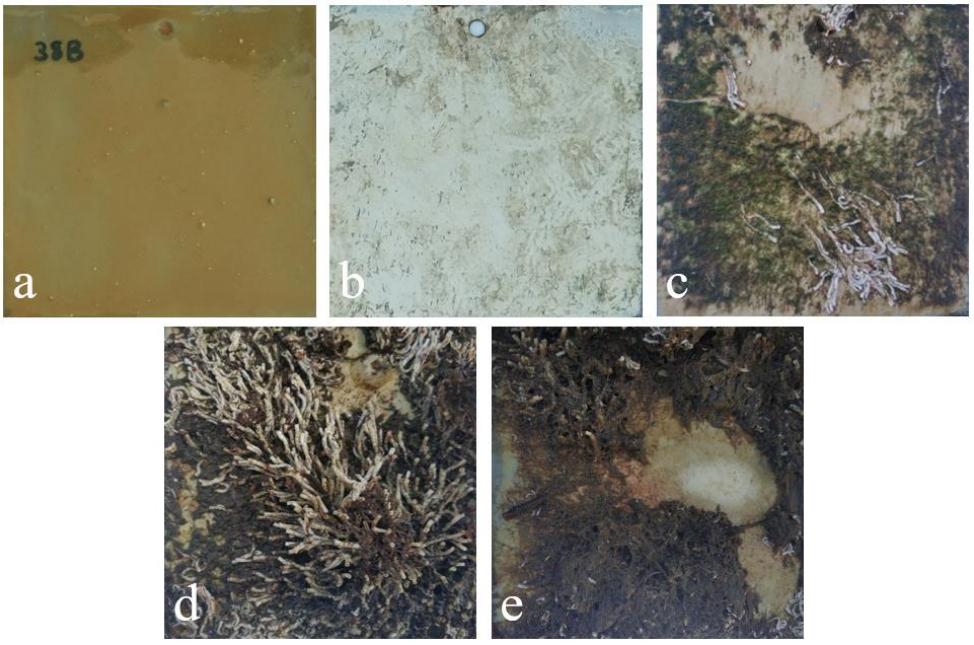


Figure 3.30 The field test results of Coating-22 (a) before immersion, (b) after 2 weeks, (c) after 4 weeks, (d) after 7 weeks, (e) after 10 weeks (Personal archive, 2022)

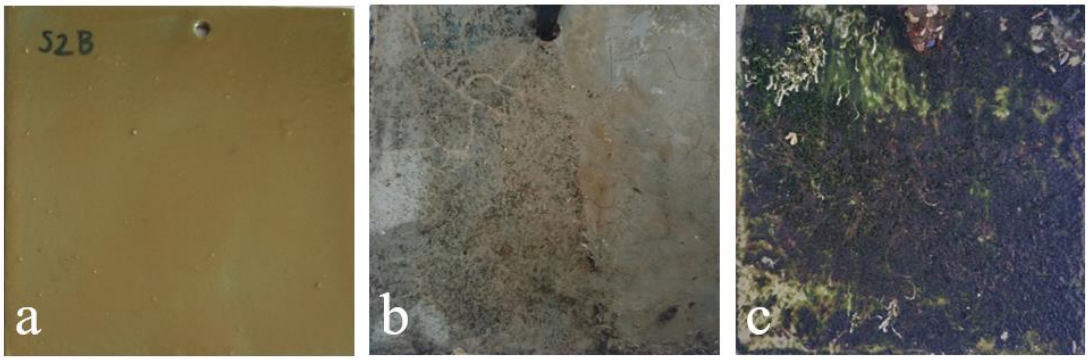


Figure 3.31 The field test results of Coating-23 (a) before immersion, (b) after 3 weeks, (c) after 6 weeks (Personal archive, 2022)

Table 3.1 Antifouling performance scores of prepared coatings

Coatings	Coating Type	Antifouling performance score			
		After 2 weeks	After 4 weeks	After 7 weeks	After 10 weeks
Uncoated	-	I	IV	V	V
Anticorrosive primer coated	Primer	I	V	V	V
Commercial antifouling paint	Commercial	-	II	III	-
1	Rosin	II	V	V	V
2	Rosin	II	IV	V	V
3	Rosin	-	V	V	-
4	Zinc rosinate	-	III	V	-
5	Zinc rosinate	-	III	IV	-
6	Zinc rosinate	-	III	IV	-
7	PVB	III	V	V	V
8	PVB	III	V	V	V
9	PVB	III	IV	V	V
10	Rosin	II	III	V	V
11	Rosin	II	III	V	V
12	Rosin	II	IV	V	V
13	Rosin	II	III	V	V
14	Rosin	II	IV	V	V
15	Rosin	II	III	V	V
16	Zinc rosinate	III	IV	V	V
17	Zinc rosinate	III	IV	V	V
18	Zinc rosinate	III	IV	V	V
19	Zinc rosinate	III	III	V	V
20	Zinc rosinate	III	IV	V	V
21	Zinc rosinate	III	IV	IV	V
22	Rosin	II	IV	V	V
23	Zinc rosinate	-	II	IV	-

3.4 Protein Determination on Plates (Field Experiment)

After immersing in seawater for 10 weeks, coating with the most biofouling and with the commercial paint were chosen for the protein determination experiment. Standard calibration graph in Figure 3.1 was used to calculate BSA concentrations.

The plates were removed from seawater, they were washed with 5 mL of deionized water 3 times. Then, biofouling on the first plate was scraped carefully and the remaining plate was washed with 5 mL of deionized water 3 times. After collecting all the samples, they were centrifuged at 800 rpm for 20 minutes and Bradford Assay was used to determine total protein concentrations in supernatants (Table 3.2). As can be seen from the Table 3.2, scraping fouling organisms from the surface did not make a noticeable difference in protein concentration. However, commercial coating had very low concentration of protein. This also supports the antifouling properties of the commercial coating since the surface had no fouling organisms.

Table 3.2 Protein concentrations on plates that used in field experiment

Samples	**Protein Concentration (µg/mL)**
Plate with Biofouling (First wash)	21.03
Plate with Biofouling (Second wash)	33.45
Plate with Biofouling (Third wash)	14.68
Plate after Scraping the Surface (First wash)	23.25
Plate after Scraping the Surface (Second wash)	20.64
Plate after Scraping the Surface (Third wash)	15.22
Plate with Commercial Coating (First wash)	3.55
Plate with Commercial Coating (Second wash)	6.80
Plate with Commercial Coating (Third wash)	11.82

3.5 Barnacle and Pseudobarnacle Adhesion Strength Tests

Table 3.3 shows barnacle adhesion strengths on the coating 4, (25% (w/w) zinc rosinate, 75% (w/w) xylene) high correlation coefficient (r=0.86) was found between diameter and removal strength of barnacles.

Table 3.3 The adhesion strengths of *Amphibalanus amphitrite* on the coating 4

Diameter (mm)	**Removal Strength (N)**	**Base Area (mm^2)**	**Strength of Adhesion (MPa)**
8	12	44	0.27
9	17	57	0.30
9	17	64	0.27
11	20	95	0.21
11	20	95	0.21
11	27	95	0.28
11	23	95	0.24
12	25	104	0.24
12	32	113	0.28
12	35	113	0.31
12	38	113	0.34
13	38	133	0.29
13	29	133	0.22

Table 3.4 shows adhesion strengths of *A. amphitrite* on the coating 10 (40% (w/w) rosin, 40% (w/w) xylene, 20% (w/w) $CaCO_3$). The correlation coefficient (r=0.87) between diameter and removal strength was high. In fact, this correlation coefficient is the highest value calculated among coatings 4, 12 and 14.

Table 3.4 The adhesion strengths of *Amphibalanus amphitrite* on the coating 10

Diameter (mm)	**Removal Strength (N)**	**Base Area (mm^2)**	**Strength of Adhesion (MPa)**
4	12	13	0.96
5	10	20	0.51
6	11	28	0.39
7	21	38	0.55
7	15	38	0.39
7	24	38	0.62
8	16	50	0.32
8	14	50	0.28
8	15	50	0.30
9	22	64	0.35
9	21	64	0.33
10	34	79	0.43
15	40	177	0.23

On the coating 12 (40% (w/w) rosin, 40% (w/w) xylene, 20% (w/w) $BaSO_4$), there were not many *A. amphitrite,* but they were well positioned for the adhesion test. According to Table 3.5, high correlation coefficient (r=0.86) was found between diameter and removal strength.

Table 3.5 The adhesion strengths of *Amphibalanus amphitrite* on the coating 12

Diameter (mm)	**Removal Strength (N)**	**Base Area (mm^2)**	**Strength of Adhesion (MPa)**
7	25	38	0.65
7	11	38	0.29
10	36	79	0.46
12	38	113	0.34

Using the data in Table 3.6, a high correlation coefficient (r=0.81) was found between diameter and removal strength on the coating 14 (40% (w/w) rosin, 40% (w/w) xylene, 10% (w/w) $CaCO_3$, 10% (w/w) $BaSO_4$).

Table 3.6 The adhesion strengths of *Amphibalanus amphitrite* on the coating 14

Diameter (mm)	**Removal Strength (N)**	**Base Area (mm^2)**	**Strength of Adhesion (MPa)**
3	9	7	1.27
4	7	13	0.56
5	12	20	0.61
7	24	38	0.62
7	16	38	0.42
9	27	64	0.42
9	11	64	0.17
11	30	95	0.32
11	18	95	0.19
12	31	113	0.27
12	33	113	0.29

Table 3.7 shows the results of pseudobarnacle tests results on anticorrosive primer coated panels after 1 and 6 hours of drying. The studs with a diameter of 20 mm could not be detached from the surface after both drying times. Since the dynamometer used can measure up to 200 N, the results were given as greater than 200 N. Strength of adhesions were not calculated because the removal force could not be known exactly. Apart from that, the removal strengths of all studs were higher compared to the coatings 10, 12 and 14, except for the 5 mm diameter studs.

Table 3.7 Pseudobarnacle test results on anticorrosive primer coated panels (± standard deviation)

	Diameter (mm)	**Mean Removal Strength (N)**	**Base Area (mm^2)**	**Strength of Adhesion (MPa)**
1 hour of drying	5	10	20	0.51 ± 0.05
	10	37	79	0.47 ± 0.21
	15	153	177	0.87 ± 0.08
	20	>200	314	N/A
6 hours of drying	5	17	20	0.84 ± 0.25
	10	96	79	1.22
	15	159	177	0.90 ± 0.03
	20	>200	314	N/A

After drying for 6 hours and conducting pseudobarnacle tests on the coatings, data in Table 3.8 were obtained. High correlation coefficients were found between diameter and removal strength on the coatings 10, 12 and 14 (r=0.96, 0.94, 0.96, respectively).

Table 3.8 Pseudobarnacle tests results on all coatings after 6 hours of drying. Different letters indicate statistical difference at 0.05. Comparisons were carried within groups (Coating 10, 12, 14) and each group compared to adhesion strength of 5 mm diameter (± standard deviation)

	Diameter (mm)	**Mean Removal Strength (N)**	**Base Area (mm^2)**	**Strength of Adhesion (MPa)**
Coating 10	5	13	20	0.66 ±0.291 [a]
	10	79	79	1.01 ±0.113 [a]
	15	83	177	0.47 ±0.088 [a]
	20	157	314	0.50 ±0.043 [a]
Coating 12	5	18	20	0.90 ±0.064 [k]
	10	42	79	0.54 ±0.174 [k]
	15	64	177	0.36 ±0.030 [l]
	20	149	314	0.47 ±0.094 [m]
Coating 14	5	19	20	0.97 ±0.181 [x]
	10	84	79	1.07 ±0.178 [x]
	15	160	177	0.90 ±0.142 [x]
	20	165	314	0.52 ±0.054 [x]

Figure 3.32 shows the relationship between removal strength and wooden stud diameter on the coating 10. Pseudobarnacle adhesion tests on the coating 10 gave acceptable R^2 values (R^2_{10}=0.9643).

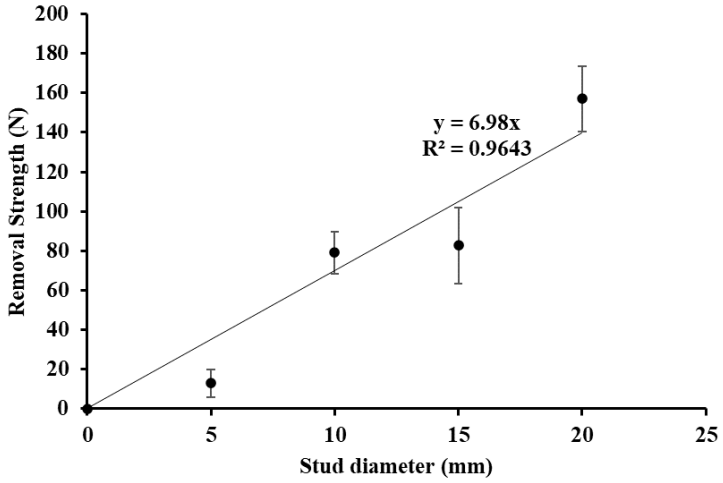


Figure 3.32 Relationship between removal strength and stud diameter on coating 10 after drying 6 hours

In Figure 3.33 the relationship between removal strength and wooden stud diameter on the coating 12 is given.

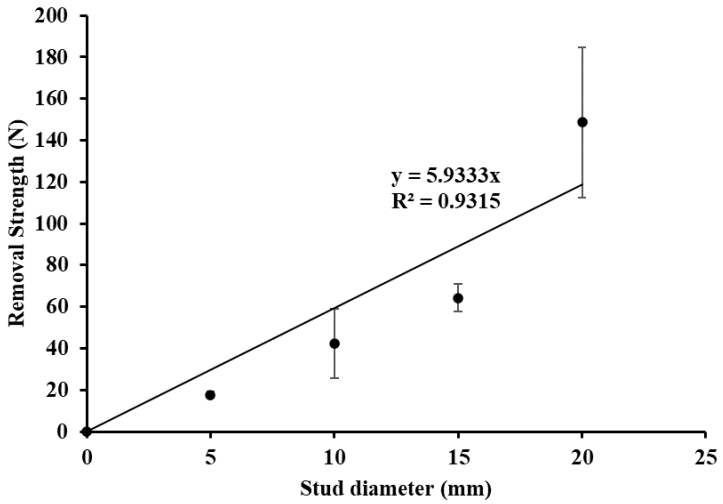


Figure 3.33 Relationship between removal strength and stud diameter on coating 12 after drying 6 hours

Figure 3.34 shows the relationship between removal strength and wooden stud diameter on the coating 14.

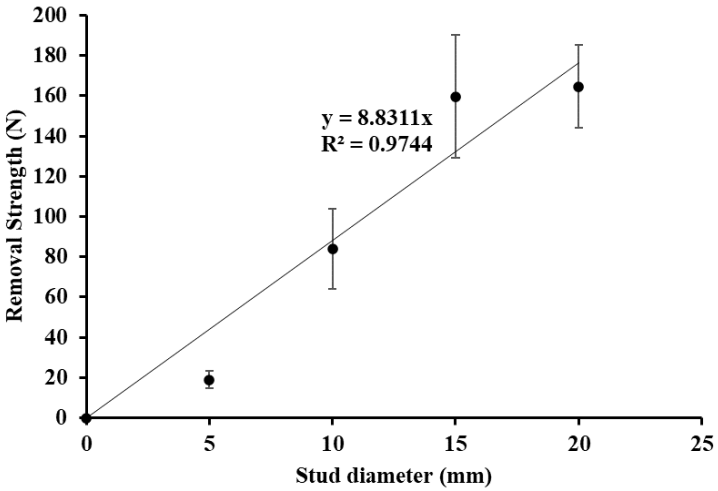


Figure 3.34 Relationship between removal strength and stud diameter on coating 14 after drying 6 hours

Figure 3.35 shows the comparison of strength of adhesion on all 3 coatings. Although the removal strength increases with the increasing stud diameter, strength of adhesion differs in each coating and diameter. There is no statistical difference ($p>0.05$) in the strengths of adhesion of 5 mm studs among the coatings 10, 12, and 14. For the 10 mm studs, although there is a significant difference ($p<0.05$) between strength of adhesions of the coatings 10 and 12, we could not observe significant difference ($p>0.05$) between the coatings 10 and 14. Adhesion strengths of 15 mm studs had no significant difference ($p>0.05$) on the coatings 10 and 12, but there is a difference ($p<0.05$) on the coating 14. Lastly, for the 20 mm studs there is no statistical difference ($p>0.05$) between all 3 coatings.

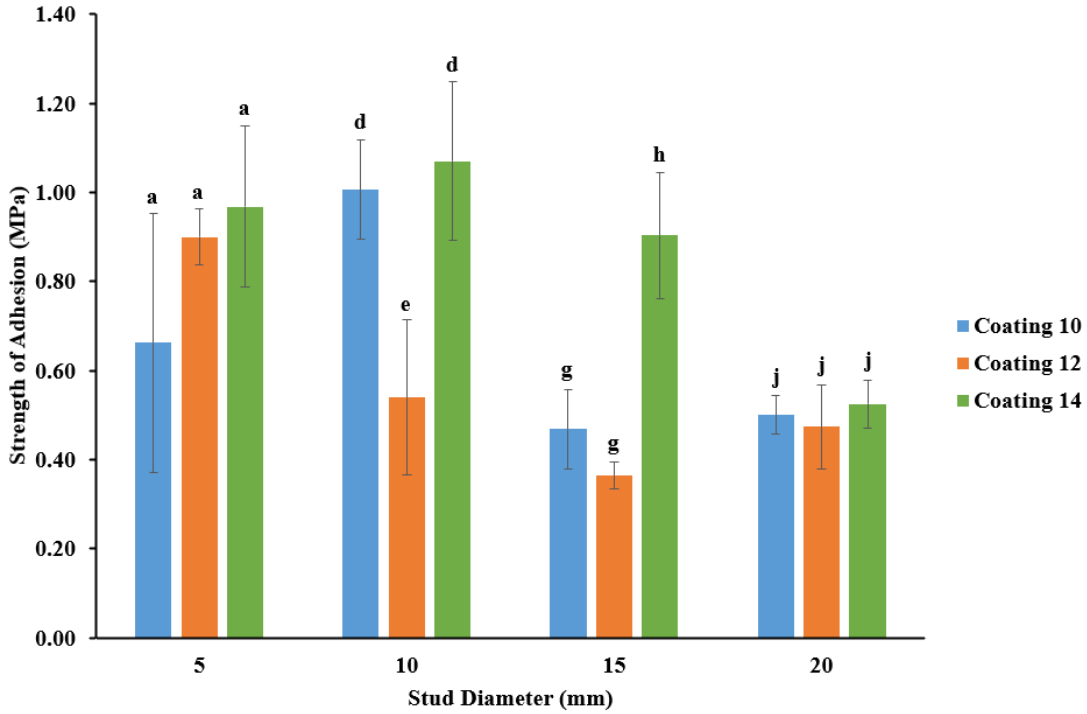


Figure 3.35 Adhesion strengths of different-sized pseudobarnacles on different coatings after 6 hours of drying. Different letters indicate statistical difference at 0.05. The comparisons were carried within groups (5, 10, 15 and 20 stud diameter)

After conducting pseudobarnacles tests, data in Table 3.9 were obtained. Even though studs with 5 mm diameter were weakly adhered to surfaces, correlation coefficient for 3 coatings were high (r_{10}= 0.93, r_{12}= 0.99, r_{14}= 0.98).

Table 3.9 Pseudobarnacle tests results on all coatings after an hour of drying. Different letters indicate statistical difference at 0.05. Comparisons were carried within groups (Coating 10, 12, 14) and each group compared to adhesion strength of 5 mm diameter (± standard deviation) (± standard deviation)

	Diameter (mm)	**Mean Removal Strength (N)**	**Base Area (mm^2)**	**Strength of Adhesion (MPa)**
Coating 10	5	6	20	0.31 ±0.072 [a]
	10	34	79	0.43 ±0.032 [a]
	15	42	177	0.23 ±0.003 [a]
	20	47	314	0.15 ±0.011 [a]
Coating 12	5	5	20	0.27 ±0.064 [k]
	10	35	79	0.45 ±0.031 [l]
	15	56	177	0.32 ±0.033 [k]
	20	86	314	0.27 ±0.024 [k]
Coating 14	5	5	20	0.25 ±0.042 [x]
	10	23	79	0.30 ±0.042 [x]
	15	82	177	0.47 ±0.023 [y]
	20	113	314	0.36 ±0.033 [z]

Figure 3.36 shows the relationships between removal strength and stud diameter that dried for an hour.

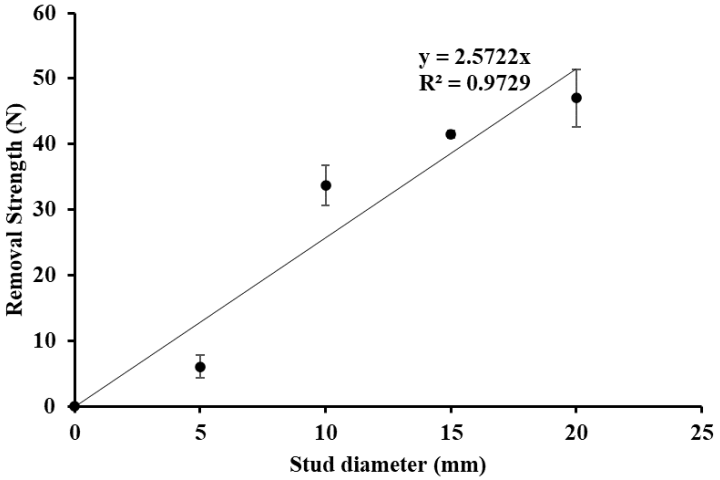


Figure 3.36 Relationship between removal strength and stud diameter on coating 10 after drying an hour

In Figure 3.37 the relationships between removal strength and stud diameter on coating 12 is given.

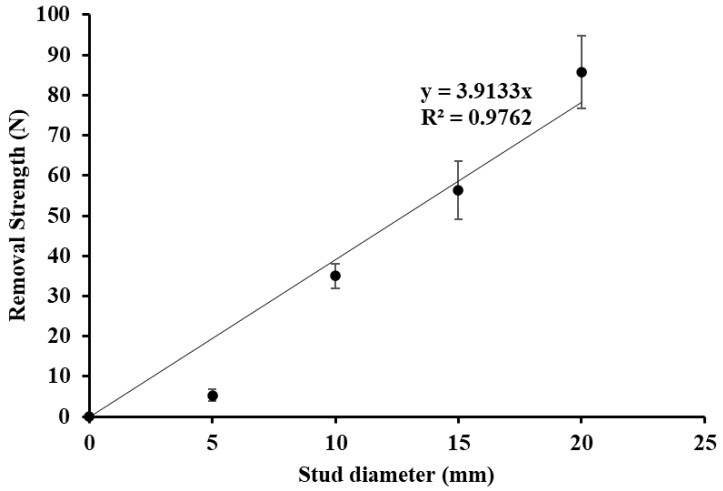


Figure 3.37 Relationship between removal strength and stud diameter on coating 12 after drying an hour

In Figure 3.38 the relationships between removal strength and stud diameter on coating 14 is given.

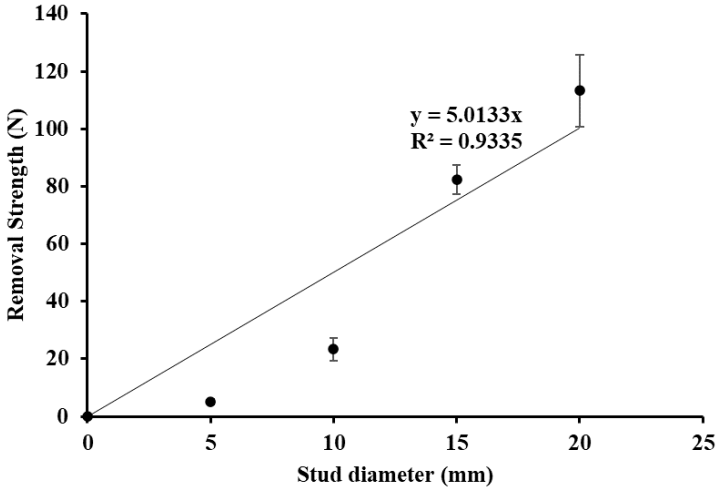


Figure 3.38 Relationship between removal strength and stud diameter on coating 14 after drying an hour

Figure 3.39 shows comparison of adhesion strengths on different coatings and pseudobarnacle diameters. These graphs are not with a constant increase or decrease even though removal strength increases with increasing diameter. For the 5 mm studs, there is no significant difference ($p>0.05$) between the adhesion strengths of the coatings 10, 12 and 14. While there is no significant difference ($p>0.05$) between the adhesion strengths of 10 mm studs on coatings 10 and 12, there is a remarkable difference ($p<0.05$) between the coating 14. 15 mm studs also show no statistical difference ($p>0.05$) between the coatings 10 and 12 but there is a difference ($p<0.05$) with the coating 14. All 3 coatings with 20 mm studs are significantly differ ($p<0.05$) from each other.

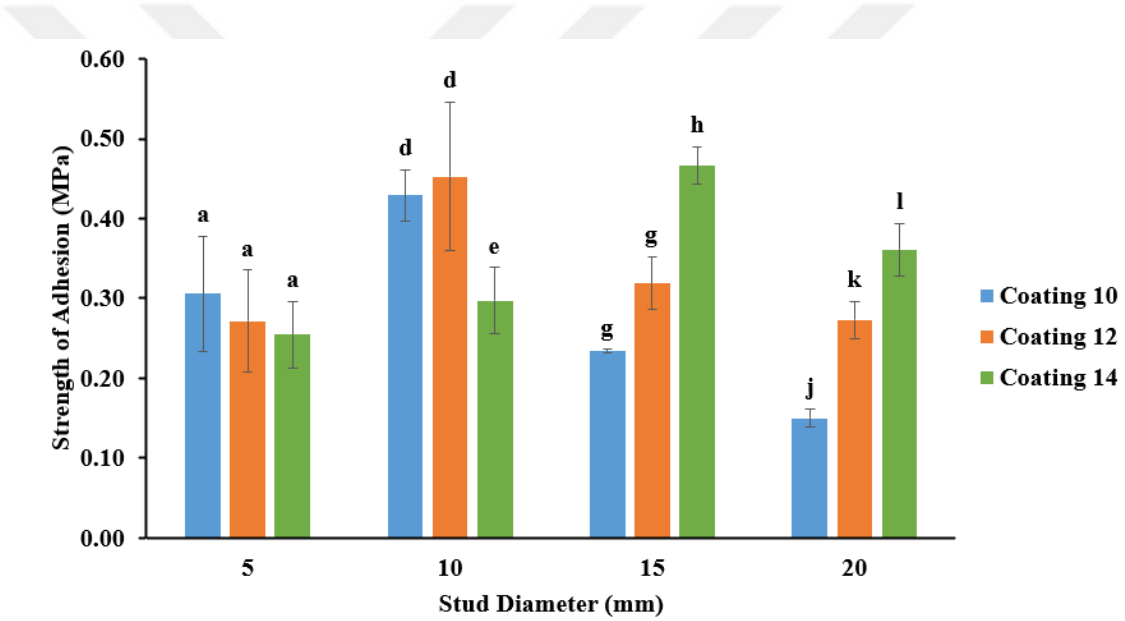


Figure 3.39 Adhesion strengths of different-sized pseudobarnacles on different coatings after an hour of drying. Different letters indicate statistical difference at 0.05. The comparisons were carried within groups (5, 10, 15 and 20 stud diameter)

3.6 Molecular Docking

3D structures of *A. amphitrite* CP-20k fragments were obtained using SWISS-MODEL. As can be seen from Figure 3.40, each fragment has different structures. Because of this docking them individually will provide more accurate results. Between

the created structures, templates with highest coverage and lowest resolution were chosen.

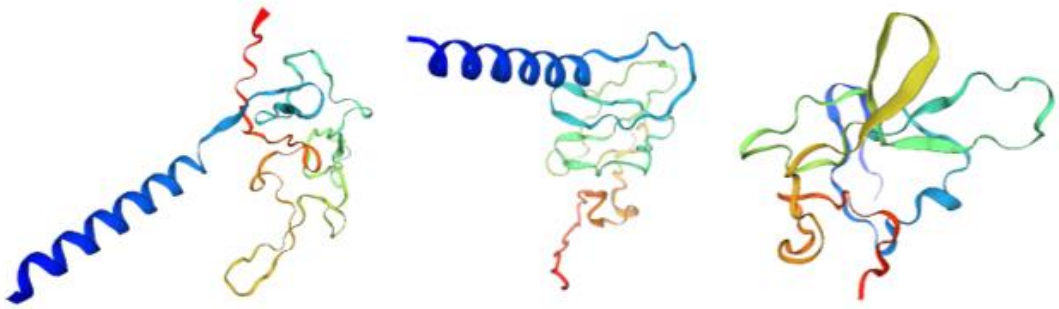


Figure 3.40 Modelled 3D structure of CP-20k-1, CP-20k-2 and CP-20k-3 by using SWISS-MODEL

After modelling all the proteins, molecular docking analysis were conducted using CB-Dock2. In the docking analysis abietic acid was used as ligand. In Table 3.10, molecular docking results of *A. amphitrite* CP-20k-1 are given. CB-Dock2 gives 5 cavities that are interaction sites. Between these cavities, Cavity 3 has the highest docking score with -6.9 kcal/mol and 317 $Å^3$ cavity volume. Contact residues between ligand and protein is also given in Table 3.10. As can be seen from Table 3.11, Cavity 1 and 2 has the highest docking score with -7.7 kcal/mol for the CP-20k-2 fragment. Their cavity volumes are 3363 $Å^3$ and 2930 $Å^3$, respectively. Compared to CP-20k-1, cavities of sites with highest vina score are bigger. Table 3.12 shows the molecular docking result of CP-20k-3. In this one Cavity 1 has the highest docking affinity with the -7.1 kcal/mol vina score. Cavity volume of this region is 3209 $Å^3$ which is very similar to the CP-20k-2 binding sites. When comparing all the 15 cavities detected by CB-Dock2, most of them have more than one Cys as contact residues. In Table 3.13, docking results of *M. rosa* MrCP-20 to abietic acid is given. Cavity 4 has the highest binding score with the -11.9 kcal/mol vina score. This binding site has 258 $Å^3$ cavity volume. As in other docking analysis, Cys residues were found in this binding site as well.

Table 3.10 The molecular docking results of abietic acid with *Amphibalanus amphitrite* CP-20k-1

Receptor (Protein)	CurPocket ID	Vina Score (kcal/mol)	Cavity volume (Å^3)	Center (x, y, z)	Docking size (x, y, z)	Contact Residues
Amphibalanus amphitrite CP-20k-1	C1	-6.3	596	2, -1, 0	21, 21, 21	**Chain A**: ARG57 CYS76 LEU79 THR80 SER85 HIS86 PRO87 CYS88 CYS105 ARG113 HIS114 PRO115 CYS116 TRP117 HIS118
	C2	-6.2	399	-8, 0, 11	21, 21, 21	**Chain A**: ALA23 ARG24 GLY25 GLN26 LYS27 ARG28 ASP106 SER107 ILE108 GLU109 CYS110 CYS116 CYS121 CYS123
	C3	-6.9	317	2, 9, 1	21, 21, 21	**Chain A**: CYS36 PHE37 HIS38 CYS39 ASP44 CYS45 SER47 GLU48 LEU50 HIS56 TRP117 GLY122 CYS123 ASN124 CYS125 THR126
	C4	-5.9	125	-5, 10, 15	21, 21, 21	**Chain A**: CYS30 ASN31 PRO32 PRO35 CYS36 PHE37 HIS38 CYS39 GLU48 LEU50 CYS125
	C5	-5.0	39	4, -8, -7	21, 21, 21	**Chain A:** ASN77 HIS78 LEU79 THR80 PRO81 CYS82 CYS103 ASP104 ASP106

Table 3.11 The molecular docking results of abietic acid with *Amphibalanus amphitrite* CP-20k-2

Receptor (Protein)	CurPocket ID	Vina Score (kcal/mol)	Cavity volume (Å^3)	Center (x, y, z)	Docking size (x, y, z)	Contact Residues
Amphibalanus amphitrite CP-20k-2	C1	-7.7	3363	3, 1, -11	29, 21, 27	**Chain A**: CYS51 CYS60 LYS61 PRO62 HIS64 PRO65 CYS66 TRP92 ASN93 LYS94 LEU110 HIS116 PRO117 CYS118
	C2	-7.7	2930	7, 0, 2	27, 27, 21	**Chain A**: CYS51 CYS60 LYS61 PRO62 HIS64 PRO65 CYS66 TRP92 ASN93 LYS94 LEU110 HIS116 PRO117 CYS118 TRP119
	C3	-6.8	83	-8, -11, -7	21, 21, 21	**Chain A**: CYS85 ASN86 HIS89 CYS91 GLN103 ARG104 CYS105 ASN106 CYS107 ASP108 TRP119 HIS120 ARG121
	C4	-6.7	56	4, 0, 16	21, 21, 21	**Chain A**: CYS60 LYS61 PRO62 ARG111 CYS112 ASN113 ARG114 HIS116 PRO117 CYS118 TRP119 CYS123 CYS125 CYS127
	C5	-5.8	340	-5, -8, -15	21, 21, 21	**Chain A**: CYS38 CYS44 TYR45 TYR46 CYS53 HIS54 HIS57 ASP58 GLN59 LYS61 HIS64

Table 3.12 The molecular docking results of abietic acid with *Amphibalanus amphitrite* CP-20k-3

Receptor (Protein)	**CurPocket ID**	**Vina Score (kcal/mol)**	**Cavity volume (Å^3)**	**Center (x, y, z)**	**Docking size (x, y, z)**	**Contact Residues**
Amphibalanus amphitrite CP-20k-3	C1	-7.1	3209	1, -3, 1	21, 27, 30	**Chain A**: PRO8 PRO11 PRO28 PRO29 PHE31 PRO32 CYS33 PHE34 LEU51 THR52 HIS58 CYS60 TYR89
	C2	-5.8	102	16, -1, -2	21, 21, 21	**Chain A**: CYS21 ALA22 LEU24 GLU43 PRO44 SER45 CYS46 ASP47 CYS48 ASN49 ARG91
	C3	-5.5	87	19, 4, 4	21, 21, 21	**Chain A**: CYS21 CYS33 LEU36 SER45 CYS46 ASP47 CYS48 ASN49 GLN50 ARG91
	C4	-5.6	76	0, 4, -13	21, 21, 21	**Chain A**: ASN12 PHE13 ASN14 THR84 SER85 HIS86 PRO87
	C5	-6.1	65	15, 6, -4	21, 21, 21	**Chain A**: PRO5 CYS6 ASN12 GLU23 LEU24 ARG25 TYR26 CYS27 PRO28 ALA30 PHE31

Table 3.13 The molecular docking results of abietic acid with *Megabalanus rosa* cement protein MrCP-20

Receptor (Protein)	CurPocket ID	Vina Score (kcal/mol)	Cavity volume (Å^3)	Center (x, y, z)	Docking size (x, y, z)	Contact residues
Megabalanus rosa MrCP-20	C1	-9.7	672	21, 0, 21	21, 27, 21	**Chain A:** VAL145 HIS72 LYS119 HIS120 ASN54 CYS56 CYS58 SER59 GLY143 GLY144 VAL145 ASN54 TYR139 ARG140 LYS141 GLU142 TYR139 VAL145 LYS57 HIS120 ASP176 CYS177 ILE63 PRO64 VAL145 GLU4 CYS27 ASP96
	C2	-11.4	330	-1, 7, -1	21, 21, 21	**Chain A:** GLU30 CYS175 ASP176 CYS177 GLU178 HIS179 MET1 ALA2 GLU4 SER173 ALA13 PRO14 CYS15 GLU4 GLU5 ASN28 LYS129 LEU130 CYS175 ASP176 CYS177 HIS179 ASP6 SER173 ASP176 HIS3 GLU4 GLU5 ASN28 PRO131
	C3	-9.6	312	-8, 9, 10	21, 21, 21	**Chain A:** LYS119 ASP117 LEU118 LYS119 HIS120 LYS172 ASP117 LEU118 LYS119 HIS120 LYS119 HIS120 ASP121 PHE32 ASP117 LEU118 LYS119 ASP117 LEU118 LYS119 HIS120
	C4	-11.9	258	16, 3, 2	21, 21, 21	**Chain A:** SER180 PRO181 GLY182 PRO183 GLU185 TYR16 GLU30 LYS129 LEU130 CYS175 ASP176 CYS177 GLU178 HIS179 SER180 PRO181 TYR16 ASP134 GLU135 GLU185 PRO183 GLU185 VAL145 HIS3 GLU5 SER184 GLU185 CYS177 GLU178 LYS129 THR171 ASP174 CYS175 HIS179 GLU178 SER180 PRO181 GLY182 PRO183 MET1 HIS3 TYR16 LYS129 CYS155 ASN156 GLU157
	C5	-9.8	200	-6, 19, 18	21, 21, 21	**Chain A:** GLU166 ASP168 THR171 GLU166 GLU166 LYS119 GLU166 LYS172 SER173 ASP174 CYS175 LYS119 ASP168 THR171 LYS172 SER173 ASP174 ASN156 HIS163 SER164 GLU166 ASP121 ASP168 VAL146 VAL170 THR171 LYS172 SER173 ASP174

To see the physical and chemical similarities of the studied protein, ProtParam was used. ProtParam is a tool that only uses protein sequence to find physicochemical properties of that protein. To find those parameters for the studied proteins, ProtParam analysis were conducted, and the results are given in Table 3.14. Most of the parameters calculated by ProtParam is self-explanatory. Among those parameters, instability index shows the stability of protein and if it is below 40, that protein is predicted as stable. As in the other analyzes performed under the bioinformatic study, the amount of Cys was found to be high in all the proteins examined by the ProtParam analysis.

Table 3.14 ProtParam results of *Megabalanus rosa* and *Amphibalanus amphitrite* CP-20k

Protein	**Number of Amino Acids**	**Molecular Weight**	**Theoretical pI**	**3 Most Abundant Amino Acids**	**Instability Index (II)**
M. rosa CP-20k	202	22466.57	4.91	Cys (C) 15.8% Asp (D) 10.4% Glu (E), His (H) 9.4%	45.92 (unstable)
A. amphitrite CP-20k-1	129	14375.26	6.16	Cys (C) 14.7% Thr (T) 10.1% His (H) 7.8%	60.64 (unstable)
A. amphitrite CP-20k-2	131	15395.57	8.68	His (H) 16.8% Cys (C) 14.5% Lys (K) 9.2%	43.57 (unstable)
A. amphitrite CP-20k-3	96	10444.52	4.59	Cys (C) 17.7% Pro (P) 12.5% Asn (N), Ser (S) 9.4%	61.19 (unstable)

Similarities between the studied CP-20k proteins were analyzed using Clustal Omega. Results of the Clustal Omega are given in Figure 3.41. Clustal Omega gives results using different symbols and colors. " * " means the residue is conserved in each sequence. " : " indicates the residues with strongly similar properties (>0.5 in the Gonnet PAM 250 Matrix). Lastly " . " shows residues with weakly similar properties (≤ 0.5 in the Gonnet PAM 250 Matrix). When it comes to colors, red shows small and hydrophobic amino acid residues. Green shows residues with hydroxyl, sulfhydryl and amine groups. While blue shows the acidic residues, magenta shows the basic ones.

As can be seen from Figure 3.41, mostly Cys residues are marked with * symbol, but there are also His and Pro residues that are fully conserved. It is clear from the docking results that there are a lot of Cys residues. With this analysis, these residues were found to be conserved between proteins.



Figure 3.41 Clustal Omega result of *Megabalanus rosa* CP-20k and *Amphibalanus amphitrite* CP-20k fragments

CHAPTER FOUR
DISCUSSION

The aim of this thesis is to evaluate the performance of antifouling paints by using field test, adhesion strength tests and *in silico* analysis. Field test was carried out at İnciraltı/İzmir between July and September (38°24'48.7"N, 27°02'03.9"E). After that, barnacle and pseudobarnacle adhesion strengths tests were carried out both in field and the laboratory. Both tests have similar methodologies, they were used to compare results. Then, molecular docking analysis were used to support the above performance tests.

According to scientific literature, very different barnacle adhesion strengths have been reported so far. The reasons behind these variances are barnacle species, size, age, seasons, physical conditions of the seawater and the test surfaces. Barnacle adhesion strength is strictly based on the antifouling coating types. Shortly, antifouling paints are classified under two groups: self-polishing and non-stick technology. In self-polishing antifouling coatings, binder is soluble in seawater. This means that the coating surface leaches out over time and release its content. When biocide release is stopped in self-polishing coatings, biofouling organisms adhere, and they must be cleaned from the surfaces. Otherwise, they cause serious issues such as speed reduction, loss of maneuverability, increased fuel consumption and increased carbon emission on ships (Ai et al., 2020). On the other hand, in non-stick coatings binder or so-called composite is not soluble in seawater. Therefore, the surface characteristics of both coatings are quite different. Nowadays, most effective, and mostly studied non-toxic fouling release surfaces are silicone-based coatings. Due to their low surface energies, PDMS-based coatings are widely used today (Nurioglu and Estecev, 2015). However, PDMS-based coatings have low mechanical properties, and this results in a short lifetime. This deficiency is compensated by adding support material, poly(urethane) (PU) and/epoxy segments (Kaffashi et al., 2012; Holberg et al., 2020).

In this thesis, it was aimed to gain similar properties to rosin-based coatings. Therefore, in this thesis, the adhesion strength of *A. amphitrite* that adhered to self-polishing coatings that do not contain biocide was examined. The results are especially important in the adjustment of the pressure to be applied in the process of cleaning fouling organisms from the surfaces. Moreover, this study is the first to demonstrate the adhesion strength of *A. amphitrite* on self-polishing coatings. Adhesion tests are mostly used to test the performance of fouling release paints. However, in this thesis, the performance of biocide-free rosin-based self-polishing coatings were tested with adhesion tests. Since there is no study with rosin, the studies performed with silicone-based coatings were given below for comparison purposes.

In the study conducted by Kaffashi et al. (2012), PDMS/silica nanocomposites were used as a paint matrix. Nanocomposites were synthesized with sol gel method. In the study, they investigated the effects of PDMS molecular weight, TEOS (tetraethyl orthosilicate) type and PDMS/TEOS weight ratios. They used TEOS as a cross-linking agent to form silica domains. To obtain these nanocomposites, they mixed PDMS and TEOS together and then added xylene to the mixture. For pseudobarnacle adhesion test, they applied each mixture to the sanded 150x100 mm aluminum plates. Film thickness was adjusted as 175 (±25) μm. They followed the instructions in ASTM D5618 for the pseudobarnacle adhesion test. They glued wooden studs with known diameters on the coatings with epoxy. After drying for 3 days, they measured the shear forces required for studs to detach from the surfaces. They used force gauge for measurements and moved plates parallel to the force gauge. As a result of the pseudobarnacle adhesion tests, samples that contain oligomeric TEOS (0.68 MPa) gave higher adhesion strengths than those with monomeric TEOS (0.008 MPa) because of the higher elastic properties.

Biofouling performance of PDMS-based coating with grafted telomer of tertiary carboxybetaine dodecafluoroheptyl ester ethyl acrylate (TCBF) was studied by Hu et al. (2021). At first, they synthesized TCBF and then telomer of TCBF (tTCBF) that they will be using in PDMS coating. Prepared coatings were applied into silicon wafer, glass slides and reinforced epoxy panel for different tests. Characterization

experiments were conducted with NMR, ATR-IR and FTIR spectroscopies. They used an automatic tester in accordance with ASTM D4541 for the adhesion test. The adhesion strength of PDMS tTCBF-x coatings were measured with an aluminum dolly that glued into surface with epoxy. After drying the pull rate was measured as 0.2 MPa s^{-1}. For the pseudobarnacle adhesion test ASTM D5618 was used. They immersed the samples in artificial seawater for 3 days before starting the experiments. After that, five aluminum studs with 10 mm diameter glued into test panels with epoxy. Adhesion strengths are measured with force gauge after drying for 3 days. While adhesion strength of PDMS is around 0.5 MPa, the adhesion strength of PDMS tTCBF was found 0.3 MPa. For the fouling resistance experiments, *Pseudomonas* sp. and *Navicula incerta* were used. Coatings were immersed in *Pseudomonas* sp. and *N. incerta* suspensions and then washed with ASW. *Pseudomonas* sp. samples were stained and counted with a fluorescence microscope while *N. incerta* samples were counted with microscopy. The coatings with 20 and 30% of tTCBF gave better fouling resistance results. As a result of these experiments coating can be used in marine applications.

Although the support material was added to the coatings prepared with rosin, it was observed that the coating broke off from the metal surface after the field trial. In addition to antifouling properties, mechanical properties are also important in coatings. In their study, Qiu et al. (2021) combined fouling release feature of PDMS with the high mechanical properties of PTU (propylthiouracil). Adhesion tests were carried to evaluate the performance of the composite they prepared. On the plates coated with PTU, the pseudobarnacle adhesion strength (~4.0 MPa) was found to be 30 times higher than the live barnacle adhesion strength (0.4 MPa) However, when the performance of the composite consisting of PTU-PDMS was examined, the two adhesion strengths (~0.1 MPa) were close to each other. Thus, when a material with low antifouling properties and molecules with high fouling release performance are combined, a coating with high performance and durability is created.

Holberg et al. (2020) synthesized PDMS-polyethylene glycol (PEG) copolymer coatings and conducted laboratory tests to investigate antifouling and fouling release performances of that coating. They conducted contact angle, pseudobarnacle test,

bacterial culture test and fresh water fouling test. Addition of PEG into PDMS decreased the water contact angle which means surface becomes more hydrophilic. It also reduced the number of bacteria that attaches to the surfaces. However, addition of PEG to PDMS had no discernible impact on pseudobarnacle adhesion strength (0.15-0.2 MPa) even though it changes the surface tension. In fresh water test, some of the coatings reduced the biofouling and some of them did not. As conclusion acceptable performance in the laboratory test do not mean that it will also be successful in real life biofouling.

Rath et al. (2010), developed two-component silicone modified epoxy resin-based coatings. They prepared two epoxy resins with different silicone contents (15% and 30%) and mixed them with polyether diamine. In the study, surface composition, surface topography and water contact angels were evaluated. Also, pseudobarnacle adhesion tests and fouling studies were also carried out to find out the antifouling properties of the coatings. 6 in. x 4 in. MS plates were degreased and coated with primer. After fully drying, prepared coatings were applied on panels. On fouling studies prepared plates were immersed in seawater for 90 days at Mumbai harbor. For pseudobarnacle tests aluminum studs with 7.5 mm diameter were used. As conclusion, pseudobarnacle adhesion strengths were decreasing with the increased amount of silicone in the coating. Using 30% silicone modified epoxy as a coating, 0.58 MPa of adhesion strength was obtained. As for the fouling studies, between 14-30 days all coatings formed slime layer. After 60 days heavy foulers start attaching to the coatings. After 90 days, panels were washed with a hose to evaluate foul release capabilities of the coatings. Coatings with 15% and 30% silicone showed 25-35% and 50-60% fouling release, respectively.

Using a statistical experimental design, Kim et al. (2007) studied the relationships between coating thickness, Young's modulus, and pseudobarnacle adhesion test. They prepared vinyl end-terminated polydimethylsiloxane-based coatings. First vinyl end-terminated polydimethylsiloxane was dissolved in methyl isobutyl ketone and mixed homogenously. Then, platinum-divinyltetramethyldisiloxane complex and tetrakis(dimethylsiloxy)silane were added as catalyst and cross-linkers, respectively.

After obtaining homogenous structure coating was poured into 1 x 3-inch glass slides and let them to dry for a week. The dry coating thickness ranged from 160 to 740 μm. Aluminum studs having a diameter of 7.2 mm were used for the adhesion testing. They were glued into silicone coating and cured until fully drying. They used customized adhesion tester that can be used at constant rate. As conclusion, it turned out that coating modulus influences both coating thickness and shear rate. Coating thickness and shear force were important variables for the soft coatings, but the effect of coating thickness decreased with the increased modulus. Shear rate was not significant for increased modulus (0.08-1.30 MPa).

Pawar et al. (2022) prepared a coating that has an anticorrosive and fouling release properties. By combining silicone and epoxy in three distinct ratios (70:30, 80:20, 90:10), three different coatings were prepared. Then desired amounts of hardener, crosslinker and catalyst were added and applied into steel and glass panels. They conducted both pseudobarnacle adhesion and fouling release tests. For the pseudobarnacle adhesion tests aluminum studs with known diameters were used. Studs were glued into coating surfaces and then adhesion test were carried out with a portable force gauge. Release forces of 0.71, 0.42 and 0.56 MPa has been recorded. To compare the results conventional coating was also used and 2.04 MPa release forces was obtained. As for the fouling release tests, coated test panels were dried 7 days. Plates were dried and then left in the sea for five months. After 5 months, fouling organisms on the coatings were removed with a portable force gauge. It was observed that removing an organism from the control coating needed 2.7 kgf of force, but only 0.2 kgf of force for the prepared coatings. According to the findings, an epoxy and silicone coating in a 70:30 ratio can be used as an antifouling paint.

Most of the time manual systems were used to calculate the adhesion strength of barnacles, but there are automatic pull-off testers to conduct adhesion tests. With the automated systems more accurate results are obtained. Singer et al. (2000) studied the barnacle adhesion strengths on transparent single-layer and duplex coatings. Pull-off testers (Quad Group's Romulus III) were used to measure the adhesion strengths of pseudobarnacle and *Balanus improvisus*. Sylgard®184 was applied to glass to create

single-layer coatings, and silicone-based adhesive was used to attach coated glass substrates to plexiglass to create duplex coatings. For barnacle adhesion test, coated glasses were immersed 20-60 cm beneath the water surface and left for 10 weeks. After 10 weeks, substrates were collected and gently brushed to remove soft fouling organisms from the surface and to make barnacles visible. Diameter range for the barnacles was 4-11 mm. After transporting panels with into laboratory, live barnacles were cleaned with acetone. Then, shells were swabbed with epoxy and wrapped with aluminum foil. After drying aluminum studs were glued into foil-wrapped barnacles. After drying tests were conducted and adhesion strengths between 1 N-13.5 N were obtained. For pseudobarnacle adhesion tests, aluminum studs with 7.2 mm and 12.5 mm diameter were glued into coatings with epoxy and air dried for 3 days. The results showed that, adhesion strengths were decreasing with the increase in coating thickness (0.17 to 0.02 MPa). As conclusion three parameters are effective in foul release coatings and those are surface energy, elastic modulus, and thickness.

Apart from the coating matrix, other parameters also affect the barnacle adhesion strength. Variables such as different methods, coating thickness, adhesive type cause different adhesion strengths to be obtained. Instead of studying standard adhesion strength methods, Rittschof et al. (2008) studied the reattachment ability of barnacles to surfaces. They collected *A. amphitrite* from the field and mass cultured it to obtain cyprises. For reattachment of barnacles, they waited until their diameters reach at least 5 mm then barnacles dislodged from old surfaces and placed on reattachment surfaces. After that panels were put in a container with seawater. They changed seawater in the container every 2 weeks and fed barnacles with brine shrimp nauplii. After measuring adhesion strengths of reattached barnacles, they compared the results of both field and reattachments tests. Adhesion strengths of reattached barnacles increased from day 1 to 7 and reached similar values to field barnacles at day 7 (from 0.01 MPa to 0.10 MPa). But overall, reattached barnacles gave lower adhesion strengths than field test barnacle (~0.10 and ~0.15 MPa, respectively). In conclusion, for the general method for barnacle adhesion strengths takes several weeks to months but for reattachment test it takes less than 4 weeks. Even though it takes short period of time results are positively correlated to field experiment results.

Dry coating thickness is one of the parameters that effects the adhesion strength of barnacles (Wendt et al., 2006). Dry coating thickness of the prepared coatings was varied between 100-178 μm. Wendt et al., (2006) also studied the adhesion strengths of *A. amphitrite* and obtained smaller adhesion strengths. But their study specified on how coating thickness affects adhesion strength, and they used silicone-based coating. Although the same species were used in present study and study of Wendt et al. (2006), different results were obtained due to coating thickness and surface characteristics.

Apart from the barnacle species and surface properties, adhesive type also affects the pseudobarnacle tests. Barnacles in nature use CPs to adhere on to surfaces (Liang et al., 2019). However, in pseudobarnacle test, commercial adhesives are used to glue aluminum or wooden studs on to surfaces. Due to the different chemical structures of these adhesives, it is sometimes not possible to obtain similar results in adhesion tests. For this reason, methodologies that can mimic barnacles specific to the adhesive type should be developed. Besides that, size and age of the barnacles also affect the adhesion strengths. Therefore, the diameter of the pseudobarnacle used should be specified in the methodology.

Finally, when *in silico* studies on the adhesion mechanisms of barnacles were investigated, very few papers were found. Instead of using cement protein, they used a protein that is responsible for the adhesive secretion. In the study carried out by Inbakandan et al. (2016), molecular docking of different metabolites to the G-protein coupled receptor (GPCR) was conducted. Metabolites from different marine sponges were used because of their antifouling performances. GPCR is a protein responsible for the secretion of adhesives. By studying the docking affinities of these molecules, preliminary work to reduce the CP secretion of the barnacles was studied. In their result, 5 of the 33 metabolites had high binding affinities (73.71, 68.08, 123.418, 72.124 and 72). They also find out that ligand-protein interactions occurred at Arg, Thr residues, which are responsible for the structural stability. When these results are examined, coatings with high antifouling properties can be produced by studying these 5 molecules with high affinity. For this reason, the results obtained from molecular docking should be supported by wet lab experiments.

CHAPTER FIVE
CONCLUSION

The aim of this study is to test the performance of antifouling paints by field test and barnacle adhesion strength tests. The obtained results were compared with *in silico* methods using molecular docking. For this purpose, field test was carried out at İnciraltı/İzmir between July and September (38°24'48.7"N, 27°02'03.9"E) (Prior to the field trial, permission was obtained from the Ministry of Environment, Urbanization and Climate Change of the Republic of Türkiye). In the field test, rosin, zinc rosinate, and PVB were used as binders, ZnO, $CaCO_3$ and $BaSO_4$ were used as supportive materials.

As a result of these field tests, the adhesion strengths of *A. amphitrite* attached to the surfaces were examined. Furthermore, pseudobarnacle adhesion tests were performed to mimic barnacle adhesion strengths in cases where field tests could not be performed. According to the tests conducted on the coating 12 (40% (w/w) rosin, 40% (w/w) xylene, 20% (w/w) $BaSO_4$), the barnacle adhesion strength was found to be 0.46 MPa while pseudobarnacle adhesion strengths was found as 0.45 MPa. Other than that, correlation of diameters and removal strengths between all barnacle and pseudobarnacle adhesion tests on coating 10, 12 and 14 gave matching results (Table 5.1). Paint manufacturers can use these data before starting their trials. However, it should not be forgotten that these values vary with different physicochemical condition of seawater.

Table 5.1 Correlations of diameters and removal strengths between barnacles and pseudobarnacles

Coating #	**Correlation Diameters between barnacles vs pseudobarnacles**	**Correlation Removal strength between barnacles vs pseudobarnacles**
10	0.845	0.625
12	0.943	0.799
14	0.950	0.663

Moreover, when the pseudobarnacle adhesion tests results were evaluated, it was found the pseudobarnacles glued to the rosin-based coating surface were detached from the surfaces with lower forces compared to the non-coated surfaces. Which means rosin-based coatings decreases the adhesion strength of pseudobarnacles. Since we have already found that there is a correlation between barnacle and pseudobarnacle adhesion tests, we can say that rosin-based coating also decreases the adhesion strength of live barnacles.

To compare our laboratory results, *in silico* analysis were also conducted. For that, molecular dockings were used. Since the species found on the Aegean Sea is *A. amphitrite*, the cement protein of this species, CP-20k, was chosen for molecular docking. Since this protein is directly related to barnacle attachment it was chosen as target protein for *in silico* tests. Since prepared coatings are based on rosin, abietic acid, which is an organic compound that highly found in the rosin was used as a ligand. 3D structure of abietic acid was readily available on PubChem. For the 3D structure of the CP-20k protein, RCSB protein data bank was searched but no data was found. Therefore, SWISS-MODEL was utilized to model the CP-20k's 3D structure. After modelling, structure was retrieved and used in the CB-Dock. Results of the molecular docking analysis were compared to the outcomes of the barnacle and pseudobarnacle adhesion tests.

In conclusion, development of eco-friendly antifouling coatings is a challenging process due to many factors such as environmental conditions, physicochemical parameters of seawater, testing organisms etc. Therefore, pseudobarnacle adhesion tests for development of eco-friendly antifouling coatings is of great importance. However, standardized conditions should be carefully studied to prevent possible differences among the laboratories. Moreover, based on field tests, a pseudobarnacle adhesion methodology was developed to mimic barnacles and the correlation between barnacle and pseudobarnacle tests was examined. Lastly, the obtained results were compared with *in silico* methodologies.

REFERENCES

Abeşka, Y. Y. (2019). *Green Synthesis of Silver Nanoparticles by Caulerpa spp* [Master's thesis]. Dokuz Eylül University.

Agarwal, S., & Mehrotra, R. (2016). An overview of molecular docking. *JSM Chemistry*, 4(2), 1024-1028. https://doi.org/10.47739/2334-1831/1024

Ai, X., Xie, Q., Ma, C., & Zhang, G. (2020). Fouling release coating consisting of hyperbranched poly(ε-caprolactone)/siloxane elastomer. *ACS Applied Polymer Materials*, 2(4), 1429-1437. https://doi.org/10.1021/acsapm.9b01056

Aldred, N., & Clare, A. S. (2008). The adhesive strategies of cyprids and development of barnacle-resistant marine coatings. *Biofouling*, 24(5), 351-363. https://doi.org/10.1080/08927010802256117

Antizar-Ladislao, B. (2008). Environmental levels, toxicity and human exposure to tributyltin (TBT)-contaminated marine environment. A review. *Environment International*, 34(2), 292-308. https://doi.org/10.1016/j.envint.2007.09.005

Arimura, H., Hiyoshi, S., Nakamura, N., Tsuboi, M. (2004). (Poly)Oxyalkylene Block Silyl Ester Copolymer, Antifouling Coating Composition, Antifouling Coating Formed from Antifouling Coating Composition, Antifouling Method Using Antifouling Coating Composition and Hull or Underwater Structure Covered with Antifouling Coating. US Patent 6,828,030 B2.

ASTM International. (2017). *Standard Test Method for Measurement of Barnacle Adhesion Strength in Shear* (D5618-94). https://doi.org/10.1520/D5618-94

ASTM International. (2020). *Standard Test Method for Testing Antifouling Panels in Shallow Submergence* (D3623-78a). https://doi.org/10.1520/D3623-78AR20

Banerjee, I., Pangule, R. C., & Kane, R. S. (2011). Antifouling coatings: recent developments in the design of surfaces that prevent fouling by proteins, bacteria, and marine organisms. *Advanced Materials*, 23(6), 690-718. https://doi.org/10.1002/adma.201001215

Barlow, D. E., Dickinson, G. H., Orihuela, B., Rittschof, D., & Wahl, K. J. (2009). *In situ* ATR–FTIR characterization of primary cement interfaces of the barnacle *Balanus amphitrite*. *Biofouling*, 25(4), 359-366. https://doi.org/10.1080/08927010902812009

Berman, H. M., Bhat, T. N., Bourne, P. E., Feng, Z., Gilliland, G., Weissig, H., & Westbrook, J. (2000). The Protein Data Bank and the challenge of structural genomics. *Nature Structural Biology*, 7(11), 957-959. https://doi.org/10.1038/80734

Bradford, M. M. (1976). A rapid and sensitive method for the quantitation of microgram quantities of protein utilizing the principle of protein-dye binding. *Analytical Biochemistry*, 72(1-2), 248-254. https://doi.org/10.1016/0003-2697(76)90527-3

Brady, R. F. (2005). Fouling-release coatings for warships. *Defence Science Journal*, 55(1), 75-81. https://doi.org/10.14429/dsj.55.1971

Bressy, C., & Lejars, M. (2014). Marine fouling: An overview. *The Journal of Ocean Technology*, 9(4), 19-28.

Briand, J. F. (2009). Marine antifouling laboratory bioassays: an overview of their diversity. *Biofouling*, 25(4), 297-311. https://doi.org/10.1080/08927010902745316

Burden, D. K., Spillmann, C. M., Everett, R. K., Barlow, D. E., Orihuela, B., Deschamps, J. R., Fears, K. P., Rittschof, D., Wahl, K. J. (2014). Growth and development of the barnacle Amphibalanus amphitrite: time and spatially resolved structure and chemistry of the base plate. *Biofouling*, 30 (7), 799-812. https://doi.org/10.1080/08927014.2014.930736

Cahill, P. L., Heasman, K., Jeffs, A., & Kuhajek, J. (2013). Laboratory assessment of the antifouling potential of a soluble-matrix paint laced with the natural compound polygodial. *Biofouling*, 29(8), 967-975. https://doi.org/10.1080/08927014.2013.822488

Callow, M. E., & Callow, J. A. (2002). Marine biofouling: a sticky problem. *Biologist*, 49(1), 1-5.

Cao, S., Wang, J., Chen, H., & Chen, D. (2011). Progress of marine biofouling and antifouling technologies. *Chinese Science Bulletin*, 56, 598-612. https://doi.org/10.1007/s11434-010-4158-4

Cao, Y., & Li, L. (2014). Improved protein–ligand binding affinity prediction by using a curvature-dependent surface-area model. *Bioinformatics*, 30(12), 1674-1680. https://doi.org/10.1093/bioinformatics/btu104

Carve, M., Scardino, A., & Shimeta, J. (2019). Effects of surface texture and interrelated properties on marine biofouling: a systematic review. *Biofouling*, 35(6), 597-617. https://doi.org/10.1080/08927014.2019.1636036

Chambers, L. D., Stokes, K. R., Walsh, F. C., & Wood, R. J. K. (2006). Modern approaches to marine antifouling coatings. *Surface and Coatings Technology*, 201(6), 3642-3652. https://doi.org/10.1016/j.surfcoat.2006.08.129

D'Souza, F., Bruin, A., Biersteker, R., Donnelly, G., Klijnstra, J., Rentrop, C., & Willemsen, P. (2010). Bacterial assay for the rapid assessment of antifouling and fouling release properties of coatings and materials. *Journal of Industrial Microbiology and Biotechnology*, 37(4), 363-370. https://doi.org/10.1007/s10295-009-0681-1

Dafforn, K. A., Lewis, J. A., & Johnston, E. L. (2011). Antifouling strategies: history and regulation, ecological impacts and mitigation. *Marine Pollution Bulletin*, 62(3), 453-465. https://doi.org/10.1016/j.marpolbul.2011.01.012

Dahlström, M., Jonsson, H., Jonsson, P. R., & Elwing, H. (2004). Surface wettability as a determinant in the settlement of the barnacle *Balanus improvisus* (DARWIN). *Journal of Experimental Marine Biology and Ecology*, 305(2), 223-232. https://doi.org/10.1016/j.jembe.2003.12.013

Diniz, W. J. S., & Canduri, F. (2017). Bioinformatics: an overview and its applications. *Genetics and Molecular Research*, 16(1), 17-37. http://dx.doi.org/10.4238/gmr16019645

Du, J., Chadalavada, S., Chen, Z., & Naidu, R. (2014). Environmental remediation techniques of tributyltin contamination in soil and water: A review. *Chemical Engineering Journal*, 235, 141-150. https://doi.org/10.1016/j.cej.2013.09.044

Ekin, A., Webster, D. C., Daniels, J. W., Stafslien, S. J., Cassé, F., Callow, J. A., Callow, M. E. (2007). Synthesis, formulation, and characterization of siloxane–polyurethane coatings for underwater marine applications using combinatorial high-throughput experimentation. *Journal of Coatings Technology and Research*, 4, 435-451. https://doi.org/10.1007/s11998-007-9039-7

Fan, J., Fu, A., & Zhang, L. (2019). Progress in molecular docking. *Quantitative Biology*, 7, 83-89. https://doi.org/10.1007/s40484-019-0172-y

Feng, D. Q., He, J., Chen, S. Y., Su, P., Ke, C. H., & Wang, W. (2018). The plant alkaloid camptothecin as a novel antifouling compound for marine paints: Laboratory bioassays and field trials. *Marine Biotechnology*, 20, 623-638. https://doi.org/10.1007/s10126-018-9834-4

Fenstermacher, D. (2005). Introduction to bioinformatics. *Journal of the American Society for Information Science and Technology*, 56(5), 440-446. https://doi.org/10.1002/asi.20133

Gabilondo, R., Graham, H., Caldwell, G. S., & Clare, A. S. (2013). Laboratory culture and evaluation of the tubeworm *Ficopomatus enigmaticus* for biofouling studies. *Biofouling*, 29(7), 869-878. https://doi.org/10.1080/08927014.2013.810214

Gasteiger, E., Hoogland, C., Gattiker, A., Duvaud, S. E., Wilkins, M. R., Appel, R. D., & Bairoch, A. (2005). Protein Identification and Analysis Tools on the ExPASy Server. In Walker, J.M. (Eds.) *The Proteomics Protocols Handbook*. Springer Protocols Handbooks. Humana Press. https://doi.org/10.1385/1-59259-890-0:571

Gohlke, H., Hendlich, M., & Klebe, G. (2000). Knowledge-based scoring function to predict protein-ligand interactions. *Journal of Molecular Biology*, 295(2), 337-356. https://doi.org/10.1006/jmbi.1999.3371

Gule, N. P., Begum, N. M., & Klumperman, B. (2016). Advances in biofouling mitigation: A review. *Critical Reviews in Environmental Science and Technology*, *46*(6), 535-555. https://doi.org/10.1080/10643389.2015.1114444

He, J., Wang, P., Wang, Z., Feng, D., & Zhang, D. (2023). TRPM7-Mediated Ca^{2+} Regulates Mussel Settlement through the CaMKKβ-AMPK-SGF1 Pathway. *International Journal of Molecular Sciences*, 24(6), 5399. https://doi.org/10.3390/ijms24065399

Henrikson, A. A., & Pawlik, J. R. (1995). A new antifouling assay method: results from field experiments using extracts of four marine organisms. *Journal of Experimental Marine Biology and Ecology*, 194(2), 157-165. https://doi.org/10.1016/0022-0981(95)00088-7

Hillisch, A., Pineda, L. F., & Hilgenfeld, R. (2004). Utility of homology models in the drug discovery process. *Drug Discovery Today*, 9(15), 659-669. https://doi.org/10.1016/S1359-6446(04)03196-4

Holberg, S., Losada, R., Blaikie, F. H., Hansen, H. H. W. B., Soreau, S., & Onderwater, R. C. A. (2020). Hydrophilic silicone coatings as fouling release: Simple synthesis, comparison to commercial, marine coatings and application on fresh water-cooled heat exchangers. *Materials Today Communications*, 22, 100750. https://doi.org/10.1016/j.mtcomm.2019.100750

Hu, P., Xie, Q., Ma, C., & Zhang, G. (2020). Silicone-based fouling-release coatings for marine antifouling. *Langmuir*, 36(9), 2170-2183. https://doi.org/10.1021/acs.langmuir.9b03926

Hu, P., Zeng, H., Zhou, H., Zhang, C., Xie, Q., Ma, C., & Zhang, G. (2021). Silicone Elastomer with Self-Generating Zwitterions for Antifouling Coatings. *Langmuir*, 37(27), 8253-8260. https://doi.org/10.1021/acs.langmuir.1c00984

Huang, S. Y., & Zou, X. (2010). Mean-force scoring functions for protein–ligand binding. In *Annual Reports in Computational Chemistry* (Vol. 6, pp. 280-296). Elsevier. https://doi.org/10.1016/S1574-1400(10)06014-7

Hunsucker, K. Z., Ralston, E., Gardner, H., & Swain, G. (2019). Specialized grooming as a mechanical method to prevent marine invasive species recruitment and transport on ship hulls. In Makowski, C., & Finkl, C. W. (Eds.) *Impacts of Invasive Species on Coastal Environments: Coasts in Crisis* (pp. 247-265). https://doi.org/10.1007/978-3-319-91382-7_7

Idora, M. S. N., Ferry, M., Wan Nik, W. B., & Jasnizat, S. (2015). Evaluation of tannin from *Rhizophora apiculata* as natural antifouling agents in epoxy paint for marine application. *Progress in Organic Coatings*, 81, 125-131. https://doi.org/10.1016/j.porgcoat.2014.12.012

Inbakandan, D., Raj, S., Kumar, C., Venkatesan, R., & Khan, S. A. (2016). Virtual Screening of Marine Natural Antifoulant: In Silico Approach to Screen Antifouling Metabolites from Marine Sponges. *Indian Journal of Geo-Marine Science*, 45(8), 1042-1048.

Jones, G. (2009). The battle against marine biofouling: a historical review. In Hellio, C., & Yebra, D. (Eds.) *Advances in Marine Antifouling Coatings and Technologies* (pp. 19-45). Woodhead Publishing. https://doi.org/10.1533/9781845696313.1.19

Kaffashi, A., Jannesari, A., & Ranjbar, Z. (2012). Silicone fouling-release coatings: effects of the molecular weight of poly(dimethylsiloxane) and tetraethyl orthosilicate on the magnitude of pseudobarnacle adhesion strength. *Biofouling*, 28(7), 729-741. https://doi.org/10.1080/08927014.2012.702342

Kamino, K. (2001). Novel barnacle underwater adhesive protein is a charged amino acid-rich protein constituted by a Cys-rich repetitive sequence. *Biochemical Journal*, 356(2), 503-507. https://doi.org/10.1042/bj3560503

Kamino, K. (2008). Underwater adhesive of marine organisms as the vital link between biological science and material science. *Marine Biotechnology*, 10, 111-121. https://doi.org/10.1007/s10126-007-9076-3

Kamino, K. (2012). Diversified material designs in biological underwater adhesives. In Thomopoulos, S., Birman, V., & Genin, G. M. (Eds.) *Structural Interfaces and Attachments in Biology* (pp. 175-199). Springer, New York. https://doi.org/10.1007/978-1-4614-3317-0_9

Kamino, K. (2013). Mini-review: barnacle adhesives and adhesion. *Biofouling*, 29(6), 735-749. https://doi.org/10.1080/08927014.2013.800863

Kamino, K. (2016). Barnacle underwater attachment. In Smith, A. M. (Eds.) *Biological Adhesives* (pp. 153-176). Springer, Cham. https://doi.org/10.1007/978-3-319-46082-6_7

Kamino, K., & Shizuri, Y. (1998). Structure and function of barnacle cement proteins. In Gal, Y. L., & Halvorson, H. O. (Eds.) *New Developments in Marine Biotechnology* (pp. 77-80). Springer, Boston. https://doi.org/10.1007/978-1-4757-5983-9_16

Kamino, K., Nakano, M., & Kanai, S. (2012). Significance of the conformation of building blocks in curing of barnacle underwater adhesive. *The FEBS Journal*, 279(10), 1750-1760. https://doi.org/10.1111/j.1742-4658.2012.08552.x

Kamino, K., Odo, S., & Maruyama, T. (1996). Cement proteins of the acorn-barnacle, *Megabalanus rosa*. *The Biological Bulletin*, 190(3), 403-409. https://doi.org/10.2307/1543033

Kiil, S., Dam-Johansen, K., Weinell, C. E., Pedersen, M. S., & Codolar, S. A. (2003). Estimation of polishing and leaching behaviour of antifouling paints using mathematical modelling: a literature review. *Biofouling*, 19(S1), 37-43. https://doi.org/10.1080/0892701021000069131

Kim, J., Chisholm, B. J., & Bahr, J. (2007). Adhesion study of silicone coatings: the interaction of thickness, modulus and shear rate on adhesion force. *Biofouling*, 23(2), 113-120. https://doi.org/10.1080/08927010701189708

Kim, S., Chen, J., Cheng, T., Gindulyte, A., He, J., He, S., Li, Q., Shoemaker, B. A., Thiessen, P. A., Yu, B., Zaslavsky, L., Zhang, J., & Bolton, E. E. (2023). PubChem 2023 update. *Nucleic Acids Research*, 51(D1), D1373–D1380. https://doi.org/10.1093/nar/gkac956

Kocak, F., Ergen, Z., & Çinar, M. E. (1999). Fouling organisms and their developments in a polluted and an unpolluted marina in the Aegean Sea (Turkey). *Ophelia*, 50(1), 1-20. https://doi.org/10.1080/00785326.1999.10409385

Korb, O., Stützle, T., & Exner, T. E. (2009). Empirical scoring functions for advanced protein− ligand docking with PLANTS. *Journal of Chemical Information and Modeling*, 49(1), 84-96. https://doi.org/10.1021/ci800298z

Kugler, S., Ossowicz, P., Malarczyk-Matusiak, K., & Wierzbicka, E. (2019). Advances in rosin-based chemicals: the latest recipes, applications and future trends. *Molecules*, 24(9), 1651. https://doi.org/10.3390/molecules24091651

Kwon, S. H., Lee, I., Park, H., & Lee, S. G. (2020). Decomposition mechanisms of self-polishing copolymers for antifouling coating materials through first-principles approach. *Progress in Organic Coatings*, 138, 105406. https://doi.org/10.1016/j.porgcoat.2019.105406

Lassmann, T., & Sonnhammer, E. L. (2005). Kalign–an accurate and fast multiple sequence alignment algorithm. *BMC Bioinformatics*, *6*(1), 1-9. https://doi.org/10.1186/1471-2105-6-298

Lejars, M., Margaillan, A., & Bressy, C. (2012). Fouling release coatings: a nontoxic alternative to biocidal antifouling coatings. *Chemical Reviews*, 112(8), 4347-4390. https://doi.org/10.1021/cr200350v

Li, H., Mishra, M., Ding, S., & Miyamoto, M. M. (2019). Diversity and dynamics of "*Candidatus Endobugula*" and other symbiotic bacteria in Chinese populations of the bryozoan, *Bugula neritina*. *Microbial Ecology*, 77, 243-256. https://doi.org/10.1007/s00248-018-1233-x

Liang, C., Strickland, J., Ye, Z., Wu, W., Hu, B., & Rittschof, D. (2019). Biochemistry of barnacle adhesion: an updated review. *Frontiers in Marine Science*, 6, 565. https://doi.org/10.3389/fmars.2019.00565

Liu, Y., Grimm, M., Dai, W. T., Hou, M. C., Xiao, Z. X., & Cao, Y. (2020). CB-Dock: A web server for cavity detection-guided protein–ligand blind docking. *Acta Pharmacologica Sinica*, 41(1), 138-144. https://doi.org/10.1038/s41401-019-0228-6

Liu, Y., Yang, X., Gan, J., Chen, S., Xiao, Z. X., & Cao, Y. (2022). CB-Dock2: Improved protein–ligand blind docking by integrating cavity detection, docking and homologous template fitting. *Nucleic Acids Research*, 50(W1), W159-W164. https://doi.org/10.1093/nar/gkac394

Maréchal, J. P., Culioli, G., Hellio, C., Thomas-Guyon, H., Callow, M. E., Clare, A. S., & Ortalo-Magné, A. (2004). Seasonal variation in antifouling activity of crude extracts of the brown alga *Bifurcaria bifurcata* (Cystoseiraceae) against cyprids of *Balanus amphitrite* and the marine bacteria *Cobetia marina* and *Pseudoalteromonas haloplanktis*. *Journal of Experimental Marine Biology and Ecology*, 313(1), 47-62. https://doi.org/10.1016/j.jembe.2004.07.016

Martinelli, E., Hill, S. D., Finlay, J. A., Callow, M. E., Callow, J. A., Glisenti, A., & Galli, G. (2016). Amphiphilic modified-styrene copolymer films: Antifouling/fouling release properties against the green alga *Ulva linza*. *Progress in Organic Coatings*, 90, 235-242. https://doi.org/10.1016/j.porgcoat.2015.10.005

Maruzzo, D., Aldred, N., Clare, A. S., & Høeg, J. T. (2012). Metamorphosis in the cirripede crustacean *Balanus amphitrite*. *PloS One*, 7(5), e37408. https://doi.org/10.1371/journal.pone.0037408

Mert, N., Topcam, G., Cavas, L. (2014). RP-HPLC optimization of econea by using artificial neural networks and its antifouling performance on the Turkish coastline. *Progress in Organic Coatings*, 77 (3), 627-635. https://doi.org/10.1016/J.PORGCOAT.2013.11.027

Mori, Y., Urushida, Y., Nakano, M., Uchiyama, S., & Kamino, K. (2007). Calcite-specific coupling protein in barnacle underwater cement. *The FEBS Journal*, 274(24), 6436-6446. https://doi.org/10.1111/j.1742-4658.2007.06161.x

Nurioglu, A. G., Esteves, A. C. C. & de With, G. (2015). Non-toxic, non-biocide-release antifouling coatings based on molecular structure design for marine applications. *Journal of Materials Chemistry B*, 3(32), 6547-6570. https://doi.org/10.1039/C5TB00232J

Nwuzor, I. C., Idumah, C. I., Nwanonenyi, S. C., & Ezeani, O. E. (2021). Emerging trends in self-polishing anti-fouling coatings for marine environment. *Safety in Extreme Environments*, 3, 9-25. https://doi.org/10.1007/s42797-021-00031-3

Oliveira, V. P., Ignacio, B. L., Martins, N. T., Dobler, L., & Enrich-Prast, A. (2019). The *Ulva* spp. Conundrum: What Does the Ecophysiology of Southern Atlantic Specimens Tell Us? *Journal of Marine Biology*, 2019, 5653464. https://doi.org/10.1155/2019/5653464

Pawar, S. S., Naik, R. B., Rath, S. K., Mahato, T. K., & Kandasubramanian, B. (2022). Pigmented silicone/epoxy novel blends for preparation of stratified nontoxic foul release coatings. *Journal of Coatings Technology and Research*, 19(4), 1269-1285. https://doi.org/10.1007/s11998-022-00610-4

Qian, P. Y., Lau, S. C. K., Dahms, H. U., Dobretsov, S., & Harder, T. (2007). Marine biofilms as mediators of colonization by marine macroorganisms: implications for antifouling and aquaculture. *Marine Biotechnology*, 9, 399-410. https://doi.org/10.1007/s10126-007-9001-9

Qiu, H., Gapeeva, A., Hölken, I., Kaps, S., Adelung, R., & Baum, M. J. (2021). Polydimethylsiloxane Microdomains Formation at the Polythiourethane/Air Interface and Its Influence on Barnacle Release. *ACS Applied Materials & Interfaces*, 13(3), 4545-4552. https://doi.org/10.1021/acsami.0c20058

Ragoza, M., Hochuli, J., Idrobo, E., Sunseri, J., & Koes, D. R. (2017). Protein–ligand scoring with convolutional neural networks. *Journal of Chemical Information and Modeling*, 57(4), 942-957. https://doi.org/10.1021/acs.jcim.6b00740

Rascio, V. J. D., Giúdice, C. A., & del Amo, B. (1988). Research and development of soluble matrix antifouling paints for ships, offshore platforms and power stations: a review. *Corrosion Reviews*, 8(1-2), 87-154. https://doi.org/10.1515/CORRREV.1988.8.1-2.87

Rath, S. K., Chavan, J. G., Sasane, S., Patri, M., Samui, A. B., & Chakraborty, B. C. (2010). Two component silicone modified epoxy foul release coatings: Effect of modulus, surface energy and surface restructuring on pseudobarnacle and macrofouling behavior. *Applied Surface Science*, 256(8), 2440-2446. https://doi.org/10.1016/j.apsusc.2009.10.084

Raval, K., & Ganatra, T. (2022). Basics, types and applications of molecular docking: a review. *IP International Journal of Comprehensive and Advanced Pharmacology*, 7(1), 12-16. https://doi.org/10.18231/j.ijcaap.2022.003

Rittschof, D., Clare, A. S., Gerhart, D. J., Mary, S. A., & Bonaventura, J. (1992). Barnacle *in vitro* assays for biologically active substances: toxicity and settlement inhibition assays using mass cultured *Balanus amphitrite amphitrite* darwin. Biofouling, 6(2), 115-122. https://doi.org/10.1080/08927019209386217

Rittschof, D., Orihuela, B., Stafslien, S., Daniels, J., Christianson, D., Chisholm, B., & Holm, E. (2008). Barnacle reattachment: a tool for studying barnacle adhesion. *Biofouling*, 24(1), 1-9. https://doi.org/10.1080/08927010701784920

Roleda, M. Y., & Heesch, S. (2021). Chemical profiling of *Ulva* species for food applications: What is in a name? *Food Chemistry*, 361, 130084. https://doi.org/10.1016/j.foodchem.2021.130084

Safarov, G. (2021). *Preparation of Natural Fiber Reinforced Self Polishing Paints and Evaluation of Antifouling Performances* [Master's thesis]. Dokuz Eylül University.

Saroyan, J. R., Lindner, E., & Dooley, C. A. (1970). Repair and reattachment in the Balanidae as related to their cementing mechanism. *The Biological Bulletin*, 139(2), 333-350. https://doi.org/10.2307/1540088

Scardino, A. J., Zhang, H., Cookson, D. J., Lamb, R. N., & de Nys, R. (2009). The role of nano-roughness in antifouling. *Biofouling*, 25(8), 757-767. https://doi.org/10.1080/08927010903165936

Schultz, M. P., Bendick, J. A., Holm, E. R., & Hertel, W. M. (2011). Economic impact of biofouling on a naval surface ship. *Biofouling*, 27(1), 87-98. https://doi.org/10.1080/08927014.2010.542809

Sharp, K. H., Davidson, S. K., & Haygood, M. G. (2007). Localization of '*Candidatus* Endobugula sertula' and the bryostatins throughout the life cycle of the bryozoan *Bugula neritina. The ISME Journal*, 1(8), 693-702. https://doi.org/10.1038/ismej.2007.78

Sievers, F., Wilm, A., Dineen, D., Gibson, T. J., Karplus, K., Li, W., Lopez, R., McWilliam, H., Remmert, M., Söding, J., & Higgins, D. G. (2011). Fast, scalable generation of high-quality protein multiple sequence alignments using Clustal Omega. *Molecular Systems Biology*, 7(1), 539. https://doi.org/10.1038/msb.2011.75

Silvestre, A. J., & Gandini, A. (2008). Rosin: major sources, properties and applications. In M. N. Belgacem, & A. Gandini (Eds.), *Monomers, Polymers and Composites from Renewable Resources* (pp. 67-88). Elsevier. https://doi.org/10.1016/B978-0-08-045316-3.00004-1

Singer, I. L., Kohl, J. G., & Patterson, M. (2000). Mechanical aspects of silicone coatings for hard foulant control. *Biofouling*, 16(2-4), 301-309. https://doi.org/10.1080/08927010009378453

Sommer, S. A., Byrom, J. R., Fischer, H. D., Bodkhe, R. B., Stafslien, S. J., Daniels, J., Yehle, C., Webster, D. C. (2011). Effects of pigmentation on siloxane–polyurethane coatings and their performance as fouling-release marine coatings. *Journal of Coatings Technology and Research*, 8, 661-670. https://doi.org/10.1007/s11998-011-9340-3

Song, C., & Cui, W. (2020). Review of underwater ship hull cleaning technologies. *Journal of Marine Science and Application*, 19(3), 415-429. https://doi.org/10.1007/s11804-020-00157-z

Stevens, M. J., Steren, R. E., Hlady, V., & Stewart, R. J. (2007). Multiscale structure of the underwater adhesive of Phragmatopoma californica: a nanostructured latex with a steep microporosity gradient. *Langmuir*, 23(9), 5045-5049. https://doi.org/10.1021/la063765e

Stewart, R. J., Weaver, J. C., Morse, D. E., & Waite, J. H. (2004). The tube cement of *Phragmatopoma californica*: a solid foam. *Journal of Experimental Biology*, 207(26), 4727-4734. https://doi.org/10.1242/jeb.01330

Studer, G., Tauriello, G., Bienert, S., Biasini, M., Johner, N., & Schwede, T. (2021). ProMod3—A versatile homology modelling toolbox. *PLoS Computational Biology*, 17(1), e1008667. https://doi.org/10.1371/journal.pcbi.1008667

Swain, G. W., Griffith, J. R., Bultman, J. D., & Vincent, H. L. (1992). The use of barnacle adhesion measurements for the field evaluation of non-toxic foul release surfaces. *Biofouling*, 6(2), 105-114. https://doi.org/10.1080/08927019209386216

Tang, Y. Z., & Gobler, C. J. (2011). The green macroalga, *Ulva lactuca*, inhibits the growth of seven common harmful algal bloom species via allelopathy. *Harmful Algae*, 10(5), 480-488. https://doi.org/10.1016/j.hal.2011.03.003

The UniProt Consortium (2023). UniProt: the Universal Protein Knowledgebase in 2023, *Nucleic Acids Research*, 51(D1), D523–D531. https://doi.org/10.1093/nar/gkac1052

Unabia, C. R. C., & Hadfield, M. G. (1999). Role of bacteria in larval settlement and metamorphosis of the polychaete *Hydroides elegans*. *Marine Biology*, 133, 55-64. https://doi.org/10.1007/s002270050442

Urushida, Y., Nakano, M., Matsuda, S., Inoue, N., Kanai, S., Kitamura, N., Nishino, T., & Kamino, K. (2007). Identification and functional characterization of a novel barnacle cement protein. *The FEBS Journal*, 274(16), 4336-4346. https://doi.org/10.1111/j.1742-4658.2007.05965.x

van Dam, J. W., Trenfield, M. A., Harries, S. J., Streten, C., Harford, A. J., Parry, D., & van Dam, R. A. (2016). A novel bioassay using the barnacle *Amphibalanus amphitrite* to evaluate chronic effects of aluminium, gallium and molybdenum in tropical marine receiving environments. *Marine Pollution Bulletin*, 112(1-2), 427-435. https://doi.org/10.1016/j.marpolbul.2016.07.015

Vinagre, P. A., Simas, T., Cruz, E., Pinori, E., & Svenson, J. (2020). Marine biofouling: A European database for the marine renewable energy sector. *Journal of Marine Science and Engineering*, 8(7), 495. https://doi.org/10.3390/jmse8070495

Waite, J. H. (1987). Nature's underwater adhesive specialist. *International Journal of Adhesion and Adhesives*, 7(1), 9-14. https://doi.org/10.1016/0143-7496(87)90048-0

Walker, G. (1972). The biochemical composition of the cement of two barnacle species, *Balanus hameri* and *Balanus crenatus*. *Journal of the Marine Biological Association of the United Kingdom*, 52(2), 429-435. https://doi.org/10.1017/S0025315400018786

Walker, G., & Yule, A. B. (1984). Temporary adhesion of the barnacle cyprid: the existence of an antennular adhesive secretion. *Journal of the Marine Biological Association of the United Kingdom*, 64(3), 679-686. https://doi.org/10.1017/S0025315400030344

Waterhouse, A., Bertoni, M., Bienert, S., Studer, G., Tauriello, G., Gumienny, R., Heer, F. T., de Beer, T. A. P., Rempfer, C., Bordoli, L., Lepore, R., & Schwede, T. (2018). SWISS-MODEL: homology modelling of protein structures and complexes. *Nucleic Acids Research*, 46(W1), W296-W303. https://doi.org/10.1093/nar/gky427

Wendt, D. E., Kowalke, G. L., Kim, J., & Singer, I. L. (2006). Factors that influence elastomeric coating performance: the effect of coating thickness on basal plate morphology, growth and critical removal stress of the barnacle *Balanus amphitrite*. *Biofouling*, 22(1), 1-9. https://doi.org/10.1080/08927010500499563

Yebra, D. M., & Weinell, C. E. (2009). Key issues in the formulation of marine antifouling paints. In *Advances in Marine Antifouling Coatings and Technologies* (pp. 308-333). Woodhead Publishing. https://doi.org/10.1533/9781845696313.2.308

Yebra, D. M., Kiil, S., & Dam-Johansen, K. (2004). Antifouling technology—past, present and future steps towards efficient and environmentally friendly antifouling coatings. *Progress in Organic Coatings*, 50(2), 75-104. https://doi.org/10.1016/j.porgcoat.2003.06.001

Yuvaraj, D., Annushrie, A., Niranjana, M., Gnanasekaran, R., Gopinath, M., & Iyyappan, J. (2021). A review on process and characterization of mussels and cirripeds for adhesive properties and applications thereof. *Current Research in Green and Sustainable Chemistry*, 4, 100092. https://doi.org/10.1016/j.crgsc.2021.100092

Zardus, J. D., Nedved, B. T., Huang, Y., Tran, C., & Hadfield, M. G. (2008). Microbial biofilms facilitate adhesion in biofouling invertebrates. *The Biological Bulletin*, 214(1), 91-98. https://doi.org/10.2307/25066663

Zhang, X., Zhou, X., & Wang, X. (2013). Basics for Bioinformatics. In Jiang, R., Zhang, X., Zhang, M. (Eds.) *Basics of Bioinformatics* (pp 1–25). Springer, Berlin, Heidelberg. https://doi.org/10.1007/978-3-642-38951-1_1

Zhou, W., Wang, Y., Ni, C., & Yu, L. (2021). Preparation and evaluation of natural rosin-based zinc resins for marine antifouling. *Progress in Organic Coatings*, 157, 106270. https://doi.org/10.1016/j.porgcoat.2021.106270